The pig as an animal model for Cystic Fibrosis – approaches to overcome the lethal intestinal phenotype

von Michaela Désirée Dmochewitz

Inaugural-Dissertation zur Erlangung der Doktorwürde
der Tierärztlichen Fakultät der Ludwig-Maximilians-Universität München

The pig as an animal model for Cystic Fibrosis – approaches to overcome the lethal intestinal phenotype

von Michaela Désirée Dmochewitz

aus Ulm

München 2016

Aus dem Veterinärwissenschaftlichen Department der Tierärztlichen Fakultät
der Ludwig-Maximilians-Universität München

Lehrstuhl für Molekulare Tierzucht und Biotechnologie

Arbeit angefertigt unter der Leitung von Univ.-Prof. Dr. Eckhard Wolf

Mitbetreuung durch Dr. Nikolai Klymiuk und Dr. Andrea Bähr

Gedruckt mit Genehmigung der Tierärztlichen Fakultät
der Ludwig-Maximilians-Universität München

Dekan:	Univ.-Prof. Dr. Joachim Braun
Berichterstatter:	Univ.-Prof. Dr. Eckhard Wolf
Korreferenten:	Univ.-Prof. Dr. Mathias Ritzmann Univ.-Prof. Dr. Katrin Hartmann Priv.-Doz. Dr. Birgit Viertlböck Univ.-Prof. Dr. Rüdiger Wanke

Tag der Promotion: 16.07.2016

Für Miky

Just because something doesn't do what you planned it to do

doesn't mean it's useless.

Thomas A. Edison

During the preparation of this thesis, the following review was published:

Dmochewitz, M. and E. Wolf (2015). "Genetic engineering of pigs for the creation of translational models of human pathologies." Animal Frontiers **5**(1).

Parts of this study were presented at the following conference:

Opening Conference COST Action BM1308 “Sharing Advances on Large Animal Models (SALAAM)”, Gene Center, LMU Munich, December 15-16, 2014.

TABLE OF CONTENTS

INDEX OF ABBREVIATIONS

aq. bidest.	Bidistilled water
aq. dest.	Distilled water
AAV	Adeno-associated virus
APS	Ammonium persulfate
ASL	Airway surface liquid
ATP	Adenosine triphosphate
BAC	Bacterial artificial chromosome
BCA	Bicinchoninic acid
BMI	Body mass index
bp	Base pair
BSA	Bovine serum albumin
BW	Body weight
cAMP	Cyclic adenosine monophosphate
CBAVD	Congenital bilateral absence of the vas deferens
cDNA	Complementary DNA
CF	Cystic Fibrosis
CFRD	Cystic Fibrosis-related diabetes
CFTR	Cystic Fibrosis Transmembrane Conductance Regulator
CT	Computed tomography
DAB	3.3’ Diaminobenzidine tetrahydrochloride
dATP	Deoxyadenosine triphosphate
dCTP	Deoxycytidine triphosphate
dGTP	Deoxyguanosine triphosphate
DIOS	Distal intestinal obstruction syndrome
DNA	Deoxyribonucleic acid
DNase	Deoxyribonuclease
dNTP	Deoxynucleoside triphosphate
DTT	Dithiothreitol
dTTP	Deoxythymidine triphosphate
EDTA	Ethylenediaminetetraacetic acid
E.g.	For example

ENaC	Epithelial sodium channel
EPI	Exocrine pancreatic insufficiency
ET	Embryo transfer
EtOH	Ethanol
FBC	Focal biliary cirrhosis
FDA	US Food and Drug Administration
gDNA	Genomic DNA
h	Hour
hCG	Human chorionic gonadotropin
H.E.	Hematoxylin and eosin
HCl	Hydrochloric acid
HIER	Heat-induced epitope retrieval
HR	Homologous recombination
i.c.	Intracardial
i.e.	That is
i.m.	Intramuscular
IF	Immunofluorescence
Ig	Immunoglobulin
IHC	Immunohistochemistry
IRT	Immunoreactive trypsinogen
IU	International unit
kb	Kilobase
KO	Knockout
L	Liter
LMU	Ludwig-Maximilians-University of Munich
M	Mole
MCT	Mucociliary transport
mg	Milligramm
MI	Meconium ileus
min	Minute
mL	Milliliter
mM	Millimolar
mmol	Millimole
MOPS	3-(*N*-morpholino) propanesulfonic acid

mRNA	Messenger RNA
MVG	Moorversuchsgut
NaCl	Sodium chloride
ng	Nanogram
NT	Nuclear transfer
NTC	Non-template control
OCT	Optimal cutting temperature compound
ORCC	Outward rectifying chloride channel
PCR	Polymerase chain reaction
PFA	Paraformaldehyde
pH	Negative log of hydrogen ion concentration in a water-based solution
PIER	Proteinase-induced epitope retrieval
PMSG	Pregnant mare's serum gonadotropin
qPCR	Quantitative PCR
rAAV	Recombinant Adeno-associated virus
rcf	Relative centrifugal force
RNA	Ribonucleic acid
RNase	Ribonuclease
rpm	Revolutions per minute
RT	Room temperature
s	Second
SCNT	Somatic cell nuclear transfer
SDS	Sodium dodecyl sulfate
SDS PAGE	SDS polyacrylamide gel electrophoresis
SNP	Single nucleotide polymorphism
TAE	Tris acetate buffer
TALEN	Transcription activator-like effector nuclease
TBS	Tris buffered saline
TEMED	Tetraethylethylenediamine
TRIS	Tris (hydroxymethyl)-aminomethane
U	Unit
UV	Ultraviolet
V.	Vene
WB	Western Blot

WT	Wild type
w/v	Weight per volume solution
µg	Microgram
µL	Microliter

I. INTRODUCTION

Cystic Fibrosis (CF) is one of the most common life-threatening hereditary diseases in people of European descent. Mutations in the gene coding for the Cystic Fibrosis Transmembrane Conductance Regulator (CFTR) lead to defective anion transport on epithelial surfaces and thereby cause a multisystemic disease mainly affecting the airways and the pancreas (Davies, Alton *et al*. 2007). From childhood on, patients have to undergo a multitude of symptomatic treatments for the management of pulmonary and gastrointestinal disease (Cystic Fibrosis Foundation 2016). Efforts in intensive symptomatic therapy have revolutionized the treatment of CF patients, leading to an increase of the median survival age from early childhood for a child diagnosed with CF in the 1950s to about 37 years for a CF patient today (Dodge, Lewis *et al*. 2007, MacKenzie, Gifford *et al*. 2014). However, treatment options are still mainly limited to symptomatic therapy.

For a better understanding of pathophysiological mechanisms involved in the onset of the disease and evaluation of novel therapeutic approaches aiming at the underlying cause of CF, animal models are an essential tool. Efforts in genome manipulation during the past decade have facilitated the establishment of different animal models for human genetic disorders. From the five CF animal models developed so far (mouse, rat, ferret, pig and zebrafish), the porcine CF model proves to be the model showing the closest resemblance to the typical CF phenotype in humans (Cutting 2015). Until now, a range of important insights, mainly regarding the inflammatory and infectious processes involved in the development of pulmonary disease, have been gained by studies on porcine CF tissue. However, the utility of the porcine CF model is still hampered, as CF piglets cannot reach adulthood due to a severe meconium ileus that occurs in 100 % of all cases. This neonatal intestinal obstruction proves to be fatal if not surgically corrected (Rogers, Stoltz *et al*. 2008, Klymiuk, Mundhenk *et al*. 2012).

The aim of this thesis was to evaluate two different approaches for the rescue of the lethal intestinal phenotype in CF piglets. The transgenic approach was driven by the idea that selective expression of *CFTR* in the intestine of a CF pig should ameliorate meconium ileus without interfering with the typical phenotype seen in other organ systems. The second approach focused on the finding that modifier genes are known to strongly influence the severity of meconium ileus in human CF patients. Therefore, it was evaluated whether modifier genes might also play a contributive role in the susceptibility for meconium ileus in CF piglets.

II. REVIEW OF THE LITERATURE

1. Cystic Fibrosis

Cystic Fibrosis (CF) is the most common lethal autosomal recessive monogenic disease in people from Caucasian origin with a prevalence of about 70,000 affected individuals worldwide (Cutting 2015). Although there was no specific characterization of the disease until the early 20th century, historic texts give a hint that characteristic symptoms of the disease, like the association between elevated sweat levels and early death, were identified much earlier:

Das Kind stirbt bald wieder, dessen Stirne beim Küssen salzig schmeckt.
"The child whose brow tastes salty when kissed will soon die."
Almanac of Children's Songs and Games from Switzerland (Rochholz 1857).

In 1938, Dorothy Anderson was the first to describe in detail the clinic and pathology of infants suffering from neonatal intestinal obstruction and intestinal and respiratory complications. Due to the characteristic histology of the pancreas with cyst-like dilated and obstructed acini and ducts surrounded by fibrotic tissue she named this disease Cystic Fibrosis (Anderson 1938). 13 years later, Kessler (1951) hypothesized, observing that CF patients were more susceptible to heat prostration and sweat depletion, that exocrine glands in CF patients were inadequate in function. This lead to the insight that the electrolyte transport is disturbed and that CF patients show elevated sodium and chloride levels in sweat (di Sant'Agnese, Darling *et al*. 1953), resulting in the development of the "sweat test" as a valuable diagnostic tool for CF, which is still in common use today. In doing so, sweating is stimulated by pilocarpine iontophoresis and sodium and chloride concentrations can be measured in the collected sweat (Gibson and Cooke 1959). This major diagnostic breakthrough did not result in a better understanding and therapy of CF until 1989, when Riordan, Rommens *et al*. (1989) identified the underlying genetic cause of CF, i.e. mutations in the gene encoding the anion channel Cystic Fibrosis Transmembrane Conductance Regulator (*CFTR*).

1.1. Genetics of Cystic Fibrosis

The *CFTR* gene is located on chromosome 7, consists of 27 exons spanning about 250 kb and encodes the CFTR anion channel. CFTR is a unique member of the ATP-binding cassette (ABC) family of membrane transport proteins (Riordan 2005), playing an important role in the chloride and bicarbonate transport across epithelia. The CFTR protein comprises 1,480 amino acids, is predominantly expressed at the apical membrane of epithelial cells (Marino, Matovcik *et al*. 1991, Denning, Ostedgaard *et al*. 1992) and occupies five functional domains – two membrane-spanning domains (MSD1 and MSD2) forming the actual channel through the membrane, two asymmetric nucleotide-binding domains (NBD1 and NBD2) regulating the gating of the channel by binding and hydrolysis of ATP, and the R-domain that mediates channel activity by cAMP-dependent phosphorylation (Sheppard and Welsh 1999). Up to 2,000 mutations in the *CFTR* gene have been reported to the CFTR mutation database. The most common mutation F508del, characterized by a deletion of phenylalanine at position 508, is found on at least one allele of 85 % of CF patients (Bell, De Boeck *et al*. 2015, Cystic Fibrosis Mutation Database 2015). Based on the functional effect on the CFTR protein, mutations are currently classified into six distinct groups (Welsh and Smith 1993). Mutations leading to deficient protein synthesis, like premature stop codons, frameshifts or nonsense mutations, are summarized in class I, whereas mutations in class II, amongst them the F508del mutation, lead to a failure in protein processing and subsequent degradation of the protein by cell quality control mechanisms in the endoplasmatic reticulum. In class III, mutations leading to alterations in the regulation of gating by failure to respond to cAMP stimulation are combined. Mutations of these first three classes produce the classic CF phenotype. In contrast, mutations of classes IV to VI often cause milder disease patterns due to defective chloride conductance (class IV), altered stability of mRNA (class V) or decreased stability of the mature protein (class VI) (Proesmans, Vermeulen *et al*. 2008, Amaral and Farinha 2013).

1.2. Pathophysiology of Cystic Fibrosis

CFTR does not only play an important role in the chloride and bicarbonate transport across epithelia, but also regulates the electrolyte transport of other channels via osmolar interaction. E.g., sodium absorption via the epithelial sodium channel ENaC and chloride efflux via the outwardly rectifying chloride channel ORCC are inhibited as a consequence (Reddy, Light *et al*. 1999, Reddy and Quinton 2001). The exact mechanism of how the dysfunction of CFTR leads to a disease that affects a range of different organs still remains unclear. However, the major outcome, the secretion by exocrine glands in the airways, intestine and pancreas with increased viscosity, decreased volume and lowered pH, is indisputable. Two main prevalent theories, the “high salt” and the “low volume” hypothesis try to answer the question of how the pathology of respiratory disease is exactly evoked. The “high salt” hypothesis focuses on the idea that reduced chloride conductance leads to an increase of NaCl in the airway surface liquid (ASL) that inhibits a naturally secreted antimicrobial protein and therefore predisposes for the development of infections (Goldman, Anderson *et al*. 1997). In contrast, the “low volume” theory claims that defective chloride secretion leads to less water efflux due to an osmotic gradient that is further intensified by the above-mentioned influences on other ion channels. The consequence is a liquid depletion on the epithelial surface causing an increase in viscosity of epithelial secretions that interferes with the function of different organs by damaging tissue and eventually destroying the organ (Boucher 2007, Ratjen 2009). In support of the “low volume” theory, studies have shown that ASL of healthy and CF individuals do not differ in the concentration of sodium and chloride (Knowles, Robinson *et al*. 1997) and that ASL volume is indeed reduced in CF airway epithelia (Matsui, Grubb *et al*. 1998).

1.3. Phenotypical abnormalities in Cystic Fibrosis

Cystic Fibrosis is a multisystemic disease affecting the airways, the gastrointestinal tract including the hepatobiliary system and pancreas, the reproductive tract and the sweat glands. The majority of CF patients die of pulmonary insufficiency associated with bronchial infections (Bell, De Boeck *et al*. 2015). The depletion of ASL causes disturbances in the mucociliary clearance leading to an increased deposit of infectious agents in the lungs. The consequence is a vicious circle of chronic inflammatory and obstructive processes like bronchiectasis and chronic infections with a predominance of *Staphylococcus (S.) aureus* and *Pseudomonas (P.) aeruginosa* in the lungs and sinuses (Proesmans, Vermeulen *et al*. 2008). The genesis of the inflammation in the airways still remains unclear. It is controversially debated whether inflammation is a consequence of infection or occurs primarily in the absence of infectious agents (Heijerman 2005). Regardless of the precise mechanism of pathogenesis, the end stages of airway disease are characterized by a series of pulmonary exacerbations leading to a decline in lung function and an increase in respiratory and systemic symptoms, resulting in fatal respiratory failure (Rosenfeld, Emerson *et al*. 2001).

About 10-20 % of all CF newborns suffer from meconium ileus (MI), a life-threatening obstruction of the intestine by fetal faeces, which is treated either conservatively by enemas or by surgical intervention. MI can be classified into simple and complex forms, the latter being complicated by additional intestinal abnormalities such as atresia or microcolon. Depending on the severity of MI, surgical methods range from simple enterostomy to resection of intestinal segments. Interestingly, although undergoing complicated surgical interventions, prolonged hospitalization and being infected with *P. aeruginosa* earlier, the long-term prognosis of CF patients presenting with MI is not affected negatively (Kappler, Feilcke *et al*. 2009). The prevalence of MI at birth shows a high correlation with more severe mutations like F508del and predisposes patients to develop the distal intestinal obstruction syndrome (DIOS) in later life (Kelly and Buxbaum 2015).

Another feature strongly associated with more severe mutations is pancreas insufficiency that occurs in 85 % of CF patients. Exocrine pancreas dysfunction (EPI) caused by extensive structural damage of the ducts and acini leads to general malnutrition, growth retardation and fat-soluble vitamin deficiency. The treatment by substitution of vitamins and pancreatic enzymes is well established. CF patients are also predisposed to develop pancreatitis and CF-related diabetes (CFRD), which is known to contribute to the progression of respiratory disease (Katkin and Schultz 2010, Brennan and Schrijver 2016). Early insulin therapy improves the lung function and is also associated with better weight gain (Hameed, Jaffé *et al*. 2015).

With improved life expectancy of CF patients, liver disease characterized by focal biliary cirrhosis (FBC), cholangiectasis, cholelithiasis and fatty liver has become the second most life-threatening feature after respiratory failure (Efrati, Barak *et al*. 2003). FBC is commonly treated by oral supplementation of the bile salt ursodeoxycholic acid that normalizes liver function. Only if hepatobiliary disease is complicated by portal hypertension, a liver transplantation is considered (Kelly and Buxbaum 2015).

All males with classic CF suffer from infertility due to the congenital bilateral absence of the vas deferens (CBAVD) and obstructive azoospermia. In contrast, only a small percentage of women affected exhibit reduced fertility, however, without any signs of structural abnormalities (O'Sullivan and Freedman 2009). It is of note that even men carrying only one mutation or being diagnosed with atypical CF without any other characteristic symptoms, are at high risk to suffer from CBAVD or other fertility problems (Mak, Zielenski *et al*. 1999).

1.4. Diagnosis of Cystic Fibrosis

As mentioned above, the gold standard for the diagnosis of CF in patients exhibiting clinical signs or symptoms is still the sweat test developed by Gibson and Cooke (1959). If chloride concentrations are greater than 60 mmol/L, a definitive diagnosis of CF can be reached, whereas intermediate concentrations between 30-59 mmol/L are only indicative of CF. In such cases, CF can only be diagnosed by identifying two CF-causing mutations on both alleles. Even for

patients with diagnostic chloride concentrations, a screening for mutations by molecular testing is commonly conducted. In order to detect CF patients before showing any clinical signs, a newborn screening for CF was established in over 40 states worldwide. Immunoreactive trypsinogen (IRT), an enzyme elevated by pancreatic injury and therefore indicative of CF, is routinely measured in the blood of newborns. If abnormal levels are detected, further tests such as mutation screening or sweat tests are performed to confirm the diagnosis of CF (Farrell, Rosenstein *et al*. 2008, O'Sullivan and Freedman 2009). In days of powerful molecular-genetic tools, screening for mutations in the *CFTR* gene can be conducted easily. Generally, a panel of 23 mutations known to cause classic CF and occurring with a frequency of more than 0.1 % in CF patients' chromosomes, is screened for by commercially available analyte specific reagents (Strom, Janeszco *et al*. 2006). In the event that mutations cannot be identified by this method, an additional assay is conducted. By sequencing all exons, splice junctional sequences, the promoter and parts of intron 11 and 19, 98.7 % of all reported mutations are detected (Strom, Huang *et al*. 2003).

1.5. Treatment strategies for Cystic Fibrosis

Although the causative agent of CF has been discovered more than 25 years ago, treatment is still focused on symptomatic therapy. For an effective treatment, close monitoring and early and aggressive intervention is recommended to fulfil the primary goals – maintaining good lung function as long as possible, assuring adequate growth and managing CF-related complications. As good nutritional status is strongly correlated with improved pulmonary function (Konstan, Butler *et al*. 2003), it is essential for CF patients with pancreatic insufficiency to keep a balanced, high-caloric diet with supplementation of fat-soluble vitamins and pancreatic enzymes (Borowitz, Baker *et al*. 2002). Management of respiratory problems depends on the different stages of CF lung disease – from airway clearing techniques and mucolytic inhalation in the pre-infectious status to aggressive intravenous and aerosol antibiotic treatment and eventual lung transplantation in the end stage (Davies, Alton *et al*. 2007). In the case of CFRD

and hepatobiliary disease, additional medication with insulin and ursodeoxycholic acid, respectively, is recommended (Kelly and Buxbaum 2015).

Over the last decades, efforts in the multidisciplinary symptomatic treatment have improved the survival age from early childhood in the 1950s to a median survival age of 37 years today (Cutting 2015). Nevertheless, novel therapeutic approaches with the aim of curing the disease by restoring the CFTR function have only evolved recently.

Gene therapy approaches for CF are based upon the concept of gene complementation, meaning that an additional WT *CFTR* cDNA copy is delivered to CF-affected cells, an approach feasible for CF patients with any genetic mutation (Gill and Hyde 2014). First results from clinical phase IIB trials with the non-viral, liposome-based vector GL67A indicate that gene therapy can lead to an improvement in lung function (Alton, Armstrong *et al*. 2015).

Another therapeutic approach is the development of novel drugs, the so-called CFTR modulators, which target specific mutation classes directly (Amaral and Kunzelmann 2007). “Suppressors” are suitable for mutations of class I by promoting the read-through of premature stop codons and thereby permitting the translation of the full-length protein. Ataluren has been successfully used in clinical phase III trials, showing a beneficial effect on lung function, but can only be used for the 5 % of CF patients carrying class I mutations (Wilschanski, Miller *et al*. 2011). “Correctors” act as chaperones by allowing the mutant protein to escape degradation and reach the cell membrane and are therefore suitable for class II mutations. Treatment of CF patients carrying the most common F508del mutation with the corrector Lumacaftor alone is insufficient, whereas in combination with the potentiator Ivacaftor it is now a commercially available drug approved by the US Food and Drug Administration (FDA) (Cystic Fibrosis Foundation 2016). “Potentiators” increase channel gating activity and are used for the treatment of class III mutations (Clancy and Jain 2012, Bell, De Boeck *et al*. 2015, Brennan and Schrijver 2016). The potentiator Ivacaftor, the first FDA-approved molecular therapeutic for CF, can be successfully used in the treatment of about 3 % of CF patients that carry the G551D mutation by increasing chloride transport through improved channel activity (Van Goor, Hadida *et al*. 2009).

2. Animal models of Cystic Fibrosis

Animal models are a unique tool for a better understanding of the pathophysiological mechanisms in Cystic Fibrosis and the development or testing of new therapeutic approaches. Among other things, they allow for the study of early pathogenesis prior to clinical manifestations and the controlled evaluation of therapeutic effects. The relevance of a disease model increases if a systematic comparison of different model species is possible (Olivier, Gibson-Corley *et al*. 2015). The rapid technological progress in the genetic manipulation of animals in the last decades (Whitelaw, Sheets *et al*. 2016) has facilitated the efficient development of animal models for Cystic Fibrosis in five different species, a unique feature among human genetic disorders (Cutting 2015). Each of these model organisms has its specific advantages, but also major limitations.

2.1. Cystic Fibrosis mice models

Historically, the first animal model for CF was the CF mouse model. Mice models bear several advantages – methods for genomic manipulation are well established, the reproduction rate is high and the costs of maintaining and housing are low.
Since the first mouse strain carrying a mutation in the *Cftr* gene was generated in 1992 (Snouwaert, Brigman *et al*. 1992), at least 14 different CF mouse models, carrying null and clinically relevant mutant *Cftr* forms like F508del, were developed (Scholte, Davidson *et al*. 2004, Fisher, Zhang *et al*. 2011). Gene targeting approaches as well as environmental influences cause slight variations in the severity of the phenotype, but there is consensus in the important phenotypical abnormalities (Davidson and Rolfe 2001, Wilke, Buijs-Offerman *et al*. 2011). The most prominent hallmark feature in CF mice is the severe intestinal phenotype characterized by electrophysiological abnormalities, mucus accumulation in the dilated crypts, goblet cell hyperplasia, a general failure to thrive and death around weaning due to intestinal obstruction. The physiological processes involved in the intestinal blockage are reminiscent of the MI complications in human CF infants, but advance differently from the clinical point of view (Guilbault, Saeed *et al*. 2007). In general, pancreatic insufficiency is clearly less pronounced than in

human CF patients, probably because of a relatively low expression of CFTR in the murine pancreatic ducts and the existence of an alternative calcium-activated fluid secretory pathway (Gray, Winpenny *et al*. 1995). Another feature absent in CF mice is obvious liver pathology. However, the murine CF gallbladder shows abnormalities like distension, inflammatory processes or an obstruction with vicious bile leading to emptying defects (Debray, Rainteau *et al*. 2012). An interesting feature in CF mice is that a lack of CFTR leads to abnormalities in enamel development in the incisors (Wright, Kiefer *et al*. 1996). Although most of the male CF mice exhibit reduced fertility, the complete bilateral absence of the vas deferens typical for humans is missing probably due to the presence of additional electrolyte transport mechanisms in the reproductive tract (Leung, Wong *et al*. 1996) . The main problem limiting the usage of the mouse as an animal model for CF is the absence of the respiratory disease typical for human CF. Although CF mice show some distinct pathological abnormalities like defects in mucociliary clearance or pulmonary parenchymal thickening, they neither develop spontaneous chronic infection nor inflammation of the lung. The reasons for this discrepancy still remain unclear, but potential explanations could be differences in the distribution of secretory cells and submucosal glands or the existence of alternative chloride channels (Grubb, Paradiso *et al*. 1994, Grubb and Boucher 1999).

In conclusion, CF mouse models have given important insights into disease mechanisms, like the role of alternative secretory pathways or potential modifier genes and the pathology of intestinal disease. They allow for the evaluation of novel therapeutic approaches, but due to their deficiency of recapitulating human airway disease, other model species are essential for CF research.

2.2. Cystic Fibrosis rat model

In 2014, the first *Cftr*$^{-/-}$ rat was generated by genome editing with Zinc finger nucleases. Advantages of the rat as a model species for CF are the fast reproduction rate, and, unlike mice, a distribution pattern of submucosal glands in the airways comparable to humans and a size allowing for surgical interventions and easier tissue collection. Similar to CF mice, *Cftr*$^{-/-}$ rats show a failure to thrive

with decreased survival at weaning because of intestinal obstruction and abnormal enamel deposition in teeth, but no obvious signs of hepatobiliary or pancreatic changes. Histological changes in the intestine include cell sloughing, mucus-dilated crypts and bacterial overgrowth. Short-circuit measurements by Ussing-chamber confirm the absence of CFTR in the intestine. Similar to human CF, male CF KO rats exhibit bilateral absence of the vas deferens and abnormalities in the airways like reduced tracheal circumference and reduced submucosal gland area. Unfortunately, the lungs appear normal without any signs of pathological or inflammatory processes (Tuggle, Birket *et al*. 2014).

2.3. Cystic Fibrosis ferret model

Since the structure of the airways resembles humans and the ferret lung is a known disease model for lung infections, the ferret is considered to be a promising model species for CF. Ferrets that are heterozygous for a disruption of the *CFTR* gene were generated by recombinant Adeno-associated virus -mediated (rAAV) gene targeting (Sun, Yan *et al*. 2008) and selectively bred for the production of litters containing WT, $CFTR^{+/-}$ and $CFTR^{-/-}$ kits (Sun, Sui *et al*. 2010). CF KO kits suffer from lethal MI with a penetrance of 75 %, but even ferrets that are able to remove MI on their own fail to thrive and die within a few days if not reared with a mixture of oral laxatives, proton pump inhibitors, antibiotics and pancreatic enzyme supplementation. Surviving CF kits exhibit crypts dilated by vicious mucus, villous atrophy, lymphoplasmacytic inflammation and bacterial overgrowth of the intestine. Although the hepatobiliary system appears normal at birth, gallbladder disease with mucous changes and mucosal proliferation occurs in CF KO ferrets older than one month. Additionally, liver enzymes are elevated, indicating early functional liver disease (Sun, Olivier *et al*. 2014). CF KO kits are born with only mild signs of exocrine pancreatic disease and slight abnormalities in endocrine function. However, during the first months a progressive destruction and remodeling of the exocrine and endocrine tissue occurs and ferrets develop exocrine pancreatic insufficiency and characteristics of CF-related diabetes (Olivier, Yi *et al*. 2012). In all male CF KO ferrets, the vas deferens is either completely absent or degenerated (Sun, Sui

et al. 2010). Most importantly, ferrets develop lung disease very similar to humans with a high susceptibility to bacterial infections, impaired mucociliary clearance and characteristic histological changes like mucus-obstruction of the airways and submucosal glands, atelectasis and inflammation (Sun, Olivier *et al*. 2014).

2.4. Cystic Fibrosis zebrafish model

A model organism principally used for the examination of early developmental effects of Cftr is the zebrafish. Studies on *cftr* knockdown zebrafish embryos show that bacterial clearance after *P. aeruginosa* infection is clearly reduced in comparison to other pathogens commonly isolated in CF patients, indicating a Cftr-mediated specific resistance to *P. aeruginosa* (Phennicie, Sullivan *et al*. 2010). Other important insights gained from zebrafish *cftr* mutants generated by TALENs are the important role of Cftr in the regulation of fluid secretion into the Kupffer's vesicles - thereby affecting left-right asymmetry (Navis, Marjoram *et al*. 2013) - and the fact that pancreatic destruction occurs without major defects in the early organ development (Navis and Bagnat 2015).

2.5. Cystic fibrosis pig models

Genetically-engineered pigs harbor great potential for use in biomedical and translational research as they share many important features with humans. The similarity in terms of anatomy, physiology, histology, immunology, metabolism and also genomics is high, the short generation time and large litter size facilitate rapid production of enough animals and environmental influences can be standardized. Additionally, the porcine lifespan allows for long-term studies regarding effects of therapeutic treatments and pathogenesis, and the body size allows for testing of human devices and surgical interventions as well as efficient and easy tissue collection (Rogers, Abraham *et al*. 2008, Aigner, Renner *et al*. 2010).

To date, three different porcine CF models either carrying a completely disrupted *CFTR* gene (Rogers, Stoltz *et al*. 2008, Klymiuk, Mundhenk *et al*. 2012) or the most common human mutation F508del (Rogers, Hao *et al*. 2008) have been generated by different genetic approaches. Rogers and coworkers targeted the *CFTR* locus in fetal fibroblasts by using rAAV vectors, followed by somatic cell nuclear transfer (SCNT) and embryo transfer, resulting in male heterozygous $CFTR^{+/-}$ offspring that was bred selectively over two generations to generate $CFTR^{-/-}$ piglets. The first European CF pig model was established by Klymiuk, Mundhenk *et al*. (2012) via sequential targeting of the *CFTR* locus in primary kidney cells using large vectors based on modified bacterial artificial chromosomes (BACs).

CF pigs show many of the characteristic phenotypic abnormalities found in human CF patients. Exocrine pancreas destruction in newborn piglets is histopathologically characterized by small, degenerated lobes with a decreased number of acinar cells, dilated ducts filled with eosinophilic material and signs of mild inflammation, surrounded by undifferentiated connective tissue (Meyerholz, Stoltz *et al*. 2010, Klymiuk, Mundhenk *et al*. 2012). Although the endocrine pancreatic tissue seems morphologically normal at birth, neonatal CF pigs exhibit functional abnormalities in glycaemic regulation and insulin secretion and, according to human CFRD, they tend to spontaneously develop hyperglycemia. This observation refuted the long-standing hypothesis that endocrine changes are mainly caused by the destruction of the exocrine pancreas (Uc, Olivier *et al*. 2015). Human focal biliary cirrhosis is mirrored in the CF piglet in a milder form with hyperplastic bile ducts surrounded by fibrotic tissue and chronic cellular inflammation. Gallbladder disease is reported in 15-30 % of human CF patients, but is a consistent finding in CF piglets, which have a micro-gallbladder obstructed by viscous bile and mucus and signs of epithelial proliferation (Welsh, Rogers *et al*. 2009). Pancreatic and biliary secretions are altered in terms of volume, pH and content of enzymes, suggesting an involvement in disease pathogenesis (Uc, Giriyappa *et al*. 2012).

CF piglets also exhibit another feature commonly found in human male CF patients, i.e. a degenerated or absent vas deferens sometimes accompanied by epididymis atresia without tubular structures (Pierucci-Alves, Akoyev *et al*. 2011). Similar to CF ferrets, CF piglets show a defect in the mineralization of enamel, suggesting an important role of CFTR in the maturation and bioformation of enamel (Chang, Lacruz *et al*. 2011). A very interesting finding is that the absence of CFTR leads directly to defects in the peripherous nervous system, a feature that is known from human CF patients but was thought to be caused by the secondary manifestations of the disease (Reznikov, Dong *et al*. 2013).

2.5.1. The value and uniqueness of the porcine CF model regarding the respiratory phenotype

Concerning pulmonary disease, the pig bears several advantages over other model species. The porcine lung has been an established model for both the healthy and sick human lung and therefore has been commonly used for the evaluation of pulmonary therapeutics long before CF pig models have been established (Rogers, Hao *et al*. 2008). The anatomy, histology and morphology of the human and porcine airways show great levels of similarity (Judge, Hughes *et al*. 2014). Lung structure, tissue modeling, volume and vascular circulation are comparable, and the distribution pattern of submucosal glands throughout the cartilaginous airways and the secretory functions that are known to affect the pulmonary phenotype in CF (Widdicombe and Wine 2015) resemble those in humans. Physiological and biochemical processes important for CF pathogenesis like transepithelial electrolyte transport or mucociliary clearance are reported to lay in the same range in humans and pigs, and in general, the porcine lung is susceptible to infection by CF-relevant human pathogens like *P. aeruginosa* or *S. aureus* (Rogers, Abraham *et al*. 2008). Another important factor for the study of infection and inflammation in CF patients is the role of the porcine innate immune system in inflammatory processes that shows great parallels to humans (Bréa, Meurens *et al*. 2012). The characterization of cellular and tissue expression patterns of porcine CFTR both on mRNA and protein level revealed that the distribution is similar to humans in

all major CF-relevant organ systems, supporting the suitability of the pig for CF research (Plog, Mundhenk *et al*. 2010).

Taken together, it does not surprise that, in contrast to most other animal models, CF piglets exhibit several phenotypic abnormalities in the airways. At birth, the lungs and submucosal glands appear morphologically normal and show no signs of infection or inflammation (Rogers, Stoltz *et al*. 2008), whereas the tracheas are misshapen with thickened cartilage and enlarged smooth muscle bundles (Klymiuk, Mundhenk *et al*. 2012). Similar to human CF, neonatal piglets have hypoplastic sinuses and spontaneously develop chronic infection (Chang, Pezzulo *et al*. 2012). Like human CF patients, CF pigs suffer from lung disease characterized by inflammation, remodeling of tissue and accumulation of mucus accompanied by defects in the eradication of bacteria (Stoltz, Meyerholz *et al*. 2010).

A range of important insights into the molecular mechanisms involved in CF pathogenesis have been gained on CF pigs or porcine CF tissue. Experiments on early pathogenesis of lung disease show that anatomical defects in the airways caused by a lack of CFTR might contribute to the onset of respiratory disease. The detection of sinus hypoplasia in newborn CF piglets prior to CF-related sinusitis could clear up the question whether sinus hypoplasia in human CF patients results out of chronical infectious processes or is a developmental consequence of lack of CFTR (Chang, Pezzulo *et al*. 2012). Inspired by the finding that CF piglets show structural abnormalities of the trachea, it was demonstrated by CT scans in CF infants and by sonography in adult CF patients that similar features are present in humans (Meyerholz, Stoltz *et al*. 2010, Diwakar, Adam *et al*. 2015). The hypothesis that air trapping and airway obstruction in human CF patients are mainly secondary consequences of infection and inflammation was refuted due to the fact that newborn piglets develop these features spontaneously in the absence of inflammatory processes. A potential explanation for these findings is the reduction in size of the proximal airways (Adam, Michalski *et al*. 2013). Another indication for the contribution of structural airway defects to early disease pathogenesis was given by the fact that structural abnormalities lead to irregular particle distribution and increased particle deposition in the porcine lung (Awadalla, Miyawaki *et al*. 2014). In addition, the porcine CF model has enabled some breakthrough studies on the genesis of inflammation and infection in CF.

CF piglets show no evidence of inflammatory processes in the lung until they become infected as a result of impaired eradication of bacteria, indicating that infection is the causative agent that triggers inflammation and not vice versa (Stoltz, Meyerholz *et al*. 2010). A possible explanation for defective eradication of bacteria in the porcine CF lung is given by Pezzulo, Tang *et al*. (2012). They postulate that decreased pH of the airway surface liquid, caused by defective HCO_3^- secretion, leads to impairment in the killing of pathogens. Hoegger, Fischer *et al*. (2014) demonstrated that besides defects in the secreted antimicrobial activity, a second important lung defence mechanism, the mucociliary transport (MCT), is disturbed. Primary MCT defects occur independently from depleted airway surface liquid due to impaired detachment of mucus strands from submucosal glands, a feature that might be mediated by the absence of bicarbonate transport (Birket, Chu *et al*. 2014). Studies on explanted tracheas from CF and WT piglets demonstrate that incubation with CF-relevant pathogens triggers CFTR-dependent ASL-secretion, a feature that would be lacking in CF patients, thereby facilitating infectious processes (Luan, Campanucci Vó *et al*. 2014). Most importantly, studies on electrolyte transport in porcine CF airway tissue have questioned the long-standing hypothesis that sodium absorption is enlarged and periciliary liquid depth is reduced in CF epithelia. Results indicate that HCO_3^- and Cl^- transport are the main pathways disturbed by the loss of CFTR function without any alteration in sodium absorption (Chen, Stoltz *et al*. 2010), a concept that could be confirmed by experiments on human airway epithelia (Itani, Chen *et al*. 2011). First trials supporting the role of the CF pig for *in vivo* testing of new therapeutic approaches have been performed using adenovirus-mediated gene transfer to correct ion transport in porcine CF sinus epithelia (Potash, Wallen *et al*. 2013).

2.5.2. The lethal intestinal phenotype impairs the utility of the CF pig model – approaches to overcome this limitation

The most prominent feature in CF piglets is intestinal disease with fatal meconium ileus. In contrast to CF infants who suffer from MI in about 15 % of all cases, MI in CF piglets occurs with a prevalence of 100 %. The site of obstruction with fetal

faeces and mucus ranges from the distal part of the jejunum to the beginning of the spiral colon. An atretic and stenotic microcolon with reduced diameter and pliability is found distal to the site of obstruction. MI proves to be fatal within 24-36 h after birth if it is not corrected surgically by ileostomy or cecostomy, as piglets develop severe enteritis and peritonitis or even perforation of the intestine (Stoltz, Meyerholz *et al*. 2010). Rather than influences of the abnormal pancreas, the primary cause for this intestinal blockage is the primary lack of CFTR in the intestine (Stoltz, Rokhlina *et al*. 2013). Another intestinal lesion found in CF pigs is diverticulosis at the mesenterial side of the jejunum distended with meconium, caused by herniation of the tuna mucosa and submucosa through the hypertrophic tuna muscularis, predisposing the intestine to rupture (Meyerholz, Stoltz *et al*. 2010, Klymiuk, Mundhenk *et al*. 2012). Both of these pathological findings are also reported in human CF patients, however, with a lower incidence rate and less severity. Histopathological findings include the obstruction of duodenal glands with mucus, atrophy of the epithelium and mucinous hyperplasia that is more pronounced in the intestine distal to the site of obstruction, whereas no obvious signs of primary inflammation are found (Meyerholz, Stoltz *et al*. 2010).

In conclusion, pathological findings in all porcine CF models strongly resemble the pathology found in human CF patients, thereby making the porcine CF pig an ideal model organism for CF research. However, the CF pig is hampered by the fatal intestinal obstruction with meconium. Although many studies can be performed on tissue or cell cultures derived from neonatal CF piglets, an essential aspect of an ideal model organism is that it can reach adulthood and thereby allows for long-term studies regarding pathogenesis and evaluation of potential therapies. To overcome the lethal intestinal obstruction in CF piglets, several approaches from different kind of scientific views are imaginable or have already been tried.

Surgical approach

As mentioned above, MI is also a feature that occurs in about 15 % of human CF newborns and has to be treated vigorously to assure survival (van der Doef, Kokke *et al*. 2011). Depending on the severity of MI, therapeutic options range from initial treatments with enemas using gastrografin or N-acetyl-cystein to complex abdominal surgeries like anastomosis or enterostomy (Karimi, Gorter *et al*. 2011). In CF piglets, non-surgical treatment with laxatives alone is not enough to rescue the severe intestinal phenotype. To ensure their survival, they have to undergo ileostomy or cecostomy to bypass the obstruction. Perioperatively, piglets have to be treated supportively with intravenous fluids, analgesics and prophylactic antibiotics (Stoltz, Meyerholz *et al*. 2010). However, surgical correction of the MI is associated with a high rate of postoperative mortality in piglets; one of the reasons could be the long time between birth and surgery that is needed to obtain genotyping results. In order to shorten this interval, Guillon, Chevaleyre *et al*. (2015) have developed a new rapid method for the identification of CF piglets via CT scan. It has to be said, however, that a surgical correction is sometimes not feasible due to atretic parts of the large intestine and that very high surgery- and intensive care-related costs hinder the production of living CF piglets on a routine basis via this approach.

Transgenic approach

The idea to rescue the severe intestinal phenotype in CF animals by transgenic expression of *CFTR* under the control of a gut-specific promoter is not new. The transgenic CFTR protein is selectively expressed in the intestine, thereby correcting the obstructive phenotype that is caused by the lack of CFTR, and in no other organ systems. Therefore, transgenic CF animals should exhibit all the characteristic features of CF apart from intestinal disease. Already in 1994, Zhou, Dey *et al*. demonstrated that expression of human *CFTR*, driven by a rat fatty-acid binding protein promoter, corrected the lethal obstructive phenotype in CF mice and restored chloride secretion (Zhou, Dey *et al*. 1994). This concept was confirmed by Ostedgaard, Meyerholz *et al*. (2011) for a truncated CFTR protein, which might be applied by viral gene therapy. A transgenic approach also works for the porcine CF model, as piglets with selective expression of *CFTR* under the

control of the rat fatty-acid binding protein promoter are able to survive meconium ileus and develop lung disease and other typical organ manifestations over time. An expression rate of about 20 % of WT *CFTR* seems to be sufficient to rescue the intestinal phenotype; however, piglets still have to be treated supportively with gastrografin enemas to ensure survival (Stoltz, Rokhlina *et al*. 2013).

Contribution of genetic modifiers to disease severity

Studies on monozygotic and dizygotic human CF twin pairs have demonstrated that disease severity shows higher concordance in homozygous twins. This implies that the phenotypic manifestation of the basic mutation is influenced by additional genetic factors, so-called modifier genes (Bronsveld, Mekus *et al*. 2001). It is now known that modifier genes contribute to the variability of several features in CF – severity of obstructive lung disease, establishment of chronic infection with *P. aeruginosa*, risk for development of CFRD, low BMI and also neonatal MI (Cutting 2015). The heritability both for developing MI and the absence of MI is estimated to be 1.0. This finding indicates the high contribution of modifier genes responsible for increased susceptibility to MI as well as protection against MI (Blackman, Deering-Brose *et al*. 2006). Genome-wide analysis has revealed several potential candidate regions, including polymorphisms in the genes coding for several members of the solute transport family of proteins, SLC4A4, SLC6A14 and SLC26A9 (Dorfman, Li *et al*. 2009, Sun, Rommens *et al*. 2012). SNPs in the *MSRA* gene coding for the methionine sulfoxide reductase have a protective effect against MI, a hypothesis supported by the fact that mice lacking *MSRA* expression do not show the typical intestinal obstruction around weaning (Henderson, Doshi *et al*. 2012).

The high contribution of modifier genes to intestinal obstruction in humans and murine CF models permits the assumption that intestinal disease severity in CF pigs might also be modified. It has to be mentioned that there is no knowledge about the existence of modifier genes in the porcine genome that might modulate the CF phenotype. In addition, insights about potential candidate genes occurring in mice and humans cannot be directly adapted to the pig.

One of the possible candidate genes in the porcine genome is the *CLCA4b* gene encoding a member of the calcium-activated chloride channel regulator protein

family. In CF humans, *CLCA4* is known to modify the intestinal phenotype by modulation of residual chloride conductance (Kolbe, Tamm *et al*. 2013). A species-specific duplication of the corresponding *pCLCA4* gene occurs in the pig. In contrast to *CLCA4a, CLCA4b* is selectively expressed in small and large intestine epithelial crypts that are the only intestinal cell type to express CFTR, suggesting a potential involvement in the modulation of MI. In addition, a deleterious mutation in the *CLCA4b* gene occurs naturally with a high prevalence in the pig population without obviously affecting the phenotype in WT animals. This might be caused by the fact that carriers of this deletion bear a selective advantage over other animals (Plog, Klymiuk *et al*. 2015).

The aim of my thesis was to find a way to increase the life expectancy of the porcine CF model by evaluation of two different approaches to overcome the lethal intestinal phenotype in *CFTR*$^{-/-}$ piglets. In the first part of this study the impact of transgenic expression of *CFTR* in the intestine on the severity of meconium ileus in *CFTR*$^{-/-}$ piglets is examined with a special focus on expression analysis of *CFTR* and the gut-specific promoter *FABP2* at mRNA level. In addition, the porcine CF model is further characterized both at genomic and protein level. The second part of my thesis focuses on the role of modifier genes in the development of meconium ileus in *CFTR*$^{-/-}$ piglets. The influence of the candidate gene *CLCA4b* on meconium ileus is investigated and other candidate loci with a potential impact on the intestinal phenotype are screened for by a genome-wide analysis. In addition, mucociliary transport mechanisms in CF KO and WT piglets are examined.

III. ANIMALS, MATERIALS AND METHODS

1. Animals

The animals included in this work were wild type (WT), heterozygous *CFTR*$^{+/-}$ or homozygous *CFTR*$^{-/-}$ piglets generated by breeding of heterozygous female and male *CFTR*$^{+/-}$ pigs. In addition, *CFTR*$^{-/-}$ piglets carrying an additional transgene for the expression of *CFTR* under the control of the *FABP2* promoter were produced by somatic cell nuclear transfer (SCNT) followed by embryo transfer (ET). These piglets are designated as gut-modified *CFTR*$^{-/-}$ piglets in the following. For the generation of heterozygous *CFTR*$^{+/-}$ piglets, the *CFTR* locus on one allele in primary kidney cells of a 3-months-old male WT boar was targeted with a bacterial artificial chromosome (BAC) vector containing large regions of homology. This lead to the insertion of a STOP box and *neo*®/*kan*® resistance cassette adjacent to the start codon in exon 1. Correctly modified cell clones were used for SCNT and embryos transferred laparoscopically to estrus-synchronized gilts (Klymiuk, Mundhenk *et al*. 2012). All animal experiments were approved by the responsible animal welfare authority (Regierung von Oberbayern, AZ 55.2-1-54-2531-78-07, 55.2-1-54-2532-70-12 and 55.2-1-54-2532-163-2014).

2. Materials

2.1. Chemicals

2-Mercaptoethanol	Roth, Karlsruhe
2-Propanol	Roth, Karlsruhe
Acetic Acid (glacial)	Roth, Karlsruhe
Acrylamide (30 %)	BioRad, Munich
Agarose UltraPure™	Invitrogen, Karlsruhe
Albumin fraction V	Roth, Karlsruhe
Amersham™ ECL™ western blotting detection reagent	GE Healthcare, Munich
Ammonium persulfate (APS)	BioRad, Munich

Bicinchoninic acid	Sigma, Steinheim
Bromophenolblue	Roth, Karlsruhe and Merck, Darmstadt
Chloroform (Trichloromethane)	Roth, Karlsruhe
Complete proteinase inhibitor cocktail tablets	Roche Diagnostics, Mannheim
Coomassie® Brilliant Blue G250	Merck, Darmstadt
$CuSO_4$ (cupric sulfate)	Sigma, Steinheim
DAB (3.3' Diaminobenzidine tetrahydrochloride)	KemEnTec, Denmark
EDTA (Ethylenediaminetetraacetic acid)	Roth, Karlsruhe and VWR, Darmstadt
Ethanol	Roth, Karlsruhe
Ethidiumbromide (1 mg/mL)	Merck, Darmstadt
Formaldehyde solution, 37 %	Sigma, Steinheim
Formamide	Roth, Karlsruhe
Glycerin (Glycerol)	Roth, Karlsruhe and Sigma, Steinheim
Glycine	Roth, Karlsruhe
H_2O_2 (Hydrogen peroxide 37 %)	Roth, Karlsruhe
HCl (Hydrochloric acid 25 %)	VWR, Darmstadt
HCl (Hydrochloric acid, 37 %)	Roth, Karlsruhe
Histokitt	Glaswarenfabrik Karl Hecht, Sondheim/Rhön
KCl (Potassium chloride)	Merck, Darmstadt
KH_2PO_4 (Potassium dihydrogen phosphate)	Merck, Darmstadt
Mayer's Hemalum solution	Merck, Darmstadt
Methanol	Roth, Karlsruhe and Sigma, Steinheim
$MgCl_2$ (Magnesium chloride)	Fluka Chemie, Schweiz
MOPS (3-(*N*-morpholino) propanesulfonic acid)	Roth, Karlsruhe
Na_2HPO_4 (Di-sodiumhydrogenphosphate-2-hydrate)	Merck, Darmstadt
NaCl (Sodium chloride)	Merck, Darmstadt
NaOH (Sodium hydroxide 2N)	Roth, Karlsruhe and VWR, Darmstadt

Paraformaldehyde	Sigma, Steinheim
Perfadex®	XVIVO Perfusion, Sweden
Ponceau S	Sigma, Steinheim
Roti-Histofix 4 %	Roth, Karlsruhe
SDS (Sodium dodecyl sulfate)	Serva Electrophoresis, Heidelberg
Sucrose	Sigma, Steinheim
SuperBlock (PBS) blocking buffer	Thermo Scientific, Schwerte
Target Retrieval Solution	Dako, Hamburg
Temed (Tetraethylethylenediamine)	Roth, Karlsruhe
Tissue-Tek® O.C.T Compound	Sakura, Staufen
Tris (Tris-(hydroxymethyl)-aminomethane)	Roth, Karlsruhe
Tri-sodium citrate dihydrate	Roth, Karlsruhe
Triton X-100	Roth, Karlsruhe
TRIzol® Reagent	Thermo Scientific, Schwerte
Tween®20	Sigma, Steinheim
Universal Agarose	Bio&SELL, Nürnberg
Vectashield Antifade Mounting Medium with DAPI	Vector Laboratories, USA
w/v nonfat dry milk (blotting grade)	Roth, Karlsruhe
Xylene	VWR, Darmstadt
Xylene cyanole	Roth, Karlsruhe

2.2. Consumables

Amersham™ Hyperfilm™ ECL high performance chemiluminescense film	GE Healthcare, Munich
Centrifuge tubes (15 mL, 50 mL)	Falcon, Becton Dickinson, Heidelberg
Cover slips for histology	Roth, Karlsruhe
Disposable plastic pipettes	Falcon, Becton Dickinson, Heidelberg
Disposal polypropylene bags	Sarstedt AG+Co, Nümbrecht
EDTA Monovette® blood collection system	Sarstedt, Nümbrecht

Gel blotting paper (Whatman paper)	BioRad, Munich
Glass Pasteur pipettes	Brand, Wertheim
Immobilon®-P nitrocellulose transfer membranes	Millipore, Billerica, USA
LightCycler® 480 Multiwell Plates 96	Roche Diagnostics, Mannheim
LightCycler® 480 Sealing Foil	Roche Diagnostics, Mannheim
Microscope slides Star Frost®	Engelbrecht, Edermünde
OP-Cover (60 × 90 cm)	A. Albrecht, Aulendorf
Parafilm® M	American Can Company, USA
PCR reaction tubes (0.2 mL)	Brand, Wertheim
Pipet tips	Eppendorf, Hamburg
Pipet tips with filter	Thermo Scientific, Schwerte
Prot, Elec^{TM} tips	BioRad, Munich
SafeGrip® latex gloves	SLG, Munich
Safe-Lock reaction tubes (1.5 mL, 2 mL)	Eppendorf, Hamburg
Saran Barrier food wrap	Dow, USA
Sempercare® nitrile gloves	Satra Technology Center, USA
Tissue culture dishes (60 mm × 15 mm)	Sarstedt, Nümbrecht
Tissue culture plate, 96 well	Falcon, Becton Dickinson, Heidelberg
Uni-Link embedding cassettes	Engelbrecht, Edermünde

2.3. Devices

Accu-jet® pro pipette controller	Brand, Wertheim
Agarose gel electrophoresis chamber	WG - Biotech, Ebersberg and OWL Inc., USA
Autotechnikon Histomaster 2050/Dl	Bavimed, Birkenau
Axiovert 200 M	Zeiss, Oberkochen
Benchtop 96 tube working rack	Stratagene, USA
Chyo Petit Balance MK-2000B	YMC Co, Japan
CryoStar NX70	Thermo Scientific, Schwerte
Eppendorf Centrifuge 5415 D	Eppendorf, Hamburg
Eppendorf Centrifuge 5417 R	Eppendorf, Hamburg

Eppendorf Centrifuge 5810 R	Eppendorf, Hamburg
Gel documentation system	BioRad, Munich
GeneQuant Pro spectrophotometer	Thermo Scientific, Schwerte
HM 315 microtome	Microm, Walldorf
Homogenizer ART-Micra D-8	ART, Müllheim
Hybridization oven	Bachofer, Reutlingen
Incubator	Memmert, Schwabach
inoLab® pH meter 7110	WTW, Weilheim
Labcycler	SensoQuest, Göttingen
LightCycler® 96	Roche Diagnostics, Mannheim
Mastercycler® gradient	Eppendorf, Hamburg
Mettler PM 6000	Mettler - Toledo, Gießen
Microwave	DAEWOO, Korea
Mini-Protean Tetra Cell	BioRad, Munich
Optimax X-ray Film processor 1170-1-0000	PROTEC, Oberstenfeld
Pipettes (1000 µL, 200 µL, 20 µL, 10 µL, 2 µL)	Gilson Inc, USA
Polytron homogenizer PT 2500E	Kinematica, Switzerland
Power Pac 300 gel electrophoresis unit	BioRad, Munich
Power Station 300 gel electrophoresis unit	Labnet International, USA
RH Basic heating plate with magnetic stirrer	IKA, Staufen
Select vortexer	Select BioProducts, USA
Sunrise™ microplate reader for ELISA	Tecan, Austria
TBS 88 paraffin embedding system	Medite, Burgdorf
Thermomixer 5436	Eppendorf, Hamburg
Trans Blot® SD Semi-Dry transfer cell	BioRad, Munich
Varioklav 400 autoclave	H+P Labortechnik, Oberschleißheim
WB 6 water bath	Preiss-Daimler Group, Puschwitz
X-ray cassette	Rego, Augsburg

2.4. Antibodies, drugs, enzymes and oligonucleotides

Primary antibodies

Monoclonal mouse anti-CFTR, clone CF3	abcam, UK
Monoclonal mouse anti-CFTR; Antibody 528	CF Foundation, USA
Monoclonal mouse anti-CFTR; Antibody 570	CF Foundation, USA
Monoclonal mouse anti-CFTR; Antibody 596	CF Foundation, USA
Monoclonal mouse anti-CFTR; Antibody 660	CF Foundation, USA
Monoclonal mouse anti-CFTR; Antibody 769	CF Foundation, USA
Monoclonal mouse anti-human CFTR; clone #24-1	R&D Systems, Wiesbaden
Polyclonal goat anti-CFTR; N-20	Santa Cruz, Heidelberg
Polyclonal rabbit anti-CFTR; #2269	Cell Signaling, Frankfurt am Main
Polyclonal rabbit anti-CFTR; H-182	Santa Cruz, Heidelberg

Secondary antibodies

Biotinylated goat anti-mouse IgM; BA-2020	Vector Laboratories, USA
Biotinylated goat anti-rabbit IgG; BA-1000	Vector Laboratories, USA
Biotinylated polyclonal AffiniPure goat-anti-mouse IgG	Jackson ImmunoResearch, USA
Biotinylated polyclonal goat anti-mouse IgG, #E0433	Dako, Hamburg
Biotinylated rabbit anti-goat IgG, BA-5000	Vector Laboratories, USA
HRP-conjugated goat anti-rabbit IgG	Cell Signaling, Frankfurt am Main
HRP-conjugated polyclonal AffiniPure mouse anti-goat IgG	Jackson ImmunoResearch, USA
HRP-conjugated polyclonal goat anti-mouse IgG	Dianova, Hamburg
Alexa Fluor 488-conjugated AffiniPure donkey anti-mouse IgG	Jackson ImmunoResearch, USA

Drugs

Altrenogest (Regumate®)	Serumwerke Bernburg, Bernburg
Azaperon (Stresnil®)	Janssen Pharmaceutica, Belgium
Choriongonadotropine (hCG) (Ovogest®)	Intervet, Unterschleißheim
Cloprostenol (Estrumate®)	Intervet, Unterschleißheim
Diatrizoate meglumine and diatrizoate sodium solution (Gastrografin®)	Bayer Health Care AG, Leverkusen
Embutramid, Mebezonium, Tetracain (T61®)	Intervet, Unterschleißheim
Glucose solution 50 %	B. Braun, Melsungen
Ketamine hydrochloride (Ursotamin®)	Serumwerke Bernburg, Bernburg
Omeprazol (OMEP®)	Hexal AG, Holzkirchen
Pancreatin (Eurobiol®)	Laboratoires Mayoli Spindler, France
PMSG (Intergonan®)	Intervet, Unterschleißheim
Potassium chloride solution 7.5 %	B. Braun, Melsungen
Sodium chloride solution 0.9 % ad us. vet.	B. Braun, Melsungen

Enzymes

BigDye® Terminator v3.1	Applied Biosystems, Weiterstadt
DNase I, RNase-free (1 U/µL)	Thermo Scientific, Schwerte
FastStart Essential DNA Green Master	Roche Diagnostics, Mannheim
Proteinase K, ready to use	Dako, Hamburg
RevertAid H Minus Reverse Transcriptase (200 U/µL)	Thermo Scientific, Schwerte
SuperScript® III Reverse Transcriptase (200 U/µL)	Thermo Scientific, Schwerte
Taq DNA Polymerase (5 U/mL)	Agrobiogen, Hilgertshausen
Uracil N-Glycosylase (UNG) (1 U/µL)	Thermo Scientific, Schwerte

Oligonucleotides

All oligonucleotides were designed with the PrimerQuest Tool by IDT and were purchased from Thermo Scientific, Schwerte.

CFTR3f	5-GAC AGT ACT GCT TAG TGG TCA G-3
CFTR3r	5-CAG ATC TAG AAT TCT GGT ATG-3
Neo3f	5-GAG AAC CTG CGT GCA ATC CAT C-3
Neo2f	5-GAG ATG AGG AAG AGG AGA ACA G-3
CFTR2f	5-GAT CTG CTA CTT AGT AGT TAC TG-3
CFTR2r	5-CAA TTC CTC AAG TAC AGA TC-3
Cg1f	5-AAT GAC ATC ACE GCA GGT CAG A-3
Cg2f	5-AGA AGA GTA GGG CCT TTG GCA T-3
Cg1r	5-TGG CTG AAC TGA GCG AAC AAG T-3
Cg2r	5-ATT CCA CCA CTG CTC CCA TTC A -3
Cg3r	5-TGG CTC ATC ACA TGC AAA GCA G-3
Cg4r	5-CCT CCA GTA TGT GTG CCA AGA A-3
Cg5r	5-AGC ACA TGT GGG TCT TAG AGT ACG-3
STOPr	5-CCA ATT ATG TCA CAC CAC AG-3
CFTR7118rv	5-GAG AAG ATG CTG GCC TTT TCC-3
CFTR5armf	5-TGA GCA GTT TGT CTG GAG CAT-3
CFTR7160rv	5-TCC AAA GCT CAG CTA GAC ACC-3
pACT954f	5-CGC TCG TGG TCG ACA ACG-3
pACT1919r	5-CTG GAT GGC CAC GTA CAT G-3
FEqf1	5-TGG CAT TTG ATG GTG CCT GGA A-3
FEqf2	5-TGC CTG GAA GAT AGA CCG CAA T-3
FEqf3	5-ACG GAA CTG AAC TCA CTG GGA A-3
FEqr1	5-GCT GCA AGT TTC CTC TTT ACC ACG-3
FEqr2	5-GTC ATG AGC TGC AAG TTT CCT C-3
FEqr3	5-TTC CCA GTG AGT TCA GTT CCG T-3
FEqr4	5-TGG GCT GTG CTC CAA GAA CAA T-3
CEqf1	5-AGA GTC ACA AGA GAG CCC ATC A-3
CEqf2	5-ACA TCC CTT CTC TGG GAA ATG GGT-3
CEqf3	5-AGT GAA CGT GTC TGC TGC CAG TAA-3
CEqr1	5-ACT TAC TGG CAG CAG ACA CGT T-3

CEqr2	5-TGC CTG GAG CTT CTG TGG TAA GAA-3
CEqr3	5-ACA TCT ACC TGT AGT GCC CAG A-3
Lars1f	5-CCT GGC AAG CTT GAT TTT G-3
Lars1ra	5-CTA AAG TCT TGT TTC TTG C-3
Lars2f	5-AAC CTG AAC AAG TTT GAT GAA G-3
Lars2r	5-AAG GCA AGT CCA CAG AAG GC-3
CFgutf1	5-CCG TGA ATG TGG ACG AAGT-3
CFgutr1	5-TCG AGC TCC TAA TGC CAA AG-3
CFgutf2	5-GAA GAA GAG GTG CAA GAA ACA AG-3
CFgutr2	5-CTG GCA ACT AGA AGG CTC AG-3
CFgutf3	5-TGA AGG AGG AAA CAG AAG AAG AG-3
CFgutr3	5-CAG ATG GCT GGC AAC TAG AA-3
CFgutf4	5-TTC TAG TTG CCA GCC ATC TG-3
CFgutr4	5-TAG GAA AGG ACA GTG GGA GT-3
CLCA4b1f	5-GAG AGG TAT TCA AGG CCA CTT AG-3
CLCA4b2f	5-TTC CAC ATG CTA CAG GAA GAA A-3
CLCA4b3f	5- CAG CTT GGA TCT GGC ATT ACT-3
CLCA4b1r	5- CTC CTC TGT ACG TCT CCT GTT A-3
CLCA4b2r	5- GAG GGC CTT AGG AAG AGA GA-3
CLCA4b3r	5-CAC AGC ACC TTC AGA GTT GA-3

2.5. Buffers and solutions

Water deionized in a Millipore device (EASYpure® II, pure aqua, Schnaitsee) and termed as aq. bidest. was used as solvent. All buffers and other solutions were stored at room temperature if not indicated otherwise.

Buffers and solutions for PCR and agarose gels

DNA loading buffer (10 ×)

10 % glycerol in aq. bidest.

1 spatula tip of Bromophenol Blue

Add 0.5 M NaOH until color turns blue.

Stored aliquoted at 4 °C.

dNTP-mix

2 mM dATP, dCTP, dGTP, dTTP

Mixed in aq. bidest.

Stored aliquoted at -20 °C.

TAE buffer (50 ×)

242 g 2 M Tris

100 mL 0.5 M EDTA (pH 8.0)

57 mL glacial acetic acid

Ad 1000 mL aq. bidest.

Buffer solution was filtrated and autoclaved for storage.

Before usage, the buffer solution was diluted to single concentration.

Gene Ruler^{TM} 1 kb DNA molecular weight standard

100 µL Gene Ruler^{TM} 1 kb DNA molecular weight standard

100 µL 6 × loading dye

400 µL aq. bidest.

Stored aliquoted at -20 °C.

Sequencing buffer (5 ×)

17.5 mL 1 M Tris/HCl (pH 9.0)

125 µL 1 M $MgCl_2$

Ad 50 mL aq. bidest.

Stored aliquoted at -20 °C.

Buffers and solutions for RNA isolation and cDNA synthesis

10 mM Tris/HCl pH 8.0

10 mM Tris

Adjust pH to 8.0 with HCl.

10 mM dNTPs

10 mM dATP, dCTP, dGTP, dTTP

Mixed in aq. bidest.

Stored aliquoted at -20 °C.

25 × MOPS

2 M MOPS

500 mM NaOAc

10 mM EDTA

Mixed in aq. bidest.

Stored in the dark at 4 °C.

RNA denaturating buffer

750 µL formamide

250 µL formaldehyde

150 µL 25 × MOPS

116 µL glycerol 86 %

122 µL bromophenol blue 0.25 %

122 µL xylene cyanole 0.25 %

6 µL EtBr

Stored aliquoted at -80 °C.

Buffers and solutions for fixation and immunological detection

Methacarn

60 % methanol

30 % chloroform

10 % acetic acid (glacial)

Prepared freshly, stored in the dark.

4 % PFA solution

4 % PFA

1 × PBS buffer

Solution was heated to 50 °C in a water bath and was vigorously shaken several times. For complete dissolution of PFA, 200 µL of 5 M NaOH were added to raise the pH. After cooling down to room temperature, the solution was adjusted to pH 7.4 with HCl, filtered and stored at 4 °C.

2 % PFA solution

2 % PFA

1 × PBS buffer

Solution was heated to 50 °C on a warming plate and mixed with a magnetic stirrer. For complete dissolution of PFA, 200 µL of 5 M NaOH were added to raise the pH. After cooling down to room temperature, the solution was adjusted to pH 7.4 with HCl, filtered and stored at 4 °C.

30 % sucrose

300 g sucrose

Ad 1000 mL aq. bidest.

After filtration the solution was stored at 4 °C.

Citrate buffer

10 mM sodium citrate pH 6

0.05 % Tween 20

Sodium citrate and aq. bidest. were mixed and pH was adjusted to 6 with HCl. Tween 20 was added and the solution was mixed well.

10 × TBS buffer for IHC

90 g NaCl

60.5 g Tris

Ad 1000 mL aq. bidest.

Adjusted to pH 7.6.

Concentrated stock solution of buffer was autoclaved and diluted to single concentration with aq. bidest. before use.

DAB solution

One tablet DAB was dissolved in 10 mL aq. bidest. in the dark and was shaken several times.

Aliquots were stored at -20 °C.

Buffers and solutions for Western Blots

Laemmli buffer (5 ×)

65.5 mL 1 M Tris pH 6.8

100 mL Glycerol (100 %)

2 mL 0.5 M EDTA pH 8

20 g SDS

0.01 % bromophenol blue

Ad 200 mL aq. bidest.

PBS buffer (10 ×)

136 mM NaCl

8.1 mM Na_2HPO_4

2.7 mM KCl

1.5 mM KH_2PO_4

Adjusted to pH 7.4.

After filtration, buffer solution was autoclaved and diluted to single concentration with aq. bidest. before use.

Complete Proteinase inhibitor solution (25 ×)

One tablet was dissolved in 2 mL aq. bidest. to obtain a 25 × stock solution.

Stored at 4 °C and used within 12 weeks.

Protein extraction buffer (1 × Laemmli)

2 mL 1 M Tris (pH7.5)

2 mL Triton X-100

20 mL 5 × Laemmli buffer

4 mL 25 × Complete proteinase inhibitor solution

76 mL aq. bidest.

Ponceau S solution

0.2 g Ponceau

3 mL glacial acetic acid

Ad 100 mL aq. bidest.

SDS running buffer (10 ×)

30.3 g Tris

144 g glycine

10 g SDS

Ad 1000 mL aq. bidest.

Stored at 4 °C.

Buffer was diluted to single concentration with aq. bidest. before use.

Transfer buffer (10 ×)

58 g Tris

29 g glycine

3.7 g SDS

Ad 1000 mL aq. bidest.

Stored at 4 °C.

Transfer buffer (1 ×)

20 mL 10x Transfer buffer

140 mL aq. bidest.

40 mL methanol

Prepared freshly.

TBS buffer for WB (10 ×)

80 g NaCl

30 g Tris

Ad 1000 mL aq. bidest.

Adjusted to pH 7.4.

Concentrated stock buffer was autoclaved.

TBS-T (0.1 %) (1 ×)

100 mL 10x TBS

1 mL Tween-20

Ad 1000 mL aq. bidest.

TBS-T-BSA

0.1 % TBS-T

5 % BSA

TBS-T-w/v nonfat dry milk

0.1 % TBS-T

5 % w/v nonfat dry milk

Elution buffer

62.5 mM Tris/HCl pH 6.7

2 % SDS

100 mM 2-mercaptoethanol

2.6. Kits

Direct-zol™ RNA MiniPrep Kit	Zymo Research, Freiburg
Double Pure Kombi Kit	Bio&SELL, Nürnberg
Easy-DNA™ Kit	Invitrogen, Karlsruhe
Isohelix DDK DNA Isolation Kit	Cell Projects Limited, UK
Nexttec™ Genomic DNA Isolation Kit	Nexttec GmbH, Leverkusen
Vectastain ABC Komplex	Vector Laboratories, UK

2.7. Other reagents

0.1 M DTT for cDNA synthesis	Thermo Scientific, Schwerte
10 × PCR buffer	Agrobiogen, Hilgertshausen
10 × DNase reaction buffer with $MgCl_2$	Thermo Scientific, Schwerte
5 × First-Strand buffer for cDNA synthesis	Thermo Scientific, Schwerte
5 × RevertAid reaction buffer	Thermo Scientific, Schwerte

6 × DNA loading dye	Thermo Scientific, Schwerte
Bovine serum albumin (BSA) fraction V	Roth, Karlsruhe
dNTPs (dATP, dCTP, dGTP, dTTP)	Thermo Scientific, Schwerte
Gelatin from cold water fish skin	Sigma, Steinheim
Gene Ruler^{TM} (1 kb DNA ladder) DNA molecular weight standard	Thermo Scientific, Schwerte
Oligo (dT) primer	Thermo Scientific, Schwerte
PageRuler^{TM} prestained protein ladder	Thermo Scientific, Schwerte
Random primer hexamers (600 µg/µL)	Thermo Scientific, Schwerte
RiboLock RNase inhibitor (40 U/µL)	Thermo Scientific, Schwerte
Serum (goat, rabbit, pig)	MP Biomedicals, France
Unstained protein molecular weight marker	Thermo Scientific, Schwerte

2.8. Software

BioEdit Sequence Alignment Editor
FinchTV Version 1.3.1, Geospiza Inc.
GraphPad PRISM version 5.02
LightCycler® 96 Application Software 1.1.0.1320
ImageJ 1.49m, National Institutes of Health, USA
AxioVision 4.0, Carl Zeiss Microscopy

3. Methods

3.1. Production of *CFTR*$^{-/-}$, *CFTR*$^{+/-}$ and WT piglets by breeding

Male *CFTR*$^{+/-}$ piglets generated by SCNT were grown to maturity and mated to female WT sows. Female and male *CFTR*$^{+/-}$ offspring were kept as a breeding herd and selectively mated to each other to produce litters with WT, *CFTR*$^{+/-}$ and *CFTR*$^{-/-}$ piglets. Female *CFTR*$^{+/-}$ gilts were either estrus-synchronized by oral administration of altrenogest (5 mL/animal) over a period of at least 15 days or mated when estrus appeared naturally. Pregnancy was controlled in regular intervals of about 3 weeks via medical ultrasonic and birth routinely induced by i.m. injection of 2 mL of cloprostenol on day 113 of the pregnancy.

Sows farrowed usually between 24 and 36 hours after the cloprostenol injection and were surveyed during the birth process.

3.2. Generation of gut-modified *CFTR*$^{-/-}$ founder animals

Gut-modified *CFTR*$^{-/-}$ piglets were generated by additive gene transfer followed by SCNT and ET. For this purpose, an expression vector constructed by N. Klymiuk, Chair for Molecular Animal Breeding and Biotechnology, LMU Munich was transfected into the primary kidney cells of *CFTR*$^{-/-}$ piglets. The DNA construct consisted of a 1.2 kb fragment of the porcine Fatty-acid Binding protein 2 (*FABP2*) promoter, a 215 bp long part of the porcine β-hemoglobin (*HBB)* gene, the 4.8 kb coding region of the porcine *CFTR* followed by the 277 bp long polyadenylation signal of the bovine Growth Hormone *(bGH*) gene and a *puromycin*® resistance cassette.

Stable transfected pooled cell clones were recognized by positive antibiotic selection, taken as donors for SCNT using in vitro matured oocytes and cloned embryos laparoscopically transferred to gilts (Kurome, Kessler *et al*. 2015). An overview of the routine workflow is given in Figure 1. Gilts were pre-synchronized by oral administration of altrenogest for at least 15 days, i.m. injection of 750 IU of PMSG 36 hours after the last altrenogest administration and i.m. injection of 750 IU of hCG 3 days after PMSG injection. ET was performed about 36 hours after hCG injection. Pregnancy was confirmed by ultrasonic examinations in regular intervals and birth routinely induced by 2 mL i.m. injection of cloprostenol on day 114 of the pregnancy. Piglets with a promising phenotype could be recloned by explantation of the euthanized animal's kidney and establishment of cell cultures of cells from this kidney that could be used for NT and SCNT.

Cell culture experiments were executed by A. Wünsch, Chair for Molecular Animal Breeding and Biotechnology, LMU Munich; SCNT and ET were performed by M. Kurome, B. Kessler, V. Zakhartchenko and T. Güngör, Chair for Molecular Animal Breeding and Biotechnology, LMU Munich.

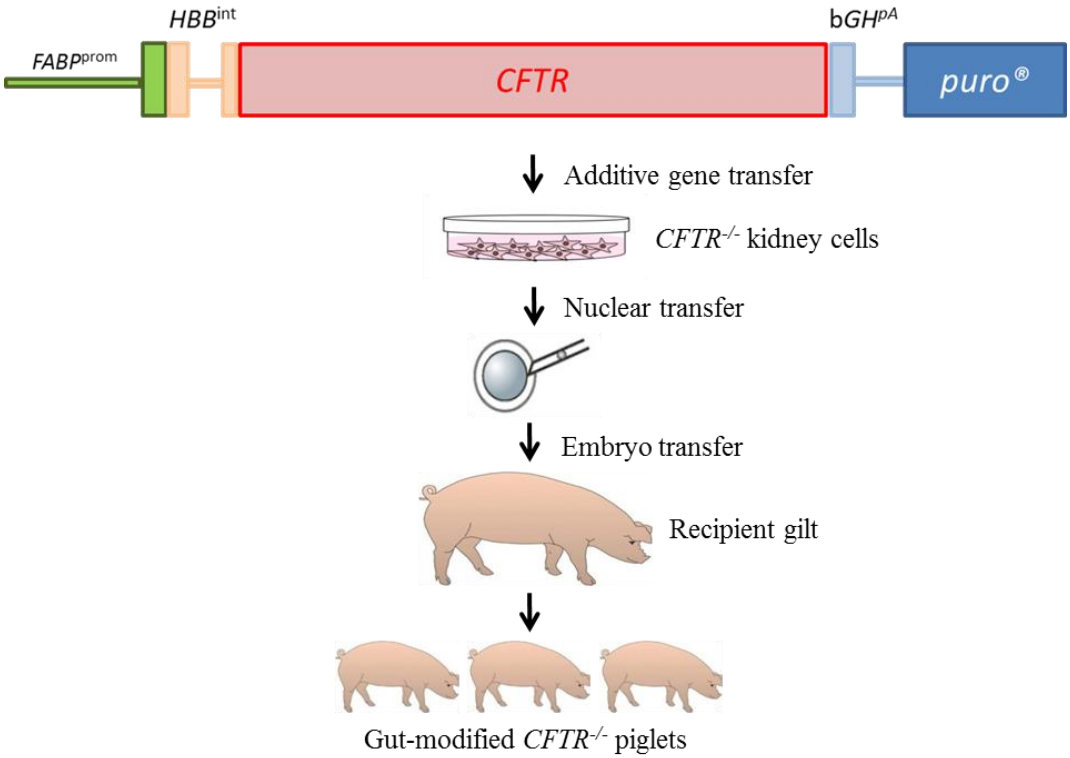

Figure 1: Generation of gut-modified *CFTR*$^{-/-}$ piglets. *CFTR*$^{-/-}$ kidney cells transfected with the transgenic DNA construct are used for somatic cell nuclear transfer and embryo transfer.

3.3. Management of neonatal gut-modified *CFTR*$^{-/-}$ piglets

After delivery, gut-modified *CFTR*$^{-/-}$ piglets were kept under 24 h surveillance and supportive treatments were undertaken to increase the probability of removing meconium ileus. The piglets were weighed immediately after birth, received ear marks for identification and their tails were docked to serve as material for genotyping. All piglets were treated with repeated gastrografin enemas every 8 h to facilitate deposit of meconium, received omeprazol as gastric protection every 12 h and pancreatic enzymes were substituted every 24 h using pancreatin. For circulation support, prewarmed 0.9 % NaCl / 5 % glucose / 0.2 % KCl was given every 4 h via stomach tube. If the piglets were not able to drink themselves, the sow was milked and the animals were fed at least 20 mL of milk via stomach tube every two hours to ensure colostrum intake. Every 2 h, the general condition of the piglets was checked with special attention to motility, defecation and abdominal pressure.

Piglets were treated according to this protocol:

Table 1: Treatment protocol for gut-modified *CFTR*$^{-/-}$ piglets.

Birth	• Earmarks and tail docking • Weighing • Ensuring colostrum intake • 1 mL gastrografin enema
Birth + 4 h	• 10 crushed grains of Eurobiol® and half the content of one capsule of OMEP® are mixed with 20 mL 0.9 % NaCl / 5 % glucose / 0.2 % KCl and fed via stomach tube
Birth + 8 h	• 20 mL 0.9 % NaCl / 5 % glucose / 0.2 % KCl via stomach tube • 1 mL gastrografin enema
Birth + 12 h	• 20 mL 0.9 % NaCl / 5 % glucose / 0.2 % KCl via stomach tube
Birth + 16 h	• 10 crushed grains of Eurobiol® in 20 mL 0.9 % NaC l/ 5 % glucose / 0.2 % KCl via stomach tube • 1 mL gastrografin enema
Birth + 20 h	• 20 mL 0.9 % NaCl / 5 % glucose / 0.2 % KCl via stomach tube
Birth + 24 h	• 20 mL 0.9 % NaCl / 5 % glucose / 0.2 % KCl via stomach tube • 1 mL gastrografin enema • Weight control

If the general condition of a piglet started to deteriorate considerably without any signs of meconium removal and the piglet showed a bloated, pear-shaped, hard abdomen, the piglet was anaesthetized i.m. with ketamine hydrochloride (2 mL/10 kg BW) and azaperone (0.5 mL/kg BW) followed by euthanization via i.c. injection of Embutramid, Mebezonium, Tetracain (1 mL/10 kg BW).

3.4. Necropsy of CF piglets

In order to compare intestinal phenotypes and expression patterns, samples were taken from gut-modified *CFTR*$^{-/-}$, WT, *CFTR*$^{+/-}$ and *CFTR*$^{-/-}$ piglets. After euthanization, a series of pictures was taken to document the severity of the intestinal phenotype, including pictures of the opened abdomen, the intestinal convolute in whole and the intestine laid out in full length. A range of organ samples were taken for expression analysis at protein and RNA level. Tissue

samples were collected from the lung, trachea, heart, liver, kidney, pancreas and from different parts of the intestine (duodenum, proximal and distal jejunum, ileum and colon).

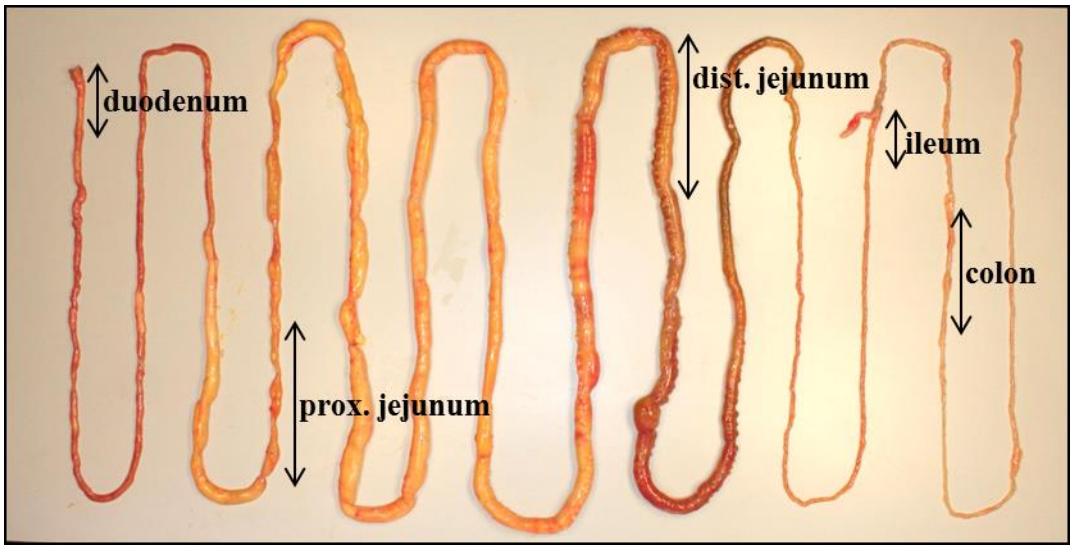

Figure 2: Sampling of the intestine. The different parts of the intestine used for sample collection are defined as follows: The duodenum reaches from pylorus to the plica duodenocolica; samples from the proximal and distal jejunum were collected within the first and the last third, respectively; the ileum is defined by the length of the plica ileocaecalis and colon samples were taken from the gyri centripetales of the colon ascendens.

For RNA and protein isolation purposes, organ samples were cut into small pieces and quick-frozen on dry ice as fast as possible to prevent degradation. Samples were wrapped in tin foil and stored at -80 °C until further examination. After the sampling of each organ, the surgical instruments were disinfected with 70 % ethanol to prevent contamination.

For immunological detection of CFTR on cryo-sections, tissue was frozen in two different ways. In the first freezing method, organs were cut into thin slices with a sharp scalpel knife, embedded in cryo-molds containing optimal cutting temperature (OCT) compound and frozen quickly on dry ice. The second freezing method consisted of a fixation step of the tissue block in 2 % PFA at RT for 1 h, followed by incubation in ice-cold 30 % sucrose overnight. The next day, tissue slides were embedded in OCT in cryo-molds and quick-frozen in a

70 % ethanol/dry ice bath. Until further processing, cryo-molds were stored at -80 °C.

For immunological detection of CFTR in paraffin sections, 1 cm × 1 cm × 1 cm blocks were cut out of organs with a sharp scalpel knife and put in falcons containing either methacarn solution or Roti-Histofix 4 % for fixation. Falcons containing methacarn solution had to be stored on ice protected from light. About 6 h after collecting the samples, the tissue blocks were cut into thin slices with a sharp microtome knife and the slices were put into embedding cassettes for further fixation in the respective fixation solution. After about 24 h, cassettes in methacarn solution were transferred directly to 70 % ethanol while cassettes in 4 % PFA were first watered with tap water for 30 min, then watered with aq. dest. for 30 min and finally transferred to 70 % ethanol. Cassettes were stored in 70 % ethanol until embedding in paraffin.

3.5. Preparation of the airways explanted from WT and *CFTR*$^{-/-}$ piglets for experiments on mucociliary transport

Before starting, the transport solution Perfadex® was prepared by adjusting the pH to 7.4 with 1 M Tris solution. Piglets were anaesthetized i.m. with ketamine hydrochloride (2 mL/10 kg BW) and azaperone (0.5 mL/kg BW), followed by euthanization via i.c. injection of Embutramid, Mebezonium, Tetracain (1 mL/10 kg BW) (Figure 3 (1)). The thorax was opened (Figure 3 (2)) and, starting from the larynx, the trachea, the lungs and the heart were explanted (Figure 3 (3)). The heart and the mediastinum containing the esophagus and big blood vessels were removed, while repeatedly bathing the airways in Perfadex® solution (Figure 3 (4)). Pulmonary tissue was carefully pulled away with forceps in a petri dish filled with Perfadex® (Figure 3 (5)) until only the bronchial system was left (Figure 3 (6 and 7)). Airways were sent in 50 mL falcons containing Perfadex® solution at 4 °C to the Mucin Biology Group, Gothenburg for further analysis (Figure 3 (8)).

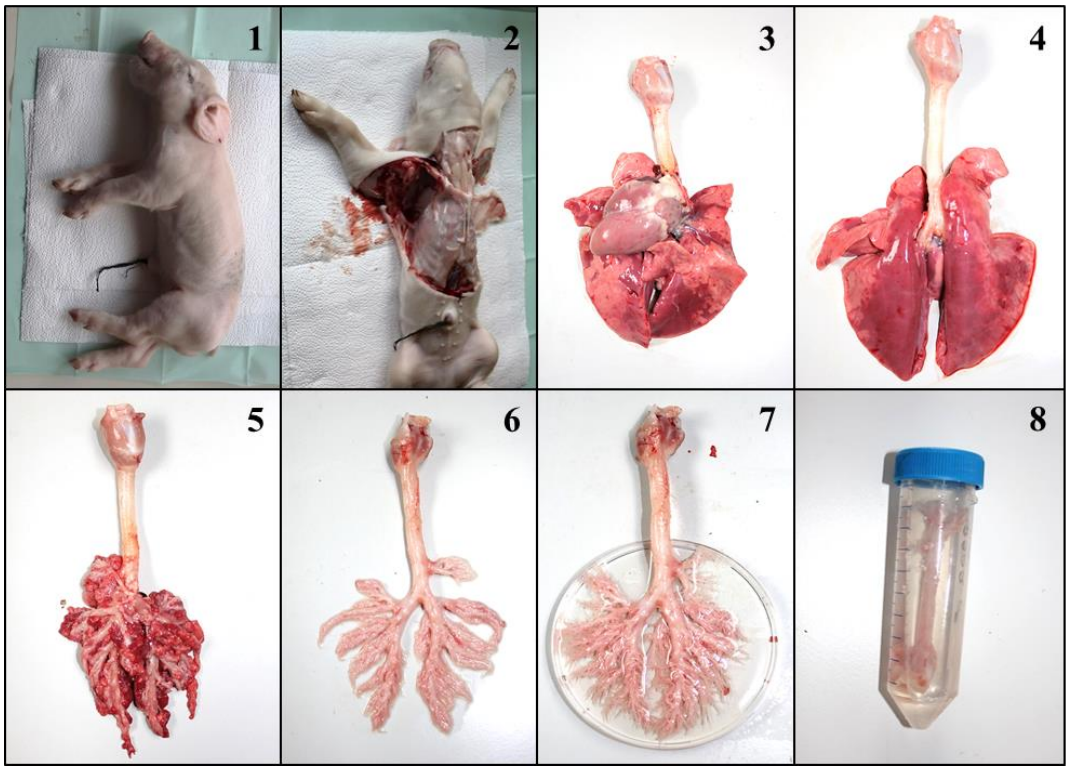

Figure 3: Preparation of the airways.

All experiments on WT and CF KO tracheas were performed by Anna Ermund from the Mucin Biology Group at the University of Gothenburg.

For video microscopy imaging of living tissue, tracheas were mounted in a petri dish containing Krebs buffer aerated with 95 % O_2 /5 % CO_2 (10 mM glucose, 5.1 mM Na-glutamate, 5.7 mM Na-pyruvate, 116 mM NaCl, 1.3 mM $CaCl_2$, 3.6 mM KCl, 1.4 mM KH_2PO_4, 23 mM $NaHCO_3$, and 1.2 mM $MgSO_4$, pH 7.4). Mucus was stained with Alcian blue 8GX. Time lapses were acquired on a Nikon stereo microscope and a Nikon color camera and strand velocity was calculated using the program NIS elements.

For Muc5b and Muc5ac antibody staining, WT and CF KO airways were fixed in 4 % PFA, paraffin embedded, sectioned and then used for immunofluorescence microscopy. The rabbit anti-Muc5b antibody was a kind gift from Dr. Mehmet Kesimer, UNC Chapel Hill and the Muc5ac antibody was the mouse monoclonal antibody clone 45M1 purchased from Sigma Aldrich. Secondary antibodies were donkey anti-rabbit Alexa Fluor 488 and donkey anti-mouse Alexa Fluor 555 (Thermo Scientific, Schwerte). Images were acquired with an upright LSM 700 Axio Examiner 2.1 confocal imaging system.

For scanning electron microscopy (SEM), WT and CF KO airways were fixed in Karnovsky fixative (2 % paraformaldehyde and 2.5 % glutaraldehyde in 0.05 M sodium cacodylate buffer, pH 7.2) for 24 h. Specimens for SEM were dehydrated in ethanol followed by immersion in hexamethyldisilazane and evaporation in a fume hood. The dried specimens were mounted on stubs and sputter-coated with palladium before examination in a Zeiss 982 Gemini field emission scanning electron microscope.

3.6. Analysis at the genomic level

As the state of health of *CFTR*$^{-/-}$ piglets started to deteriorate after about 12 h post-partum because of failure to remove meconium, a very fast genotyping protocol had to be established to differentiate between genotypes, including rapid DNA isolation and a time-saving genotyping Polymerase Chain Reaction (PCR).

3.6.1. Genotyping of piglets

Three DNA isolation procedures using different starting materials were compared in order to establish the fastest and most reliable protocol.

Isolation of genomic DNA from tails

Genomic DNA from freshly docked tails of newborn piglets was isolated using the nexttec™ Genomic DNA Isolation Kit from Tissue and Cells (nexttec GmbH, Leverkusen) according to the manufacturer's instructions. A very small amount of tissue (about 3 small pieces with a diameter < 1 mm) was incubated in lysis buffer in a 2 mL Eppendorf tube using a thermomixer with 1,200 rpm at 60 °C for 30 min. 3 µL DTT were added to each sample to ensure proper lysis and to increase the DNA yield. The sample was vortexed vigorously several times to accelerate the lysis of tissue pieces. After 30 min, the lysate was purified on an equilibrated cleaning column and the eluate containing the purified DNA was immediately used for PCR.

Isolation of genomic DNA from buccal swabs

The Isohelix DDK DNA Isolation Kit (Cell Projects Limited, UK) was employed for the isolation of genomic DNA from buccal swabs. For this purpose, buccal cells were collected by scratching the oral mucosa of newborn piglets with Isohelix buccal swabs. Afterwards, the DNA was isolated according to the manufacturer's instructions taking all optional steps to increase DNA yield and improve purity. The volume for resuspension of the DNA pellet was decreased to an amount of 55 µL TE solution to achieve a higher DNA concentration. The DNA concentration was measured at 260 nm with the GeneQuant Pro photometer and the purity was checked by measuring 260 nm/ 280 nm and 260 nm/ 230 nm ratios. The DNA sample was then immediately used as a template for PCR.

Isolation of genomic DNA from blood samples

For the isolation of genomic DNA from blood samples, the Easy-DNA™ Kit, protocol #2 – 30 min DNA extraction from blood samples (Invitrogen™, Karlsruhe) was used. 1 mL of venous blood was taken from the V. cava with EDTA monovettes and the DNA was isolated according to the manufacturer's instructions. The DNA pellet was resuspended in 105 µL T-buffer to increase DNA yield and to stabilize the DNA. After isolating the DNA, the concentration and purity were measured using the GeneQuant Pro spectrophotometer, the DNA was diluted to a concentration of 100 ng/µL and then used as a template for PCR.

PCR

Two different sets of primers detecting the WT and the transgenic sequence of the *CFTR* locus were tested for genotyping of CF piglets. To identify gut-modified *CFTR*$^{-/-}$ piglets, an additional PCR detecting specific parts of the expression vector was established. To identify optimal conditions, different annealing temperatures were tested via temperature gradient PCR and different primer concentrations were checked. The PCR components were mixed on ice to a final volume of 25 µL in 0.2 mL reaction tubes. Previously isolated genomic DNA from WT, *CFTR*$^{+/-}$ and *CFTR*$^{-/-}$ piglets served as control and aq. dest. was used as a non-template control. Details for master mix ingredients and PCR conditions are listed in Table 2 and Table 3 below.

Table 2: Master mix composition for genotyping PCRs.

10 × PCR buffer	2.5 µL
$MgCl_2$ (15 mM)	2.5 µL
dNTPs (2 mM)	2.5 µL
Primer f (10 µM)	Xx µL
Primer r (10 µM)	Xx µL
Taq Polymerase (5 U/µL)	0.2 µL
aq. dest.	Ad 24 µL
DNA template	1 µL

Table 3: Cycler protocol for genotyping PCRs.

Denaturation	95 °C	5 min	
Denaturation	95 °C	30 s	35 ×
Annealing	Xx °C	30 s	
Elongation	72 °C	1 min	
Final elongation	72 °C	10 min	
Termination	4 °C	15 min	

Agarose gel electrophoresis

To prove the presence of amplified DNA, agarose gel electrophoresis was employed. For this purpose, a 1 % agarose gel was prepared by heating 1 × TAE buffer with 1 g/100 mL Universal Agarose in the microwave until the agarose had completely dissolved. After cooling down to about 55 °C, ethidium bromide was added to the mixture in a concentration of 0.5 µg/mL and the gel was poured into an electrophoresis chamber (OWL Inc., USA) for polymerization. After termination of the PCR, 2.5 µL 10 × DNA loading buffer were added to each PCR sample and the chamber was filled with 1 × TAE buffer as running buffer. 6 µL of Gene Ruler^{TM} 1 kb DNA molecular weight standard for the determination of the fragment size as well as the samples were pipetted into individual gel slots. By application of an electric field with a voltage of about 130 V, the DNA samples were separated according to their size and were visualized under UV light afterwards. The size of the bands could be estimated on the basis of the DNA marker.

3.6.2. Sequencing of PCR products

For verification of the correct amplification of the DNA, bands of the correct size were cut out of the gel, the DNA was eluted and then sequenced.

DNA elution

For sequencing purposes, amplified DNA as well as a Gene Ruler™ 1 kb DNA molecular weight standard were loaded onto a 1 % UltraPure™ Agarose/ 1 × TAE buffer gel. Under UV light, bands of the correct size were cut out of the gel. DNA was eluted from the gel according to "protocol 1: isolation of DNA from agarose gels" from the Bio&Sell Double Pure Kombi Kit. All steps were performed according to the manufacturer's instructions. For final DNA elution (step 8), 30 µL of elution buffer, preheated to 50 °C, were used to increase the DNA yield. To confirm the successful elution,

2 µL DNA elute
2 µL 10 × DNA loading buffer
15 µL aq. bidest.

were mixed together and loaded on a 1 % agarose gel. A Gene Ruler™ 1 kb DNA molecular weight standard was used as marker.

Sequencing PCR

The DNA base sequences of the amplified DNA were determined via the Sanger-DNA sequencing approach. For this purpose, PCR components were mixed on ice to a final volume of 10 µL in 0.2 mL reaction tubes (see Table 4). Each sample was sequenced twice, once with a forward, and once with a reverse primer. The same primers used for genotyping were employed for the sequencing reaction.

Table 4: Master mix composition for sequencing PCRs.

5 × Sequencing buffer	4 µL
BigDye	1 µL
Primer (10 µM)	1 µL
aq. dest.	2 µL
DNA template	2 µL

Table 5: Cycler protocol for sequencing PCRs.

Denaturation	95 °C	1 min	
Denaturation	95 °C	5 s	40 ×
Annealing	50 °C	10 s	
Elongation	60 °C	4 min	
Termination	4 °C	15 min	

Ethanol Precipitation

After terminating the PCR run, an ethanol precipitation was performed for purification of the cycle-sequenced products. 2.5 µL of 125 mM EDTA and 30 µL of 100 % EtOH, precooled to -20 °C, were added to the amplified PCR mix and the mixture was transferred to a fresh 1.5 mL tube. Subsequently, the samples were incubated on ice for 15 min. After centrifugation at 13,000 rpm for 30 min at 4 °C, the supernatant was removed with a pipette and the pellet was washed in 50 µL of 70 % EtOH. Afterwards the samples were centrifuged at 13,000 rpm for 2.5 min, the liquid supernatant was removed with a pipette and the pellet was air-dried for 6 min. The pellet was resuspended in 30 µL aq. dest. and transferred to a sequencing plate. The analysis of the fluorescently labeled DNA fragments was carried out at the Genome Analysis Center, Helmholtzzentrum Munich, with the automated capillary electrophoresis system ABI 3730 48-capillary DNA Analyzer.

Nucleotide sequences were evaluated bioinformatically with FinchTV Version 1.3.1, Geospiza Inc. and the BioEdit Sequence Alignment Editor.

3.7. Expression analysis at the RNA level

For expression analysis at the RNA level, RNA had to be isolated from tissue samples and reverse transcribed into cDNA. An absolute quantification of *CFTR* and gut-modified *CFTR* expression was performed via quantitative PCR (qPCR) in comparison to the ubiquitously expressed housekeeping gene *TBP2*. An additional qPCR experiment was established for *FABP2*, as the *FABP2*-promoter served as intestine-specific promoter for the gut-modified *CFTR* construct.

3.7.1. RNA isolation

Two different methods for the isolation of tRNA from tissue material were compared – the time-consuming acid guanidinium thiocyanate-phenol-chloroform extraction with TRIzol® and the RNA isolation via Direct-zol™ RNA MiniPrep Kit.

RNA isolation with TRIzol®

Tissue samples stored at -80 °C were put into liquid nitrogen and ground thoroughly using a pestle and mortar standing in liquid nitrogen. All working steps were performed under a hood in a seperate room where no DNA isolation was performed to avoid possible DNA contamination. A maximal amount of 100 mg of tissue powder was transferred with a microspoon to a 2 mL tube filled with 1 mL TRIzol® and homogenized immediately for 10 s at 30,000 rpm with the Polytron PT 2500 E rotor stator. Between different samples, the rotor was cleaned with aq. dest., 0.2 M NaOH and aq. dest. again to avoid carry-over. After an incubation step of 10 min at RT, the samples were centrifuged at 12,000 rcf for 10 min at 4 °C and the supernatant was transferred to new 1.5 mL tubes. 200 µL of chloroform were added to each sample, which were shaken vigorously for about 15 s and incubated at RT for 3 min. Following centrifugation at 12,000 rcf for 15 min at 4 °C, the mixture separated into the lower phenol/chloroform phase, an interphase and the upper aqueous phase containing the RNA. The upper phase was transferred carefully with a pipette to a new 1.5 mL tube without disturbing the interphase. For RNA precipitation, the aqueous phase was mixed with 500 µL of isopropyl alcohol and the samples were incubated for 10 min at RT. After

centrifugation at 12,000 rcf for 10 min at 4 °C, the precipitated RNA formed a pellet at the bottom of the tube and the supernatant could be removed. The pellet was washed with 1 mL of 75 % ethanol, vortexed vigorously and subsequently centrifuged at 7,500 rcf for 5 min at 4 °C. The supernatant was removed completely and the pellet was left to air-dry at RT for 6 min. The RNA pellet was resuspended in 10 mM Tris, pH 8; the volume was chosen according to the size of the pellet, and incubated for 10 min at 60 °C.

The RNA concentration was determined by measuring the absorbance at a wavelength of 260 nm and 280 nm with a spectrophotometer. The 260 nm/ 280 nm and 260 nm/ 230 nm ratios were used to assess the purity of the RNA. If the ratio was lower than 1.9 and 2.0, respectively, this could be due to a contamination of the RNA with chemicals with stronger absorbance, like TRIzol® or protein.

If required, the overall quality of the isolated RNA was assessed by gel electrophoresis on a denaturating 1 % agarose gel. The gel was prepared by heating 1.5 g Universal agarose with 135 mL aq. dest. in the microwave until the agarose was completely dissolved. Before the gel was poured into a gel electrophoresis chamber in the hood, 6 mL 25 × MOPS and 7.5 mL formaldehyde were added to the mixture. 1 × MOPS buffer was used as running buffer. The RNA samples were prepared as follows:

10 µL aq. dest.
5 µL Denaturating Buffer
2 µL RNA (500 ng/µL)

Accordingly, a Gene Ruler™ 1 kb DNA molecular weight standard was prepared:

4 µL aq. dest.
5 µL Denaturating Buffer
6 µL Gene Ruler™ 1 kb DNA molecular weight standard

The samples were then incubated at 55 °C in a thermomixer for 15 min to denature the secondary structures and finally cooled on ice for 2 min. Samples were loaded on the gel and the integrity of the RNA was determined by observing the visibility of intensive 18S and 28S bands.

RNA isolation with the Direct-zol™ RNA MiniPrep Kit

Tissue samples were prepared as mentioned above, the tissue was homogenized in TRIzol® and the supernatant was transferred to a new tube after centrifugation to remove any particulate debris. Afterwards, all steps of part II (RNA purification) were executed according to the manufacturer's instructions. RNA concentration and integrity were determined as mentioned above.

DNase digestion

To remove a possible contamination with genomic DNA, RNA samples were treated with DNase I, RNase-free, an endonuclease that digests single- and doublestranded DNA. For this purpose,

2 µL	10 × reaction buffer with $MgCl_2$
2.5 µL	DNase I, RNase-free
10.5 µL	aq. dest.
5 µL	RNA (500 ng/µL)

were mixed together and the samples were incubated at 37 °C. DNase was inactivated by heating the mixture to 65 °C for 10 min after addition of 2 µL 50 mM EDTA.

3.7.2. cDNA synthesis

8 µL of the DNase digest, equivalent to 1000 ng RNA, were applied for cDNA synthesis. Two different reverse transcriptase enzymes were tested in order to obtain the optimal results. The integrity of the obtained cDNA was confirmed by amplification of the ubiquitously expressed housekeeping gene *ACTB.* To check for a possible contamination with gDNA, the DNase digest was loaded on the gel in addition to the cDNA samples.

cDNA synthesis with RevertAid H Minus Reverse Transcriptase

All steps including all optional procedures were executed according to the manufacturer's instructions. To ensure an as complete as possible cDNA synthesis, 1 µL of Oligo (dT) and 1 µL of Random Primer Hexamers were used as primers. The obtained cDNA was stored at -20 °C until further processing.

cDNA synthesis with SuperScript™ III Reverse Transcriptase

First strand cDNA synthesis with SuperScript™ III Reverse Transcriptase was executed according to the manufacturer's instructions. Oligo (dT) was used as primer. The obtained cDNA was stored at -20 °C until further processing.

3.7.3. qPCR

The aim of qPCR is to determine the amount of an expressed gene in a tissue sample by measuring the number of copies of an mRNA transcript in relation to the inserted amount of RNA. The amplification of the selected reverse-transcribed cDNA can be monitored in real-time by application of a fluorescent dye like SYBR Green that intercalates into double-stranded DNA and thereby causes the fluorescence to rise with increased concentration of the amplified product.

The amount of expression of four different genes was determined in the collected tissue samples of WT, *CFTR*$^{-/-}$ and gut-modified *CFTR*$^{-/-}$ piglets. The expression of gut-modified *CFTR* was measured by amplification of a specific sequence of the expression vector spanning the different domains of the vector. The expression level of *CFTR* could be determined by amplification of a region lying within the coding sequence of *CFTR*, thereby detecting both endogenous and transgenic *CFTR*. As the promoter of *FABP2* served as intestine-specific promoter for the gut-modified expression vector, another qPCR was set up for the determination of *FABP2*. To enable the comparison between different animals, a part of *TBP2*, a housekeeping gene coding for the transcription factor TATA-box binding protein 2, was amplified.

Primers for the different sets of qPCR were tested first in an endpoint PCR run. cDNA from intestinal WT and gut-modified *CFTR*$^{-/-}$ piglets tissue, respectively, served as a template. Promising primer pairs were then tested for their suitability in qPCR. For this purpose, the following four serial 1:4 dilutions were prepared from cDNA and served as template in duplicates:

1:4	10 µL cDNA	+ 30 µL aq. bidest.
1:16	10 µL 1:4 dilution	+ 30 µL aq. bidest.
1:64	10 µL 1:16 dilution	+ 30 µL aq. bidest.
1:256	10 µL 1:64 dilution	+ 30 µL aq. bidest.

Different primer concentrations and annealing temperatures were tested to achieve optimal results. PCR components were mixed on ice to a final volume of 10 µL in a LightCycler® 480 Multiwell Plate 96. To eliminate a carry-over DNA contamination from previous runs, Uracil N-Glycosylase (UNG) was included in the master mix. The PCR reaction batch and conditions are described in Table 6 and Table 7. A melting curve analysis was performed following the two-step amplification process to assess that one single, specific product was amplified.

Table 6: Master mix composition for qPCRs.

FastStart Essential DNA Green Master	6.25 µL
UNG	0.075 µL
Primer f (10 µM)	Xx µL
Primer r (10 µM)	Xx µL
aq. bidest.	Ad 10 µL
Template (cDNA)	2.5 µL

Table 7: Cycler protocol for qPCRs.

UNG activation	50 °C	2 min	
Denaturation	95 °C	10 min	
Denaturation	95 °C	10 s	45 ×
Annealing	Xx °C	Xx s	
Melting	95 °C	10 s	
Cooling	37 °C	30 s	

To enable a comparison between the different runs and thus establish the optimal conditions, standard curves were constructed and analyzed according to Bustin (2004). If the linear regression analysis showed a high coefficient of determination ($R^2 > 0.98$) and the slope of the standard curve was approximately 3.32 (equivalent to an amplification efficiency of 100 %), these conditions were used for the detection of the corresponding genes.

Four serial four-fold dilutions of the cDNA of all organ samples of an individual served as template performed in duplicates. A non-template control (NTC) served as a negative control. Standard curves were established for each tissue and the

expression of the selected genes was quantified based on the amplification efficiency and C_t values.

To verify the correct amplification, qPCR products were sequenced via the Sanger approach following the same protocol as mentioned under 3.6.2 “Sequencing of PCR products” above.

3.8. Expression analysis at the protein level

The presence of the CFTR protein should be demonstrated in a set of selected tissue samples (see 3.4). Immunohistochemical (IHC) and immunofluorescent (IF) staining was employed both for the identification and localization of CFTR in tissue sections, whereas western blot (WB) analysis was used for the detection of CFTR in protein lysates extracted from snap-frozen tissue. Tissue from WT and *CFTR*$^{-/-}$ piglets, respectively, served as positive and negative controls.

3.8.1. Immunohistochemical and immunofluorescent detection of CFTR

The aim of this study was to establish an immunological assay for the reliable and specific detection of CFTR in porcine tissue sections. A range of antibodies for the detection of porcine CFTR in paraffin-embedded or cryo-sections are commercially available. However, evidence for the specificity was limited by the unavailability of a real negative control. Therefore, the usage of these antibodies for specific detection of porcine CFTR was evaluated with WT lung and intestinal tissue as a positive control and tissue of the well-characterized *CFTR*$^{-/-}$ piglets, that are known not to express any CFTR, as a real negative control.

Processing of fixated tissue material

Formalin- and methacarn-fixated tissue was routinely processed in a carousel tissue processor (Autotechnikon Histomaster 2050/Dl), as described in Table 8.

Table 8: Tissue processing for paraffin histology.

Ethanol 70 %	30 min
Ethanol 70 %	2 × 1.5 h
Ethanol 100 %	2 × 1.5 h
Xylene	2 × 30 min
Xylene	1.5 h
Paraffin at 60 °C	2 h
Paraffin	3 h

Following paraffin embedding with the TBS 88 Paraffin Embedding System, sections of about 4 µm were cut with a HM 315 microtome, mounted on 3-aminopropyltriethoxysilane-treated glass slides and stored at 37 °C until immunohistochemical staining.

Frozen tissue blocks were transferred to a cryotome cryostat (CryoStar NX70) holding a temperature of -20 °C. After equilibration of the block temperature to the cryotome temperature, sections of about 8 µm were cut and mounted on 3-aminopropyltriethoxysilane-treated glass slides. Sections were dried overnight at room temperature and stored at -80 °C.

Immunohistochemical staining

The avidin-biotin-complex technique with 3.3’ Diaminobenzidine tetra-hydrochloride (DAB) as chromogen was used for the detection of CFTR in lung and intestine sections.

Paraffin sections were deparaffinized and rehydrated through a descending alcohol row according to Table 9.

Table 9: Deparaffinization and rehydration of paraffin sections.

Deparaffinization	Xylene	2 × 20 min
Rehydration	Ethanol 100 %	2 × 5 min
	Ethanol 96 %	2 × 5 min
	Ethanol 70 %	5 min
Washing	aq. dest.	2 × 1 min

Sections from formalin-fixated tissue had to be pre-treated with antigen retrieval agents to break the protein cross-links formed by formalin fixation and thereby restoring hidden antigenic sites. In general, at least one heat-induced epitope retrieval (HIER) technique, in this case heating by microwave, and the proteinase-induced epitope retrieval (PIER) with proteinase K were evaluated. For selected antibodies, three different HIER methods were tested. Dilutions of H_2O_2, serum and antibodies were prepared with TBS buffer. All steps were performed at RT if not indicated otherwise. An overview of the workflow of the standard IHC protocol with HIER is given in Table 10.

Table 10: Standard IHC protocol with HIER.

	Procedure	**Agent**	**Conditions**
STEP 1	HIER	10 mM Citrate buffer pH 6 + 0.05 % Tween	800 W until boiling, 15 min 320 W in microwave Cooling 30 min
		10 mM Citrate buffer pH 6 + 0.05 % Tween	45 min at 800 W in pressure cooker in microwave Cooling 20 min
		DAKO target retrieval solution	20 min at 97 °C in water bath Cooling 20 min
STEP 2	Washing	TBS buffer	10 min
STEP 3	Blocking of endogenous peroxidase activity	1 % H_2O_2	15 min
STEP 4	Washing	TBS buffer	10 min
STEP 5	Serum blocking	5 % serum	1 h at RT
STEP 6	Primary antibody		4 °C overnight
STEP 7	Washing	TBS buffer	10 min
STEP 8	Secondary antibody		1 h at RT
STEP 9	Washing	TBS buffer	10 min
STEP 10	Detection	ABC complex	30 min
STEP 11	Washing	TBS buffer	10 min
STEP 12	Substrate	DAB	
STEP 13	Rinsing	Floating tap water	5 min
STEP 14	Counterstaining	Mayer’s Hemalum	30 s
STEP 15	Rinsing	Floating tap water	5 min

In paraffin sections that were treated with proteinase K, endogenous peroxidase activity was first blocked with 1 % H_2O_2 for 15 min, followed by a 10 min washing step with TBS buffer. Next, sections were incubated with proteinase K as antigen retrieval and subsequently all steps from the standard protocol, beginning with STEP 4, were executed.

For sections from methacarn-fixated tissue that did not need any antigen retrieval, the standard protocol was used from STEP 2 onwards.

Cryo-sections were treated in two different ways. In the first protocol (cryo method 1), tissue frozen in OCT compound on dry ice was used, while in the second protocol (cryo method 2), tissue incubated in 2 % PFA for 1 h at RT, subsequently incubated in ice-cold 30 % sucrose overnight and frozen in OCT compound in an ethanol/dry ice bath was used. For cryo method 1, cryo-sections were air-thawed and fixated in 4 % PFA for 5 min first. After two washing steps with TBS for 2 × 5 min, sections were permeabilized by incubation in 100 % EtOH at -20 °C for 2 min followed by another washing step with TBS for 5 min. Afterwards, all steps from the standard protocol, beginning with STEP 3, were performed. In the second protocol (cryo method 2), cryo-sections were air-thawed, rehydrated in PBS for 2 × 5 min and then permeabilized by incubation in 0.2 % Triton X-100 for 5 min. After a washing step in TBS buffer for 5 min, all steps from the standard protocol, beginning with STEP 3, were executed. Deviating from the standard protocol, serum was diluted in Super-Block and the sections were only incubated for 45 min in STEP 5 and the primary antibody was incubated for 2 h at 37 °C in STEP 6. For details on primary and secondary antibodies, dilutions and serum, see Table 17.

Immunofluorescent detection of CFTR

For immunofluorescent staining of CFTR, only cryo-sections from tissue frozen with the second freezing method (1 h 2 % PFA RT, 30 % ice-cold sucrose overnight and freezing in OCT compound in ethanol/dry ice bath) were used. Frozen tissue blocks were processed as described above. Cryo-sections were air-thawed, rehydrated in PBS for 2 × 5 min and permeabilized in 0.2 % Triton X-100 for 5 min. After two washing steps with PBS for 5 min, sections were incubated with 5 % donkey serum in Super-block for 45 min to reduce non-specific binding.

Subsequently, sections were incubated with the primary antibody Ab 596 from the CF Foundation, USA (1:50 in Super-Block) for 2 h at 37 °C and washed for 10 min in PBS. Sections were then incubated with the alexa fluor 488-conjugated secondary antibody donkey anti-mouse diluted 1:250 in 2 % pig serum for 1 h. From incubation with the secondary antibody onwards, all steps were performed in the dark to avoid bleaching of the fluorescence. After a last washing step with PBS for 10 min, slides were coverslipped with Vectashield antifade solution containing 4',6-diamidino-2-phenylindole (DAPI) for the staining of cell nuclei and afterwards stored at 4 °C in the dark. Images were acquired with an inverted epifluorescence microscope (Axiovert 200 M; Zeiss, Oberkochen).

3.8.2. Detection of CFTR by Western Blot

The applicability of commercially available antibodies for the detection of CFTR in protein lysates via Western blot (WB) was evaluated with tissue of a WT piglet, human liver tissue and human T84 cells as a positive control and tissue of a *CFTR*$^{-/-}$ piglet as a real negative control.

Protein isolation from tissue

40 mg of snap frozen tissue material were transferred to a 12 mL tube containing 1 mL of protein extraction buffer and was homogenized for 2 min on ice with the homogenizer ART-Micra D-8 at 23,500 rpm. To avoid contamination, the rotor was cleaned three times with aq. bidest. and once with PBS between different samples. Protein extracts were left on ice for 30 min, transferred to 1.5 mL Eppendorf tubes and incubated for 15 min at 60 °C. After cooling on ice for 3 min, the samples were centrifuged at 15,000 rcf for 5 min at 4 °C and the supernatant was transferred to a new 1.5 mL Eppendorf tube. Protein lysates were stored at -20 °C until further processing.

Measurement of protein concentration by BCA assay

To quantify the total amount of protein in the extracted tissue lysates, the Bicinchoninic acid (BCA) assay was used. The principle of this method is that the protein concentration is indicated by a change of color in the sample solution from green to purple in proportion to the protein concentration, which can then be

measured photometrically by establishing a calibration curve using protein standard solutions of known concentration.

For this purpose, protein standard solutions of known concentration were prepared by a six-fold dilution row (50 µL each) of a BSA stock solution (4 mg/mL) in PBS/protein extraction buffer (4:1 v:v). 10 µL of each protein lysate were diluted with 40 µL PBS. Bicinchoninic acid was mixed with 4 % $CuSO_4$-solution in a ratio of 50:1 and 200 µL of this mixture were pipetted to each standard and unknown sample. 100 µL of each reaction mixture were pipetted in duplicates to a 96 well plate and the plate was incubated at 37 °C for 30 min. Extinction values were measured at 562 nm with the Sunrise™ microplate reader for ELISA and protein concentrations were determined via the standard curve.

SDS PAGE

Proteins were separated according to their size by gel electrophoresis. The SDS PAGE is based on the principle that sodium dodecyle sulfate (SDS) denatures proteins and covers them with a negative charge so that they can be separated according to their molecular weight in a polymerized gel matrix when an electrical field is applied.

An 8 % SDS polyacrylamide separating gel was prepared according to Table 11, poured into the Mini Protean® Tetra system and covered with a layer of water for polymerization.

Table 11: Composition of 8 % SDS polyacrylamide separating gel.

aq. dest.	4.63 mL
1.5 M Tris (pH 8.8)	2.5 mL
30 % Acrylamid/Bis Solution	2.67 mL
10 % SDS	100 µL
10 % APS	100 µL
Temed	5 µL

After 45 min, the water was removed carefully, the separating gel was overlaid with a 5 % stacking SDS polyacrylamide gel (see Table 12) and a 15-well comb inserted at the top.

Table 12: Composition of 5 % SDS polyacrylamide stacking gel.

aq. dest.	3.5 mL
0.5 M Tris pH 6.8	0.75 mL
30 % Acrylamid/Bis Solution	0.75 mL
10 % SDS	50 µL
10 % APS	50 µL
Temed	2.5 µL

During polymerization of the stacking gel, the samples were diluted with 1 × Laemmli buffer containing 5 % β-mercaptoethanol and 1 × Laemmli buffer, respectively, to a final concentration of 15 µg protein in 18.5 µL of total volume. For denaturation, the samples were heated to 60 °C for 15 min. The gel electrophoresis chamber was filled with 1 × SDS running buffer and the prepared samples were loaded onto the gel. A PageRuler^{TM} prestained protein ladder and an unstained Protein Molecular Weight Marker were loaded onto the gel as protein weight markers. Electrophoresis ran at 100 V until the proteins, concentrated to a narrow band, had entered the running gel, whereupon the voltage was raised to 140 V. Gel electrophoresis was stopped when the 55 kDa band of the prestained protein ladder had leaked from the gel.

Semi-dry Blot

Proteins were transferred electrophoretically from the polyacrylamide gel to a nitrocellulose membrane via the semi-dry blot method using the Trans Blot® SD Semi-Dry transfer cell. Nitrocellulose membranes were activated for 10 min with 100 % methanol followed by incubation in 1 × transfer buffer for 30 min. The polyacrylamide gel was placed on the nitrocellulose membrane, enclosed by two extra thick blotting Whatman papers soaked within 1 × transfer buffer, and the proteins were blotted to the membrane with 15 V for about 90 min. As confirmation of successful blotting, the membranes were stained reversibly with Ponceau S solution for 2 min, washed three times with aq. dest. for destaining and subsequently stored at 4 °C.

Western Immunoblot

CFTR was detected via antigen-antibody coupling in an immunoblot. All steps were conducted in 50 mL falcons in a hybridization oven at room temperature if not indicated otherwise. Primary antibodies were diluted in TBS-T-BSA, while secondary antibodies were diluted in TBS-T-w/v nonfat dry milk. An overview of the standard protocol is given in Table 13.

Table 13: Standard western blot protocol.

	Procedure	**Agent**	**Conditions**
STEP 1	Activation	100 % methanol	1 min
STEP 2	Washing	TBS-T	3 × 5 min
STEP 3	Blocking	TBS-T-w/v nonfat dry milk	1 h
STEP 4	Washing	TBS-T	1 × 15 min, 2 × 5 min
STEP 5	Primary antibody		4 °C overnight
STEP 6	Washing	TBS-T	1 × 15 min, 2 × 5 min
STEP 7	Secondary antibody		1 h
STEP 8	Washing	TBS-T	1 × 15 min, 2 × 5 min
STEP 9	Detection	ECL™ detection reagent	

Signals were detected with the ECL detection reagent on Hyperfilm™ ECL chemiluminescense films in a darkroom. After suitable exposition time, films were developed in the Optimax X-ray Film processor 1170-1-0000.
An overview of the tested antibodies and dilutions is given in Table 18.

Stripping of the membranes

If membranes were to be used in further experiments, bound antibodies had to be removed by stripping of the membranes. For this purpose, the membranes were incubated in elution buffer for 30 min at 70 °C, followed by two washing steps in aq. bidest. for 10 min and one washing step in TBS-T in a new falcon for 10 min. Afterwards, the membranes could be used for another antibody incubation, starting with STEP 3 of the standard protocol.

IV. RESULTS

1. Transgenic expression of *CFTR* in the intestine modifies the severity of meconium ileus in gut-modified *CFTR*$^{-/-}$ piglets

Since a surgical correction of the fatal intestinal obstruction in newborn CF piglets is not feasible to produce large numbers of living animals, we decided to take another approach. By transgenic expression of porcine *CFTR* under the control of a promoter selectively expressed in the intestine, the severity of MI should be ameliorated and thereby ensure the survival of the CF piglets without affecting the other typical organ manifestations. As those pigs should have the potential to avoid MI, they are designated as potentially "gut-modified" in the following.

1.1. Generation of gut-modified *CFTR*$^{-/-}$ piglets

Gut-modified *CFTR*$^{-/-}$ piglets were generated by additive gene transfer of the expression vector (see Figure 4) in porcine *CFTR*$^{-/-}$ kidney cells, followed by SCNT and ET. This work was performed by N. Klymiuk, A. Wünsch, M. Kurome, V. Zakhartchenko, B. Kessler and T. Güngör, Chair for Molecular Animal Breeding and Biotechnology, LMU Munich.

Figure 4: DNA construct for generation of gut-modified *CFTR*$^{-/-}$ piglets. The expression vector consists of different functional parts: a 1.2 kb fragment of the porcine fatty-acid binding protein 2 promoter (*FABP2*) for the selective expression in the intestine, a 215 bp long part of the porcine β-hemoglobin (*HBB)* gene to increase the expression capacity by introducing a synthetic intron, the 4.8 kb coding region of the porcine *CFTR* followed by the 277 bp long

polyadenylation signal of the bovine Growth Hormone *(*b*GH*) gene as termination signal and a *puromycin*® (*puro*®) resistance cassette for positive selection.

A total of 1401 gut-modified *CFTR*$^{-/-}$ embryos were transferred to 12 pre-synchronized sows, resulting in four pregnancies. Three pregnancies went to full term with the birth of 13 living and 5 stillborn piglets. The efficiency of NT experiments, as defined by the number of living piglets per number of transferred embryos and per number of successful embryos, respectively, was about 0.9 % and 3.7 %. 25 % of all performed ETs resulted in the birth of living offspring. To exclude a potential influence on the outcome of pregnancy rates and the phenotype, *CFTR*$^{-/-}$ kidney cells from different genetic backgrounds were employed for additive gene transfer. In the first 11 experiments, cells from a cloned *CFTR*$^{-/-}$ piglet (#1267) and pooled cells from several cloned *CFTR*$^{-/-}$ piglets (#1268, 1270, 1274) were used. In the last NT experiment, pooled cells from *CFTR*$^{-/-}$ piglets (#2353, 2358) produced by normal breeding were employed to avoid the negative effects of repeated reproduction by cloning (for details see Table 14).

1.2. Analysis of the intestinal phenotype in gut-modified *CFTR*$^{-/-}$ piglets

Immediately after birth, the gut-modified CF piglets were repeatedly treated with enemas. Medication for gastric protection and circulation support was applied and pancreatic enzymes were supplemented to increase the likelihood of MI removal (for details see treatment protocol in Table 1). The gut-modified CF piglets from the litter of sow 1 and sow 12 exhibited a clearly impaired viability since birth, as they were unable to suckle on their own and had to be fed artificially to ensure colostrum and energy intake. The piglets were kept under 24 h surveillance and as soon as a piglet started to show a considerably deteriorated behavior, characterized by reduced motility, inability to suckle milk and a pear-looking, bloated abdomen with enhanced abdominal pressure in the absence of any signs of meconium removal, it was euthanized for controlled phenotypical analysis and sample collection.

All 13 living piglets had to be euthanized within the first 24 h after birth as, in spite of all the supportive measures taken, they were not able to remove meconium and therefore developed the severe characteristic symptoms mentioned above. For a detailed evaluation of the severity, localization and extension of MI in comparison to “normal” CF piglets and WT piglets of the same age, see Figure 5 and

Figure **6**. Summarized, the severity of the intestinal phenotype was improved in comparison to normal CF KO piglets in all examined gut-modified *CFTR*$^{-/-}$ piglets. The localization of stuck meconium was consistently found in more distal parts of the intestine and in a large percentage of gut-modified CF piglets, diverticulosis was less pronounced.

Table 14: Results of SCNT experiments using gut-modified *CFTR*$^{-/-}$ embryos.

Recipients	Genetic background	No. of transferred embryos	No. of successful embryos	Pregnancy	Result	
					Living piglets	Stillborn piglets
Sow 1	#1267	121	121	+	3 (#2128-2130)	3 (#2131-2133)
Sow 2	#1267	120	-	-	-	-
Sow 3	#1267	89	-	+	Preterm abortion	
Sow 4	#1267	99	-	-	-	-
Sow 5	#1267	111	-	-	-	-
Sow 6	#1267	136	136	+	6 (#2477-2482)	2 (#2494, 2507)
Sow 7	#1267	119	-	-	-	-
Sow 8	#1267	118	-	-	-	-
Sow 9	#1267	95	-	-	-	-
Sow 10	#1267	139	-	-	-	-
Sow 11	#1268, 1270, 1274	159	-	-	-	-
Sow 12	#2353, 2358	95	95	+	4 (#2736-2739)	-
Total		**1401**	**352**	**3**	**13**	**5**
Efficiency		**~0.9 %**	**~3.7 %**	**25 %**	**~72.2 %**	**~27.8 %**

Efficiency of NT experiments is calculated as number of living piglets per number of transferred or successful embryos. Pregnancy rate is calculated as number of pregnancies resulting in the birth of living piglets per ETs in total. Percentage of living and stillborn piglets, respectively, is calculated by correspondent number of piglets per total number of born piglets.

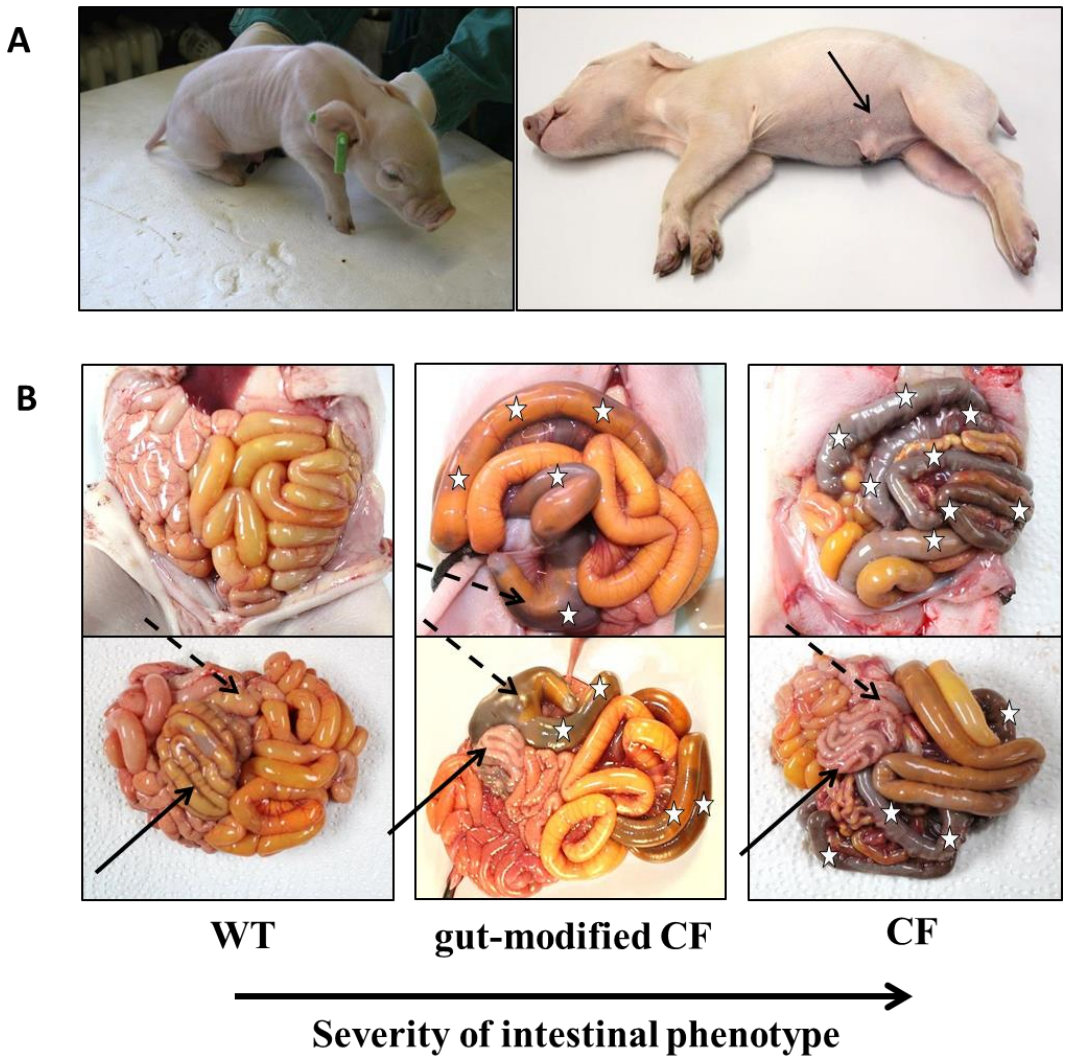

Figure 5: Intestinal phenotype of WT, gut-modified *CFTR*$^{-/-}$ and *CFTR*$^{-/-}$ piglets. (A) Detoriation of the general condition in a gut-modified CF piglet is illustrated by the decreased ability to move on its own and a severely bloated abdomen with prominent blood vessels (black arrow). (B) View of the intestinal convolute after opening the abdominal cavity and after complete resection. White asterisks mark the presence of meconium in dilated intestinal loops. In WT piglets, meconium has been completely deposited after about 24 h and the intestine shows a healthy brownish color and intestinal loops of equal diameter. Both in normal and gut-modified CF piglets, intestinal loops are blocked by black meconium. Compared to normal CF piglets, the blockage by meconium appears in the more distal parts of the intestine in gut-modified CF piglets, extending until the beginning of the colon. Discontinuous black arrows point to the cecum, which is severely enlarged by stuck meconium in gut-modified CF piglets. The colon is

marked by black arrows. Gut-modified CF piglets exhibit the microcolon characteristic for normal CF piglets, although a small portion of the meconium has entered the proximal parts of the colon ascendens.

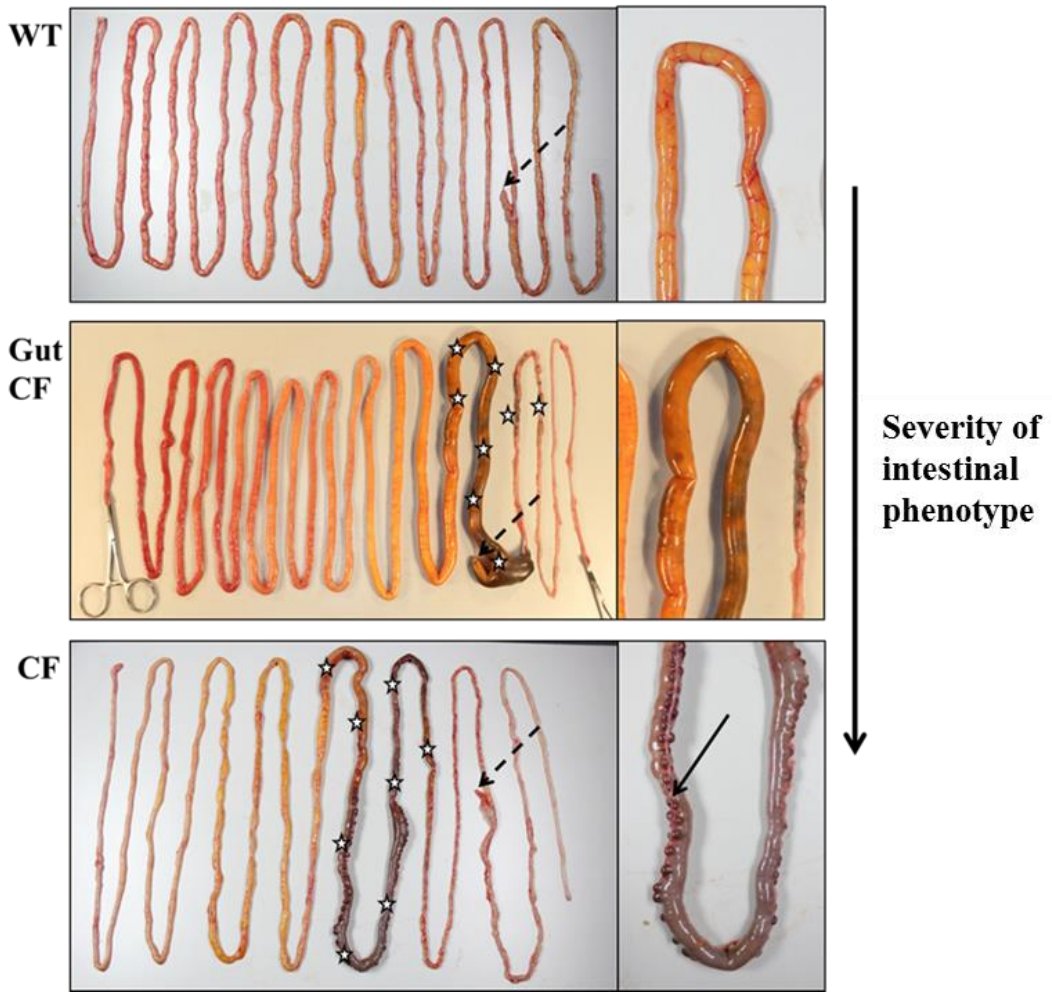

Figure 6: Range of MI in WT, gut-modified *CFTR*$^{-/-}$ (gut CF) and *CFTR*$^{-/-}$ piglets. As a reference point, the cecum is marked by discontinuous black arrows. The range of MI (marked by white asterisks) differs in the location between gut-modified and normal CF piglets. In all examined normal CF piglets, stuck meconium is mainly located in the middle and distal parts of the jejunum, whereas gut-modified CF piglets exhibit a slightly improved phenotype with meconium consistently localized in the distal jejunum, cecum and proximal colon. The prominent feature of diverticulosis (black arrow), that is consistently found in all normal CF piglets and illustrates the severity of the intestinal phenotype, is considerably less pronounced or even missing in gut-modified CF piglets.

1.3. Selection of founder animals for recloning

Founder #2478 had to be euthanized after 24 h due to rapid deterioration of its general condition, but no signs of meconium were detected in the intestinal convolute and it did not exhibit a microcolon. Therefore, its kidney was explanted under sterile conditions, a primary cell line was established and primary kidney cells were employed for SCNT and ET. An overview of the recloning experiments is given in Table 15. Compared to the results of the generation of gut-modified *CFTR*$^{-/-}$ founder animals by SCNT in Table 14, it has to be mentioned that, although the pregnancy rate in the recloning experiments is much higher (55 % compared to 25 %), the cloning efficiency, defined as number of living piglets per number of successful embryos, is impaired (1.9 % compared to 3.7 %) as well as the average number of living piglets per litter (2.6 living piglets/litter compared to 4.3 living piglets/litter). The percentage of stillborn piglets is increased (35 % compared to 27.8 %).

The recloned piglets were supportively treated and analyzed the same way as the gut-modified *CFTR*$^{-/-}$ founder piglets. All 13 living piglets exhibited a strongly reduced viability, were not able to suckle or swallow on their own and had to be fed artificially. A high percentage of piglets had enlarged tongues, a well-known side effect of SCNT, hindering a self-dependent milk intake (see Figure 7 (A)). All 13 piglets had to be euthanized within the first 24 h because of the severe deterioration of their general condition due to the characteristic symptoms of the severe intestinal phenotype. Close examination of the intestine revealed that the improvement of the phenotype in piglet #2478 was not reproducible in recloned animals. The range of MI resembled the one found in other gut-modified *CFTR*$^{-/-}$ founder animals, with the main part of the meconium stuck in the distal parts of the jejunum and the enlarged cecum. A microcolon was a consistent finding in all piglets and diverticulosis was existent in variable degrees (see Figure 7 (B)).

Table 15: Recloning experiments of founder #2478.

Recipients	Recloning of founder	No. of transferred embryos	No. of successful embryos	Pregnancy	Result	
					Living piglets	Stillborn piglets
Sow 1	#2478	194	194	+	1 (#2870)	2 (#2869, 2871)
Sow 2	#2478	118	118	+	1 (#2906)	1 (#2906)
Sow 3	#2478	119	-	-	-	-
Sow 4	#2478	152	-	-	-	-
Sow 5	#2478	187	-	-	-	-
Sow 6	#2478	135	-	-	-	-
Sow 7	#2478	122	122	+	2 (#4008, 4009)	-
Sow 8	#2478	127	127	+	4 (#4051-4054)	-
Sow 9	#2478	134	134	+	5 (#4280, 4283-4286)	4 (#4279, 4281, 4282, 4287)
Total		**1288**	**695**	**5**	**13**	**7**
Efficiency		**~1.0 %**	**~1.9 %**	**~55 %**	**65 %**	**35 %**

Efficiency of NT experiments is calculated as number of living piglets per number of transferred or successful embryos. Pregnancy rate is calculated as number of pregnancies resulting in the birth of living piglets per ETs in total. Percentage of living and stillborn piglets, respectively, is calculated by correspondent number of piglets per total number of born piglets.

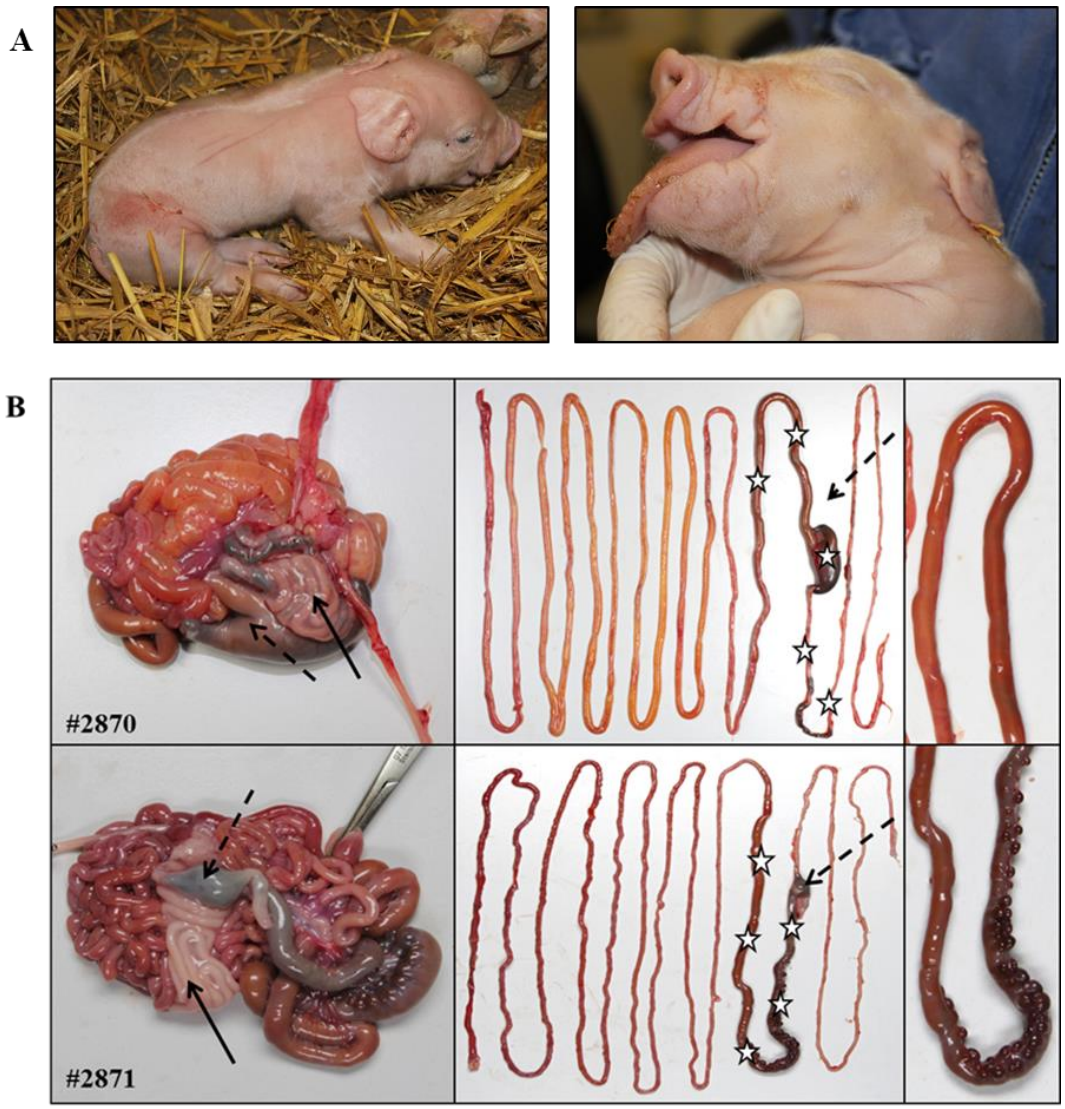

Figure 7: Phenotype of recloned founder piglets. (A) Abnormal findings in recloned piglets. All recloned piglets show reduced viability, a high percentage of them has an enlarged tongue and the number of stillborn piglets or mummies is increased. (B) Intestinal phenotype of two exemplary piglets. The cecum is marked with a discontinuous black arrow, the continuous black arrow points to the microcolon. The range of MI is marked with white asterisks. Meconium is stuck in the distal parts of the jejunum, cecum and the beginning of the colon ascendens. All piglets exhibit a microcolon with reduced diameter. Thus, the range of MI resembles other founder animals with a slight improvement compared to normal CF KO piglets, but not the clearly improved phenotype of #2478. The range of diverticulosis differs strongly between all examined recloned piglets.

1.4. Analysis of gut-modified *CFTR*$^{-/-}$ piglets at the genomic level

Considering the fact that the health of normal *CFTR*$^{-/-}$ piglets started to deteriorate within 24 h after birth because of the severe intestinal phenotype, it was essential to establish a rapid method for the genotyping of gut-modified CF piglets, including a time-sparing DNA isolation method and an extremely shortened PCR protocol.

DNA isolation

Three different fast DNA isolation kits were compared in terms of suitability, time duration and reliability of PCR results – the nexttec™ Genomic DNA Isolation Kit from Tissue and Cells, the Easy-DNA™ Kit, protocol #2 – 30 min DNA extraction from blood samples and the Isohelix DDK DNA Isolation Kit.

Table 16: Comparison of DNA isolation methods.

	Source	**Suitability**	**Time duration**	**Reliability of PCR results**
Nexttec kit	Docked tail	Tail docking is routinely performed in all litters to prevent tail biting	60 min	high
Easy-DNA kit	Blood	Blood collection is critical in neonatals	30 min	low
Isohelix kit	Buccal swabs	Easy to handle	90 min	medium-high

After comparing all critical aspects, the DNA isolation from docked tails via the nexttec kit proved to be the safest, fastest and most reliable method for the isolation of genomic DNA in newborn piglets.

Establishment of genotyping PCRs

To confirm the *CFTR*$^{-/-}$ genotype, two sets of regular PCR amplifying the WT and the mutated *CFTR* sequence were established. The integration of the gut-modified *CFTR* expression vector in the *CFTR*$^{-/-}$ genome was confirmed by amplifying a specific part of the expression vector. As the nexttec DNA isolation protocol is very time-saving but produces DNA of inferior quality, a range of primer pairs for amplification of the WT (see Figure 8) and mutant *CFTR* (see Figure 9) sequence

had to be tested and best pairs were further optimized. To determine whether the gut-modified *CFTR* expression vector had been integrated in the *CFTR*$^{-/-}$ genome, primer pairs amplifying specific parts of the expression vector in the 3'- and 5'-UTR-regions flanking the porcine *CFTR* sequence were tested and the conditions were further optimized (see Figure 10).

	WT primer pairs		
	Primer f	Primer r	length
1	CFTR3f	CFTR3r	1070 bp
2	CFTR3f	CFTR2r	1090 bp
3	CFTR2f	CFTR2r	1020 bp
4	CFTR2f	CFTR3r	1000 bp
5	CFTR5armf	CFTR7118rv	500 bp
6	CFTR5armf	CFTR7160rv	550 bp
7	Cg1f	Cg5r	430 bp
8	Cg1f	Cg3r	900 bp
9	Cg1f	Cg4r	550 bp
10	Cg2f	Cg3r	860 bp
11	Cg2f	Cg4r	510 bp
12	Cg2f	Cg5r	390 bp

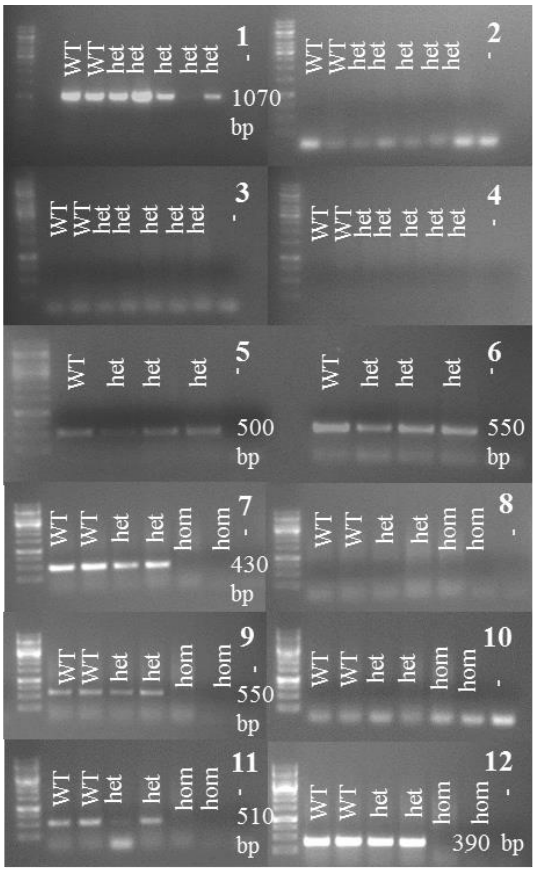

Figure 8: Testing of primer pairs for the detection of WT *CFTR*. Primer pairs were first tested with an annealing temperature of 58 °C and a starting volume of 0.5 µL each. DNA isolated with the nexttec 1 h-protocol from WT, *CFTR*$^{+/-}$ (het) and *CFTR*$^{-/-}$ (hom) piglets served as template. Conditions of promising pairs (1 and 12) were optimized by temperature gradient PCR and comparison of different primer concentrations.

	TG primer pairs		
	Primer f	Primer r	length
1	Neo2f	CFTR2r	600 bp
2	Neo2f	CFTR3r	590 bp
3	Neo3f	CFTR2r	670 bp
4	Neo3f	CFTR3r	660 bp
5	CFTR5armf	Cg1r	800 bp
6	CFTR5armf	STOPr	960 bp
7	Cg1f	Cg1r	430 bp
8	Cg1f	Cg2r	730 bp
9	Cg2f	Cg1r	390 bp
10	Cg2f	Cg2r	690 bp

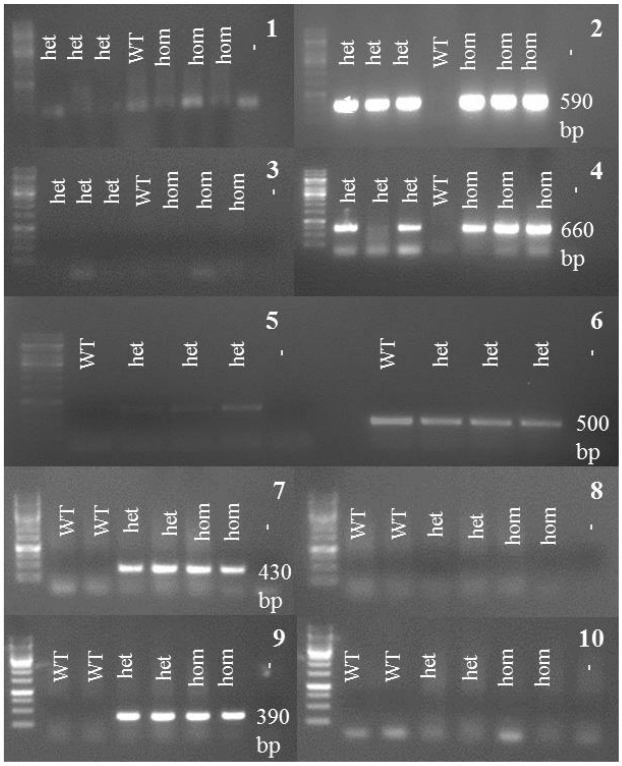

Figure 9: Testing of primer pairs for the detection of mutant (TG) *CFTR*. Primer pairs were first tested with an annealing temperature of 58 °C and a starting volume of 0.5 µL each. DNA isolated with the nexttec 1 h-protocol from WT, *CFTR*$^{+/-}$ (het) and *CFTR*$^{-/-}$ (hom) piglets served as template. Primer pair 6 detects bands of the wrong size (about 500 bp instead of 960 bp) in the mutant animals as well as in the WT animal that serves as negative control. Conditions of promising pairs (2 and 9) were optimized by temperature gradient PCR and comparison of different primer concentrations.

	Primer pairs gut-modified *CFTR*		
	Primer f	Primer r	length
1	CFgutf1	CFgutr1	110 bp
2	CFgutf2	CFgutr2	250 bp
3	CFgutf3	CFgutr3	130 bp
4	CFgutf4	CFgutr4	80 bp

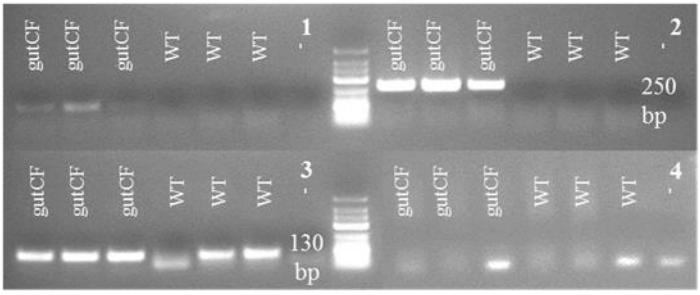

Figure 10: Testing of primer pairs for the detection of the gut-modified *CFTR* expression vector. Primer pair 1 is located in the 5'-UTR region; the other primer pairs are located in the 3'-UTR region of the expression vector. Primer pairs were first tested with an annealing temperature of 58 °C and a starting volume of 0.5 µL each. DNA from gut-modified *CFTR*$^{-/-}$ (gutCF) and WT piglets isolated with the nexttec 1 h-protocol served as template. Primer pair 3 also detects a signal in the WT piglets that serve as negative controls. Conditions for the promising primer pair 2 were optimized by temperature gradient PCR and comparison of different primer concentrations.

In conclusion, the time necessary for the genotyping of gut-modified CF piglets could be minimized to less than three hours between birth and genotyping results, including one hour for DNA isolation and one hour for the final genotyping PCRs (see Figure 11). DNA isolated with the nexttec 1 h-protocol was of sufficient quality for regular genotyping PCR.

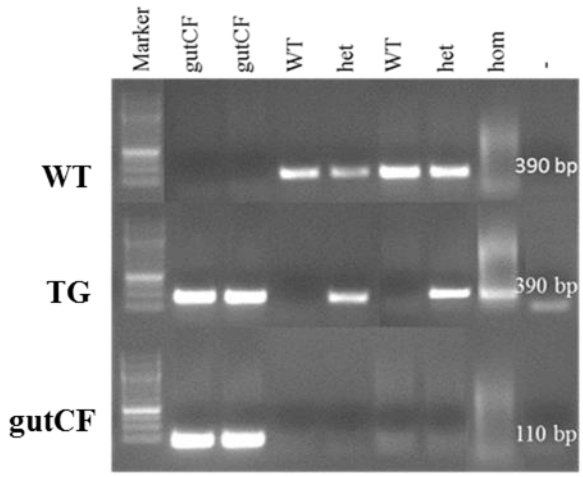

WT:	Cg2f/Cg5r 0.5 µL		
TG:	Cg2f/Cg1r 0.5 µL		
gutCF:	CFgutf2/CFgutr2 0.5 µL		

Denaturation	95 °C	5 min	
Denaturation	95 °C	15 s	35 x
Annealing	56 °C	15 s	
Elongation	72 °C	30 s	
Elongation	72 °C	5 min	
Termination	4 °C	5 min	

Figure 11: Example of genotyping gut-modified *CFTR*$^{-/-}$ (gutCF), WT, *CFTR*$^{+/-}$ (het) and *CFTR*$^{-/-}$ (hom) piglets. All three genotyping PCRs detecting the WT, the mutant (TG) and the gut-modified (gutCF) *CFTR* sequence are run under the same conditions in one machine. The time duration of all PCR steps was minimized as far as possible, until the whole run took about one hour.

Verification of the correct amplification of the PCR products

The detection of bands of the correct bp size using the agarose gel electrophoresis has to be approved by a further method. To confirm that primers annealed to the correct DNA sequences and that the requested base sequences were amplified, DNA was eluted from bands of the correct bp size and sequenced via the Sanger sequencing approach. The detailed comparison of the base sequences derived from sequencing chromatograms to the target sequences revealed that all primers annealed correctly to the sequences and that target and amplified sequences were identical (see Figure 12).

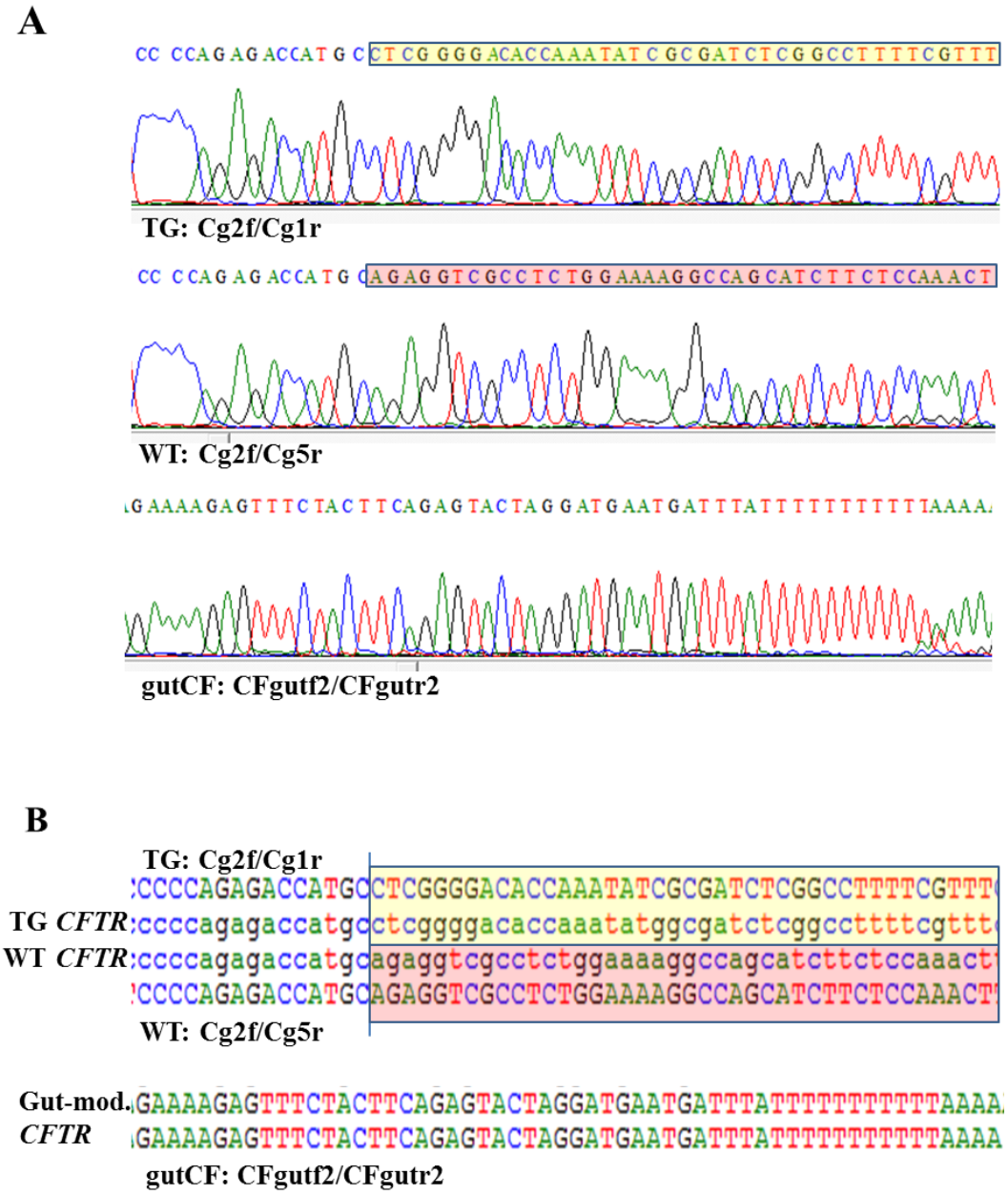

Figure 12: Verification of genotyping PCR products. (A) Electropherograms of PCR products amplified with primers for WT, mutant (TG) and gut-modified *CFTR*. In the mutant and WT *CFTR* chromatograms, the 5'-parts are identical as the forward primer Cg2f, which is used for both PCRs, anneals to a part of the *CFTR* sequence present in both sequences. The sequences specific for WT and mutant *CFTR* further downstream are highlighted in red (WT) and yellow (TG). (B) Comparison of amplified sequences to target sequences.

1.5. Expression analysis of *CFTR*$^{-/-}$ and WT piglets at the protein level

For a functional evaluation of the porcine CF model, the absence of CFTR expression had to be confirmed at the protein level. Therefore, CFTR expression in WT and CF KO piglets was examined by immunohistochemical or immunofluorescent approaches and by western blot. A range of commercially available primary antibodies are described to detect CFTR in tissue derived from pigs. Exclusively in this study, the specificity of the antibodies was evaluated with a best-optimal negative control, tissue derived from CF KO animals.

Detection of CFTR by immunohistochemistry and immunofluorescence

Initially, the utility of the well-characterized antibody Ab 596 (CF Foundation, USA) for the detection of CFTR in cryo-sections from tissue frozen with the complicated freezing method 2 was evaluated in IF and IHC, according to a published protocol (Stoltz, Rokhlina *et al*. 2013). However, the primary aim of the study was to find an antibody that reliably detected CFTR in paraffin-embedded tissue, as the morphology of paraffin-embedded tissue is better preserved and the fixation and sectioning works very well compared to cryo-sections. For a detailed evaluation of the antibodies, at least one HIER and one PIER method were tested using formalin-fixated tissue. As some antibody-specific protocols preferred the usage of cryo-sections for IHC, the specificity of all antibodies was also evaluated on paraffin slides from methacarn-fixated tissue. Methacarn fixation is reported to produce tissue slides with a quality similar to cryo-sections (Mitchell, Ibrahim *et al*. 1985). The specificity of the antibodies from the CF Folding consortium was also evaluated using cryo-sections from tissue frozen with freezing method 1with cryo method 1, an established protocol for the detection of CFTR in human tissue (Kreda and Gentzsch 2011). Table 17 gives an overview of all antibodies, fixations and conditions tested in immunohistochemistry.

Table 17: Overview of all tested immunohistochemical conditions.

Primary antibody	Fixation	Antigen retrieval	Dilution	Secondary antibody	Dilution	Serum
CF Folding consortium Ab 528	Formalin	Microwave	1:100; 1:300; 1:900	Biotinylated goat anti-mouse IgG + 5 % serum pig	1:200	Goat
		Proteinase K	1:200; 1:600			
	Methacarn	-	1:100; 1:300; 1:900			
	Cryo method 1	-	1:250; 1:1,000	Biotinylated AffiniPure goat anti-mouse IgG	1:250	
CF Folding consortium Ab 570	Formalin	Microwave	1:100; 1:300; 1:900	Biotinylated goat anti-mouse IgG + 5 % serum pig	1:200	Goat
		Proteinase K	1:200; 1:600			
	Methacarn	-	1:100; 1:300; 1:900			
	Cryo method 1	-	1:250; 1:1,000	Biotinylated AffiniPure goat anti-mouse IgG	1:250	
CF Folding consortium Ab 596	Formalin	Microwave	1:100; 1:300; 1:900	Biotinylated goat anti-mouse IgG + 5 % serum pig	1:200	Goat
		Water bath	1:300; 1:900; 1:2,700			
		Pressure cooker	1:300; 1:900; 1:2,700			
		Proteinase K	1:200; 1:600			
	Methacarn	-	1:100; 1:300; 1:900			
	Cryo method 1	-	1:250; 1:1,000	Biotinylated AffiniPure goat anti-mouse IgG	1:250	
	Cryo method 2	-	1:300; 1:900	Biotinylated AffiniPure goat anti-mouse IgG + 2 % serum pig	1:250	

CF Folding consortium Ab 660	Formalin	Microwave	1:100; 1:300; 1:900	Biotinylated goat anti-mouse IgG + 5 % serum pig	1:200	Goat
		Proteinase K	1:200; 1:600			
	Methacarn	-	1:100; 1:300; 1:900			
	Cryo method 1	-	1:250; 1:1,000	Biotinylated AffiniPure goat anti-mouse IgG	1:250	
CF Folding consortium Ab 769	Formalin	Microwave	1:100; 1:300; 1:900	Biotinylated goat anti-mouse IgG + 5 % serum pig	1:200	Goat
		Proteinase K	1:200; 1:600			
	Methacarn	-	1:100; 1:300; 1:900			
	Cryo method 1	-	1:250; 1:1,000	Biotinylated AffiniPure goat anti-mouse IgG	1:250	
Abcam CF3	Formalin	Microwave	1:100; 1:300; 1:900; 1:1,500; 1:1,800; 1:3,000; 1:6,000; 1:12,000	Biotinylated goat anti-mouse IgM + 2 % serum pig	1:100	Goat
		Water bath	1:1,500; 1:3,000; 1:6,000; 1:12,000			
		Proteinase K	1:1,500; 1:3,000; 1:6,000; 1:12,000			
	Methacarn	-	1:100; 1:300; 1:900; 1:1,500; 1:1,800; 1:3,000; 1:6,000; 1:12,000			

Cell Signaling #2269	Formalin	Microwave	1:100; 1:300; 1:900	Biotinylated goat anti-rabbit IgG + 5 % serum pig	1:200	Goat
		Proteinase K	1:300			
	Methacarn	-	1:100; 1:300; 1:900			
R&D 24-1	Formalin	Microwave	1:25; 1:75; 1:250	Biotinylated goat anti-mouse IgG + 5 % serum pig	1:200	Goat
		Water bath	1:150; 1:300; 1:900			
		Pressure cooker	1:150; 1:300; 1:900			
		Proteinase K	1:100; 1:350			
		-	1:100; 1:200; 1:500			
	Methacarn	-	1:100; 1:300; 1:900			
Santa Cruz H 182	Formalin	Microwave	1:100; 1:300; 1:900	Biotinylated goat anti-rabbit IgG + 5 % serum pig	1:200	Goat
		Proteinase K	1:50; 1:100; 1:200; 1:300			
	Methacarn	-	1:100; 1:300; 1:900			
Santa Cruz N-20	Formalin	Microwave	1:100; 1:300; 1:900	Biotinylated rabbit anti-goat IgG + 5 % serum pig	1:200	Rabbit
		Proteinase K	1:50; 1:150; 1:450			
	Methacarn	-	1:100; 1:300; 1:900			

The single method specifically detecting CFTR is marked in red.

Staining with the primary antibody Ab 596 (CF Foundation, USA) of cryo-sections derived from tissue frozen with the complicated freezing method 2 worked reliably using cryo method 2 for the specific detection of CFTR in intestinal tissue both in IF and IHC (see Figure 13 and Figure 14). Staining patterns in IF and IHC were identical.

In WT animals, CFTR was strongly expressed in the crypts of the intestine and showed a decreasing gradient along the villi from the crypts to the villous top. Several single villous cells with normal enterocyte-like morphology, presumably an equivalent to the CFTR High expresser cells found in human and rat proximal small intestine (Jakab, Collaco *et al*. 2013), showed a strong CFTR signal. In the staining with IF detection, fetal faeces showed a strong autofluorescence, a feature that was reproduced using IHC, where fetal faeces were stained in brown in the negative control. In WT lung tissue, a very weak CFTR signal was detected in the submucosal glands, whereas the respiratory epithelium was not stained. In CF KO animals, CFTR was neither detected in intestinal nor in lung tissue. Staining with antibody Ab 596 confirmed thereby the absence of any CFTR protein in the *CFTR*$^{-/-}$ piglets.

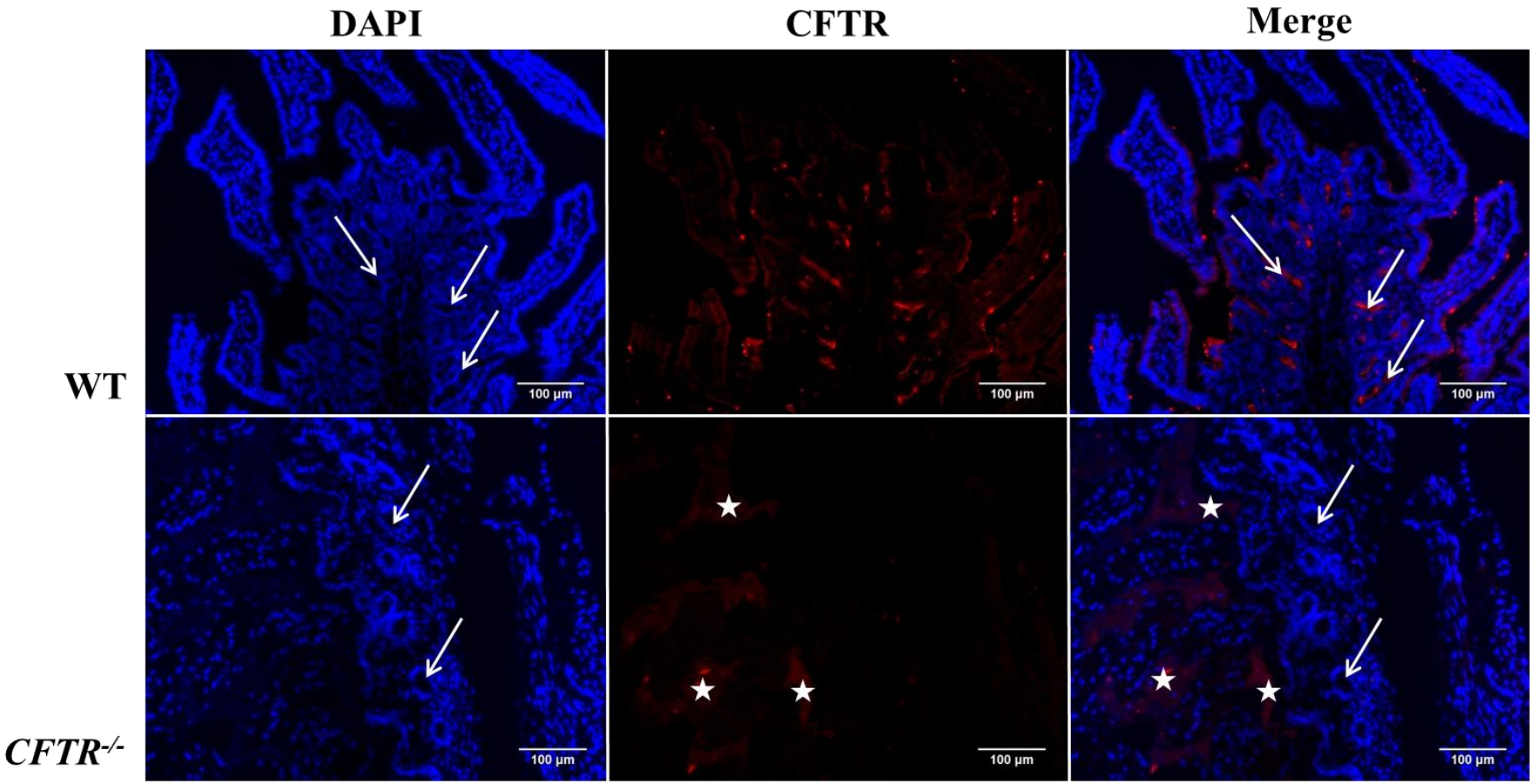

Figure 13: Immunofluorescent detection of CFTR in the intestine of WT and *CFTR*$^{-/-}$ piglets with Ab 596. Images show staining for cell nuclei (DAPI, blue) and CFTR (red). Intestinal crypts are marked with a white arrow. In WT piglets, CFTR is mainly localized in the intestinal crypts with a decreasing gradient along the villous axis and strong staining of single villous cells. In CF KO piglets, CFTR is not detected, faeces show a strong autofluorescence (marked with white asterisks).

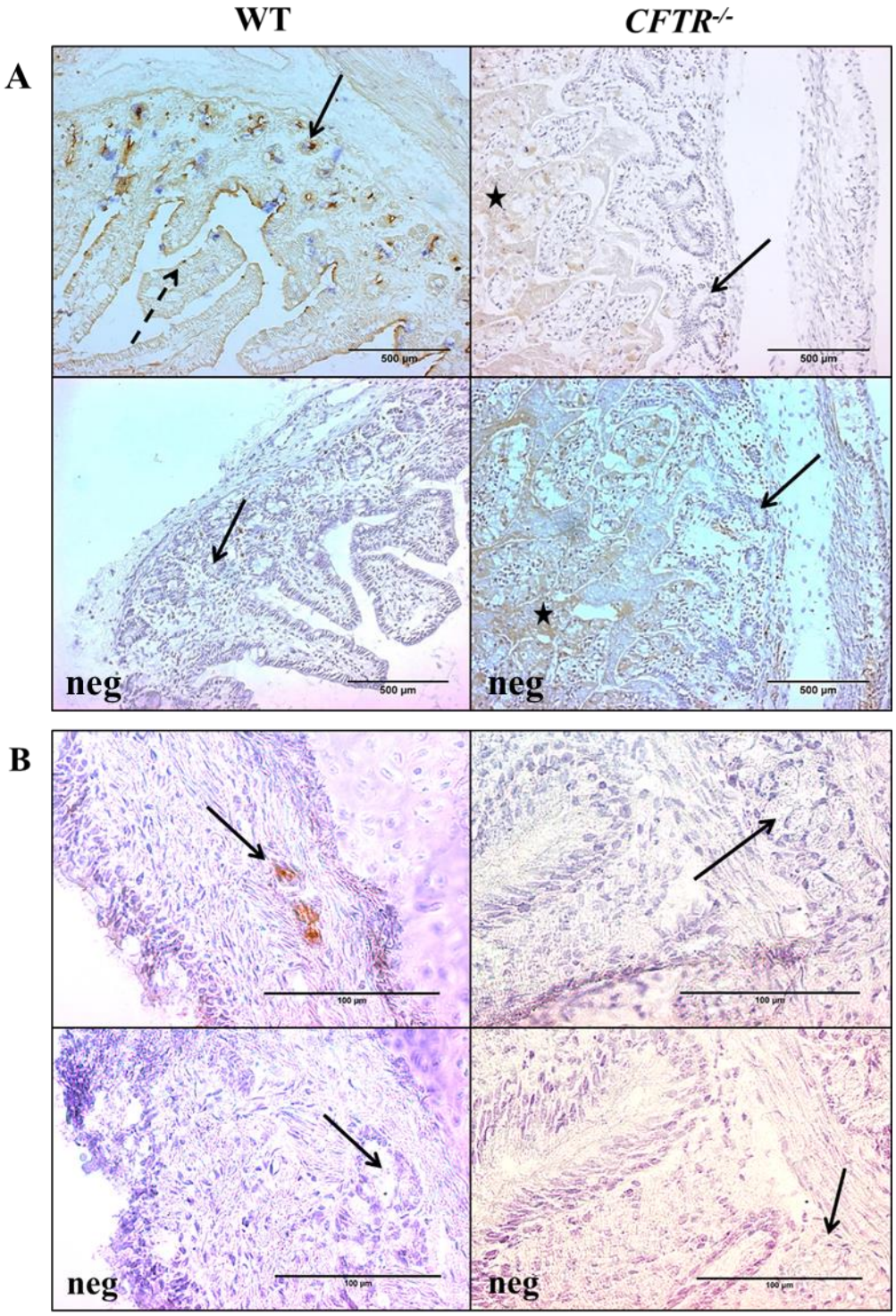

Figure 14: Immunohistochemical detection of CFTR in WT and *CFTR*$^{-/-}$ intestine and lung with Ab 596. (A) Detection of CFTR in the intestine of WT and CF KO piglets. Intestinal crypts are marked with black arrows. The discontinuous arrow points to a single strongly-stained cell. Negative controls

(neg) are stained with the secondary antibody only. Faeces are stained in brown both in the stained slide and the negative control of the CF KO intestine (marked with black asterisks). (B) Detection of CFTR in the lung from WT and CF KO piglets. Black arrows point to submucosal glands.

Since the detection of CFTR on cryo-sections with Ab 596 was not sensitive enough to detect CFTR in lung tissue and the tissue morphology showed freezing artefacts in spite of the cryo-protective freezing process, several commercially available antibodies for the detection of CFTR on paraffin-embedded tissue were tested. As the lung is the major organ of interest in CF, the antibodies were first evaluated on lung tissue from WT and *CFTR*$^{-/-}$ piglets (see Figure 15). Two antibodies showed an obvious difference of staining pattern between WT and CF KO piglets, all other antibodies detected no specific signal. Ab 596 (1:900, HIER by water bath) showed strong apical cytoplasmatic staining of the respiratory epithelium and very weak staining of the submucosal glands in formalin-fixated WT lung tissue, whereas the CF KO lung tissue was negative (see Figure 15 (B)). Ab 24-1 (1:900, HIER by pressure cooker) recognized a weak apical cytoplasmatic signal of the respiratory epithelium and submucosal glands with very strong staining on the apical surface of the respiratory epithelium in formalin-fixated WT tissue, while CF KO tissue was negative (see Figure 15 (D)). However, when these two antibodies were employed under the same conditions for the detection of CFTR in intestinal tissue, they detected the same staining pattern both in WT and CF KO tissue (see Figure 16). To exclude a single animal-specific effect, both antibodies were tested with the same conditions on a larger number of WT and CF KO animals. As the unspecific staining on intestinal tissue was reproducible for all tested animals, these antibodies were not suitable for a specific detection of CFTR. None of the other evaluated antibodies detected a specific CFTR signal in WT and simultaneously no signal in CF KO piglets in lung and intestinal paraffin-embedded tissue. Either the signal pattern was completely unspecific with strong staining of the wrong tissue, e.g. smooth muscle (see Figure 15 (C)), or the expression pattern seemed correct, however, with no difference between WT and CF KO animals. Cryo method 1 did not give a specific signal for CFTR, when porcine tissue was used.

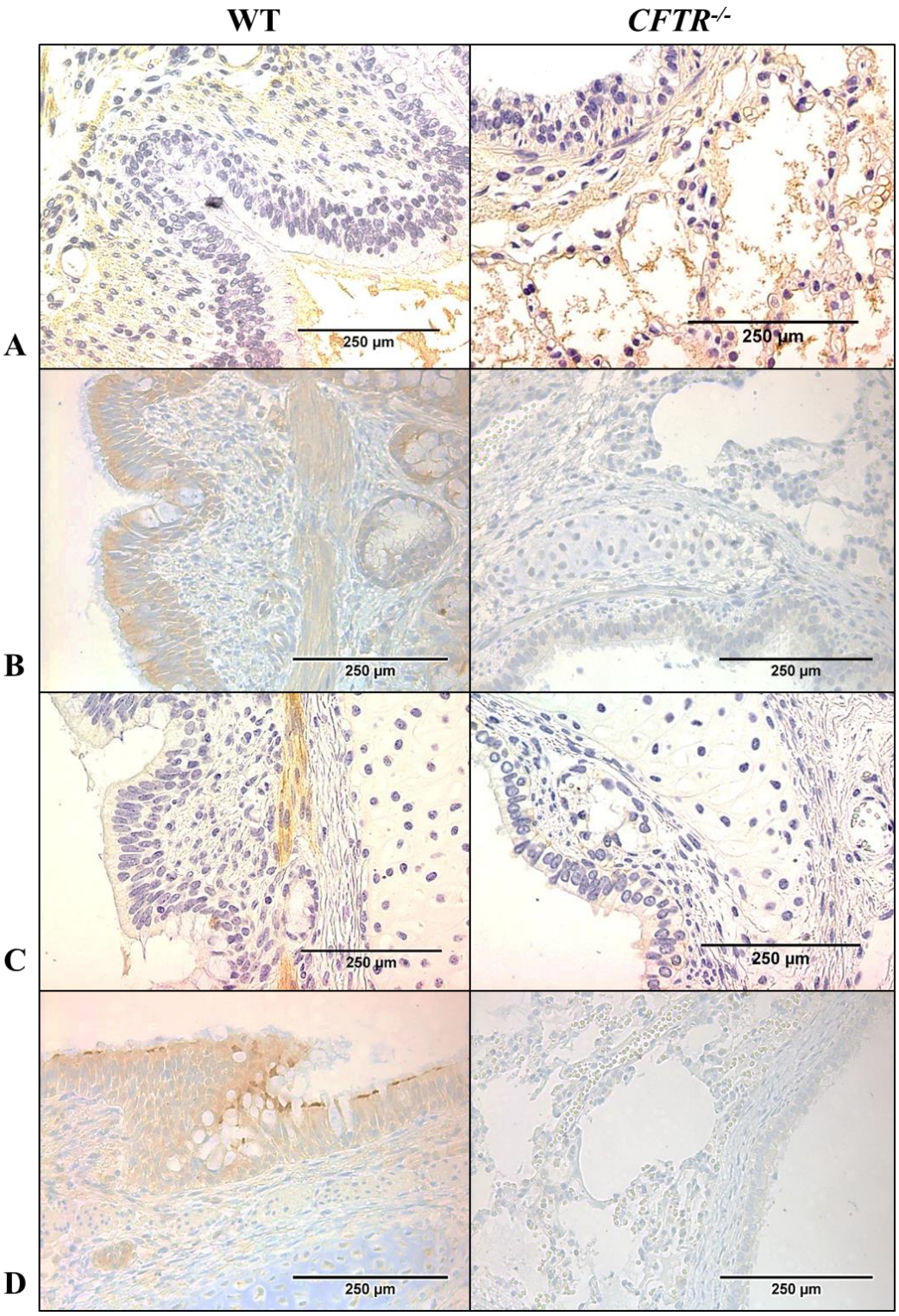

Figure 15: Testing of antibodies on paraffin-embedded lung tissue from WT and *CFTR*$^{-/-}$ piglets. (A) Ab 528 (CF Foundation, USA), 1:900 on methacarn-fixated lung tissue. (B) Ab 596 (CF Foundation, USA), 1:900 on formalin-fixated lung tissue with HIER by water bath. (C) Ab CF3 (abcam, UK), 1:12,000 on

formalin-fixated tissue with PIER by proteinase K. (D) Ab 24-1 (R&D systems, Wiesbaden), 1:900 on formalin-fixated tissue with HIER by pressure cooker.

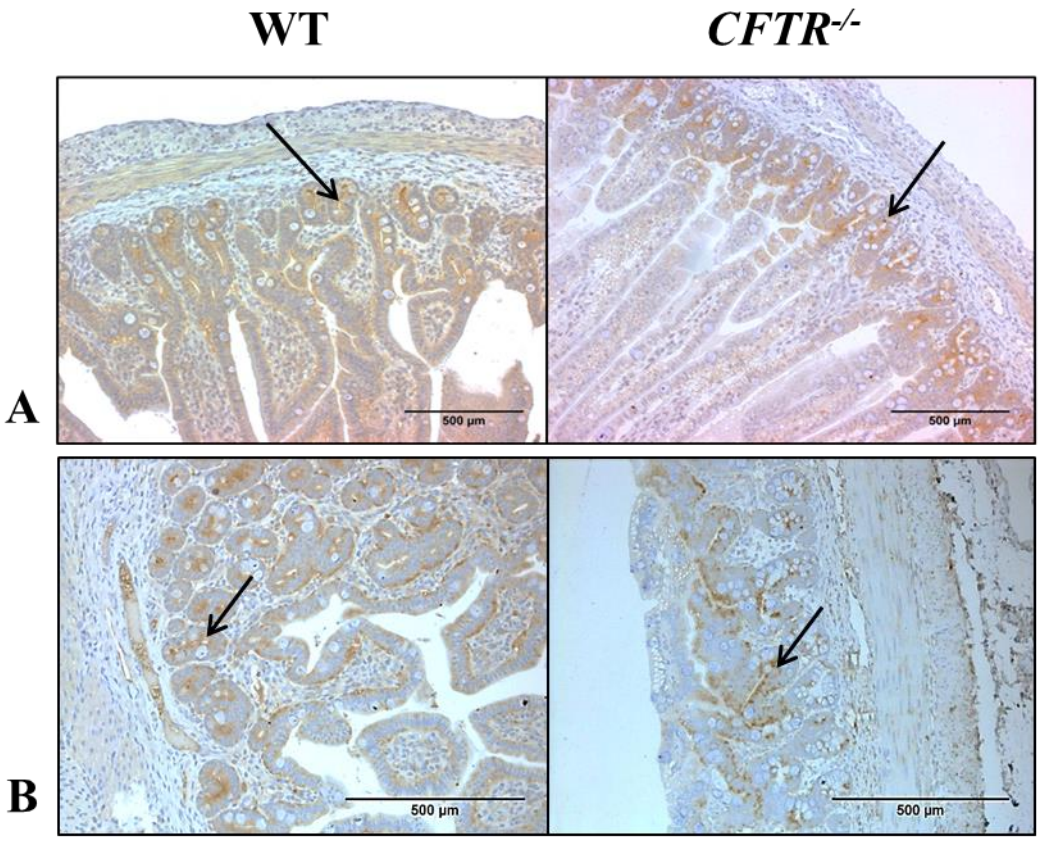

Figure 16: Unspecific staining of CFTR in the intestine of WT and *CFTR*$^{-/-}$ piglets. (A) IHC on formalin-fixated intestinal tissue with HIER by water bath using Ab 596 in a dilution of 1:900. The staining shows the correct pattern, with main localization in the intestinal crypts (marked with a black arrow), but WT and CF KO slides show no difference in staining patterns. (B) IHC on formalin-fixated intestinal tissue with HIER by pressure cooker using ab 24-1 in a dilution of 1:900. Staining shows the correct pattern, but no difference between WT and CF KO tissue.

Detection of CFTR by western blot

The aim of this study was to evaluate whether commercially available antibodies for the detection of CFTR in WB can specifically recognize CFTR in native tissue derived from WT and CF KO piglets. For testing the sensitivity of the antibodies,

protein lysates from pig organs with high (proximal jejunum) and low (lung and heart) expression levels of CFTR were employed for analysis. As all antibodies were designated to detect human CFTR, human liver and T84 cells, a human colon carcinoma cell line with endogenous CFTR expression levels, were additionally used as positive controls. Table 18 gives an overview of the tested primary and secondary antibodies with correspondent dilutions.

None of the tested antibodies specifically recognized the two typical CFTR bands (B band and C band) at about 150 kDa and 180 kDa in porcine tissue lysates. The B band indicates the presence of the core-glycosylated form of the protein and the C band the fully-glycosylated mature form of CFTR (Farinha, Penque *et al*. 2004). Either no bands of the correct size were detected (see Figure 17 (B)) or bands of the correct size were also detected in the negative control, tissue derived from the CF KO piglet (see Figure 17 (A)). Only one antibody, Ab 24-1 (R&D systems, Wiesbaden) gave a specific signal for the detection of endogenous levels of human CFTR in human T84 cells (see Figure 17 (A)).

Table 18: Overview of tested western blot conditions.

Primary antibody	**Dilution**	**Secondary antibody**	**Dilution**
CF Folding consortium Ab 528	1:1,000	HRP goat anti-mouse IgG	1:5,000
CF Folding consortium Ab 570	1:1,000	HRP goat anti-mouse IgG	1:5,000
CF Folding consortium Ab 596	1:2,000	HRP goat anti-mouse IgG	1:5,000
CF Folding consortium Ab 660	1:750	HRP goat anti-mouse IgG	1:5,000
CF Folding consortium Ab 769	1:1,000	HRP goat anti-mouse IgG	1:5,000
Cell Signaling #2269	1:1,000	HRP goat anti-rabbit IgG	1:2,000
Abcam CF3	1:1,500	HRP goat anti-mouse IgG	1:5,000
R&D 24-1	1:400	HRP goat anti-mouse IgG	1:5,000
Santa Cruz H 182	1:1,200	HRP goat anti-rabbit IgG	1:2,000
Santa Cruz N-20	1:200	HRP mouse anti-goat IgG	1:5,000

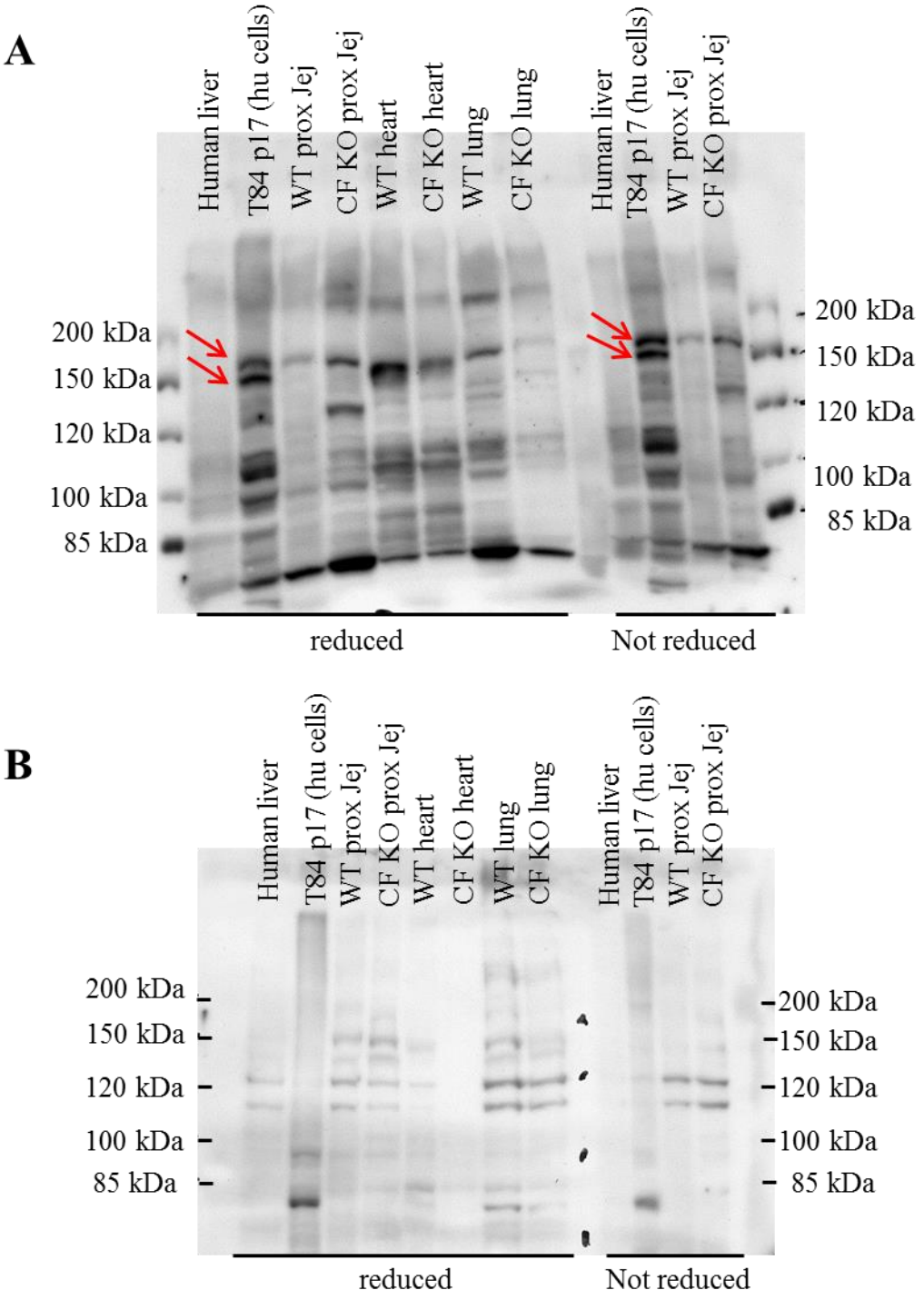

Figure 17: Detection of CFTR by WB. (A) Detection of CFTR with antibody R&D 24-1. The sharp B band and C band (red arrows) typical for the core- and fully glycosylated CFTR protein are detected in protein lysate from human T84 cells. In porcine tissue, bands of the size of the C band are detected both in WT and CF KO piglets. (B) Detection of CFTR with antibody Ab 528. No bands of the correct size are detected.

1.6. Expression analysis of gut-modified *CFTR*$^{-/-}$ piglets at the RNA level

The detection of endogenous CFTR protein levels by immunological methods proved to be difficult, limited by both specificity and sensitivity of the available antibodies. Thus, the expression levels of *CFTR* were examined at the more sensitive mRNA level. To assess whether gut-modified *CFTR* is transcribed into mRNA and whether gut-modified *CFTR* transcripts are restricted to the intestine, the expression level of gut-modified *CFTR* in different parts of the intestine, lung, trachea, heart, liver, kidney and pancreas was measured using qPCR. To determine the expression levels of *CFTR* in WT animals, another qPCR was set up for the detection of endogenous *CFTR* transcripts. In addition, gut-modified CFTR expression was compared to the transcript level of *FABP2*, whose promoter was used to drive the transgene. To enable a comparison between different animals and organs, the expression of *TBP2*, a lowly expressed housekeeping gene coding for the transcription factor TATA-box binding protein 2, was determined.

The comparison of two methods for the isolation of RNA from tissue, the RNA isolation with Trizol® and the Direct-zol™ RNA MiniPrep Kit revealed that the purity and concentration of the extracted RNA was higher when RNA was isolated with Trizol®. The quality of RNA and cDNA was controlled at different levels. RNA concentration and purity were measured with a photometer and only if the ratios for the wavelengths 260 nm/ 280 nm and 260 nm/ 230 nm were above 1.8 and 1.9, respectively, the RNA was employed for cDNA synthesis. The integrity of RNA was assessed by electrophoresis on a denaturating RNA gel; RNA of good overall quality exhibited sharp 28S and 18S ribosomal RNA bands with an approximate intensity of 2:1 under UV light. Degraded RNA appeared as a smear and was not employed for any further analysis (see Figure 18 (A)).

The integrity of cDNA and the possible contamination with gDNA was assessed in a PCR amplifying a part of the ubiquitously expressed housekeeping gene *beta-actin.* Compared to the RevertAid Reverse Transcriptase, the intensity of bands in the control actin-PCR on cDNA appeared stronger when the SuperScript™ III Reverse Transcriptase was used for cDNA synthesis, implying a more efficient reverse transcription. Only if sharp bands were detected in the samples containing cDNA template and the samples containing the DNase digest were clearly negative, cDNA was employed for further qPCR analysis (see Figure 18 (B)).

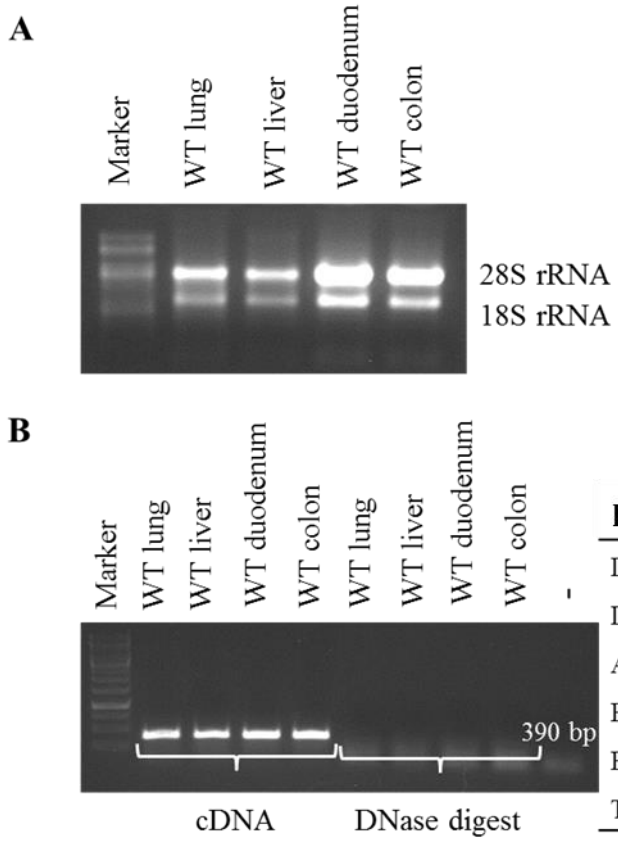

pAct954f/pAct1919r 0.5 µL			
Denaturation	95 °C	5 min	
Denaturation	95 °C	30 s	35 x
Annealing	60 °C	30 s	
Elongation	72 °C	30 s	
Elongation	72 °C	10 min	
Termination	4 °C	15 min	

Figure 18: Quality assessment of RNA and cDNA. (A) Assessment of RNA integrity using a denaturating RNA gel. Overall quality of loaded RNA samples appears to be good, as sharp 28s and 18s bands in an approximate ratio of 2:1 are visible. (B) *beta-actin* PCR on cDNA and corresponding DNase digest templates. cDNA as template gives sharp bands, whereas DNase digest samples are negative, indicating no contamination with gDNA.

Primers for qPCR were first evaluated in endpoint-PCR. Primers for the detection of gut-modified *CFTR* were already tested for genotyping (see Figure 10) and the utility of primers for the amplification of *TBP2* was already proven in previous studies. Primers for the detection of *CFTR* were designed to anneal to the 3'-UTR or 5'-UTR regions of *CFTR* that are distinct between endogenous and transgenic *CFTR*. However, all primers tested for the detection of endogenous *CFTR* also amplified unspecific products and were therefore not suitable for the determination of endogenous *CFTR* (see Figure 19 (A) and (B)). Therefore, the exon-spanning primers Lars2f and Lars2r, lying within the coding region of *CFTR*, were utilized, enabling a direct comparison of *CFTR* expression between WT and gut-modified CF animals (see Figure 19 (C)). For the detection of *FABP2* expression, exon-spanning primers were evaluated (see Figure 20) and the best primer pair 6, FEqf2 and FEqr3 was finally utilized for qPCR.

Final conditions such as primer volumes, annealing temperature and duration of PCR steps were optimized in the qPCR by comparing the slopes of standard curves that were calculated from serial dilutions of cDNA templates. If the linear regression analysis showed a high coefficient of determination ($R^2 > 0.98$) and the slope of the standard curve was approximately -3.32 (equivalent to an amplification efficiency of 100 %), these conditions were used for the determination of the correspondent genes. Final optimized conditions are given in Table 19.

A

	Endogenous *CFTR* primer pairs		
	Primer f	Primer r	length
1	CEqf1	CEqr1	240 bp
2	CEqf2	CEqr1	100 bp
3	CEqf2	CEqr2	190 bp
4	CEqf2	CEqr3	220 bp
5	CEqf3	CEqr2	120 bp
6	CEqf3	CEqr3	150 bp
7	CEqf11	CEqr11	90 bp
8	CEqf14	CEqr14	115 bp

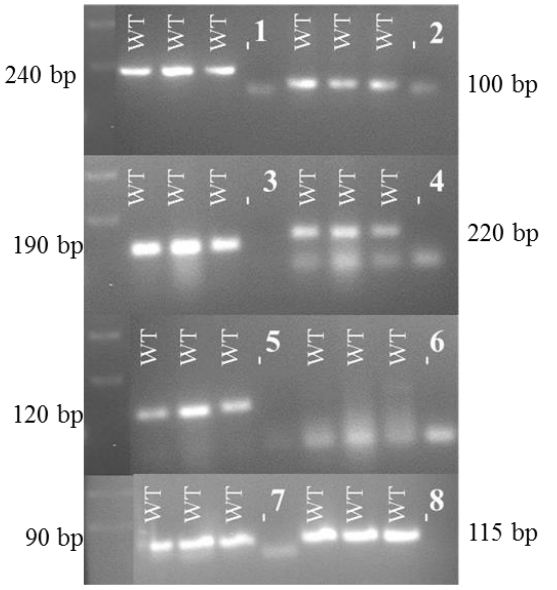

B

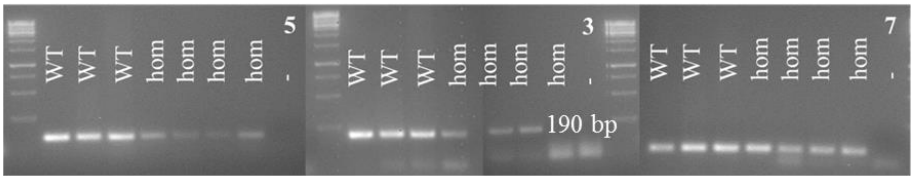

C

	CFTR primer pairs		
	Primer f	Primer r	length
9	Lars1f	Lars1r	450 bp
10	Lars2f	Lars2r	120 bp

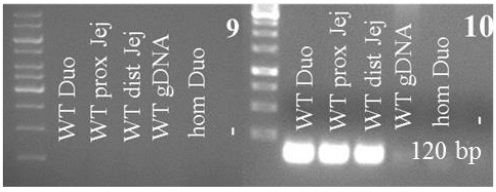

Figure 19: Testing of primer pairs for the detection of *CFTR* in qPCR. Primer pairs were first tested with an annealing temperature of 58 °C and a starting volume of 0.5 µL each. (A) Primer pairs for the detection of endogenous *CFTR* were tested first with WT gDNA as template. (B) Specificity of promising primer pairs was evaluated with gDNA from WT and *CFTR*$^{-/-}$ piglets (hom) as template. All primer pairs amplify a product both in WT and *CFTR*$^{-/-}$ piglets. (C) Exon-spanning primer pairs 9 and 10 are designed to amplify products lying within the coding region of *CFTR*. Primer pair 10 detects a specific band in cDNA isolated from WT intestine (duodenum (Duo), proximal jejunum (prox Jej) and distal jejunum (dist Jej)), but not in gDNA or in cDNA from the duodenum of *CFTR*$^{-/-}$ piglets (hom Duo).

	FABP2 primer pairs		
	Primer f	Primer r	length
1	FEqf1	FEqr1	90 bp
2	FEqf1	FEqr2	100 bp
3	FEqf1	FEqr3	220 bp
4	FEqf2	FEqr1	85 bp
5	FEqf2	FEqr2	90 bp
6	FEqf2	FEqr3	220 bp
7	FEqf3	FEqr4	190 bp

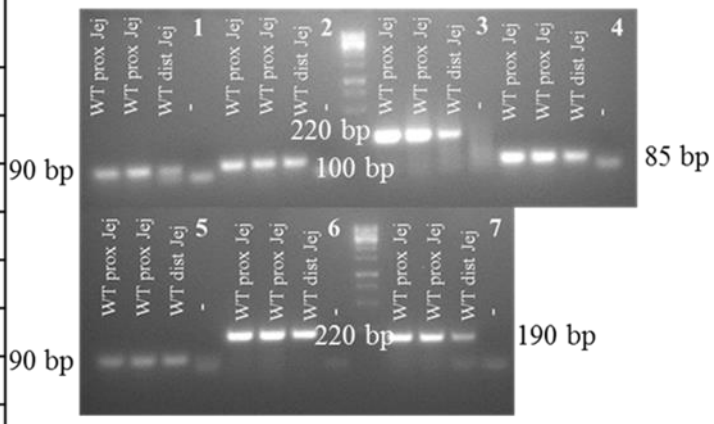

Figure 20: Testing of primer pairs for the detection of *FABP2* in qPCR. Primer pairs were first tested with an annealing temperature of 58 °C and a starting volume of 0.5 µL each. Exon-spanning primers were tested with WT cDNA from intestinal tissue material (proximal jejunum (prox Jej) and distal jejunum (dist Jej)).

Table 19: Final conditions for qPCR.

Gene	Primer pair	Concentration	Annealing temperature	Annealing time
TBP2	tbpf/tbpr	0.7 µL	63 °C	60 s
FABP2	FEqf2/FEqr3	0.3 µL	60 °C	30 s
gutCFTR	CFgutf2/CFgutr2	0.6 µL	65 °C	30 s
CFTR	Lars2f/Lars2r	0.8 µL	63 °C	60 s

The expression level, measured in copies per ng RNA inserted into cDNA synthesis, was calculated for each examined gene from C_t -values and the PCR efficiency derived from the slopes of standard curves. The measurement of the expression of the housekeeping gene *TBP2* served as internal quality control. Especially the integrity of cDNA from pancreatic tissue was evaluated on the basis of the *TBP2* expression. If no *TBP2* expression was detected in a specific organ sample, the cDNA was not further analyzed. The expression of *TBP2* was approximately within the same range of several hundred copies per ng RNA for all examined organs and genotypes (see Figure 21).

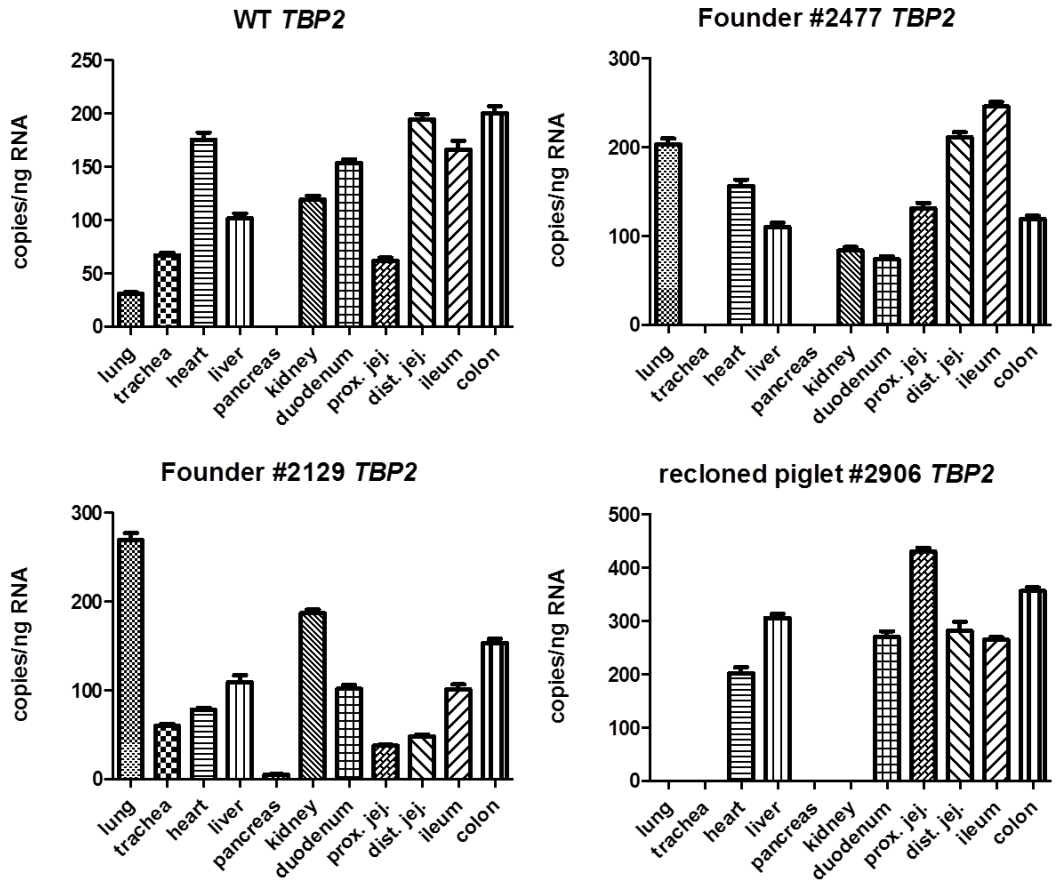

Figure 21: Expression levels of *TBP2* in different organs and genotypes. Expression levels of *TBP2* in copies per ng RNA inserted in cDNA synthesis are calculated from C_t-values and PCR efficiency. The exemplary graphs show that in cDNA from pancreatic or tracheal tissue of several animals no expression of *TBP2* is detected, meaning that cDNA synthesis unsuccessful.

The *FABP2* expression was investigated for the evaluation of the utility as intestine-specific promoter for the gut-modified construct. The expression pattern of *FABP2* did not differ among different genotypes. As expected, expression levels lying within a range of several hundred to several thousand copies per ng inserted RNA could be detected throughout the small intestine. Expression levels increased from the duodenum to the proximal parts of the jejunum, where the highest levels of mRNA expression were determined. From the proximal jejunum to the ileum, a clear decline of the *FABP2* expression was observed (see Figure 22). In the other examined organ systems, as well as in the colon, no quantifiable amount of transcripts was measured. It is of note; that *FABP2* expression was

consistently higher in the intestine of CF KO or gut-modified CF piglets, correlating with the suggested suitability of increased *FABP2* levels as marker for epithelial intestinal damage (Schellekens, Grootjans *et al*. 2014).

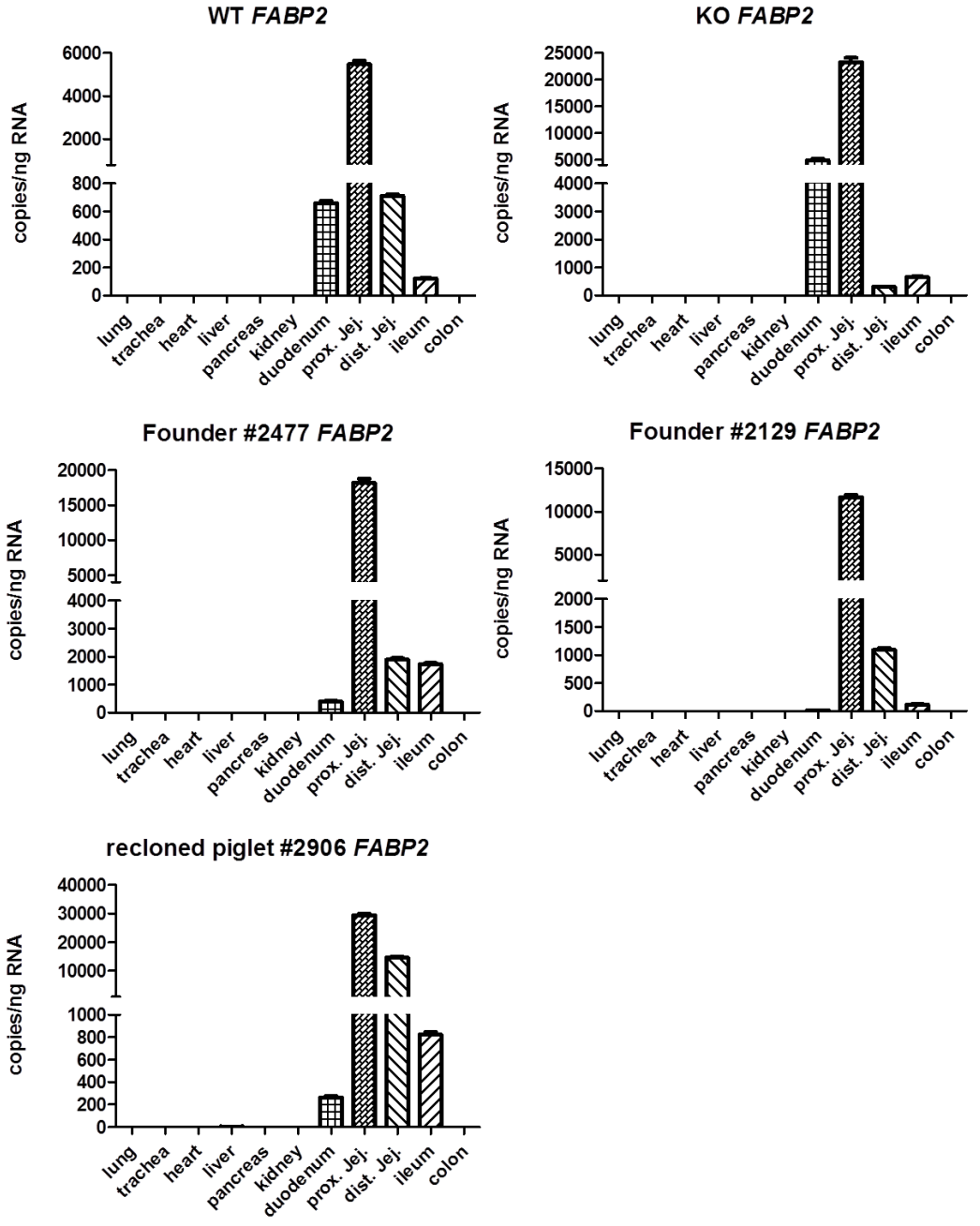

Figure 22: Expression levels of *FABP2* in different organs and genotypes. Expression levels of *FABP2* in copies per ng RNA inserted in cDNA synthesis are calculated from C_t -values and PCR efficiency. *FABP2* expression shows a consistent pattern throughout all examined genotypes. Expression levels increase

from duodenum to proximal jejunum, where the highest levels are detected, and decrease up to the ileum. In the colon, no quantifiable expression can be measured.

Expression levels of the gut-modified *CFTR* construct were examined in eight founder animals and two recloned piglets. In WT and CF KO piglets, no quantifiable amount of expression was detected. In five founder animals (#2128, 2130, 2477, 2480 and 2482) and in the recloned piglets (#2870 and 2906), expression of gut-modified *CFTR* was limited to the small intestine, with the highest expression levels in the proximal parts. This expression level corresponded to the expression of *FABP2*. Three founder animals (#2129, 2479 and 2736) showed expression of the gut-modified construct throughout all the examined organ systems, although the expression levels in the intestine were higher compared to other organs (see Figure 23).

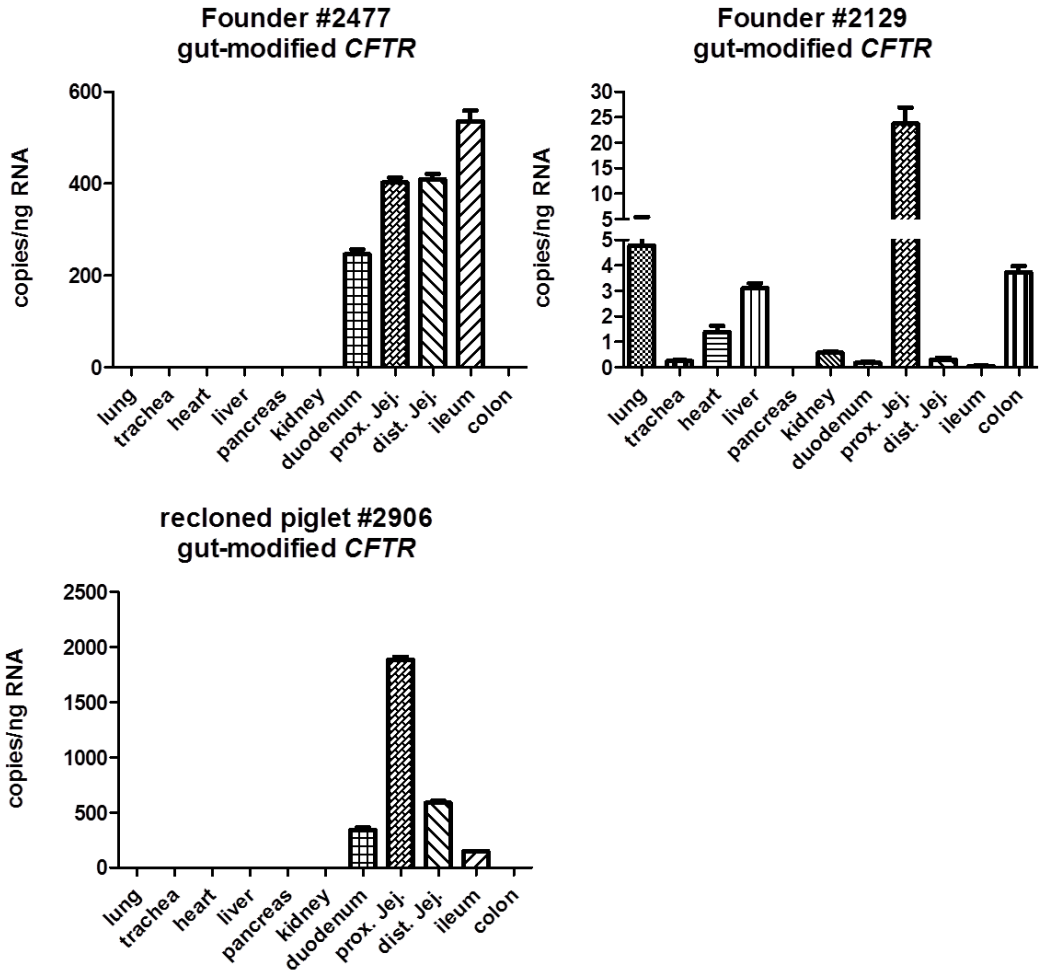

Figure 23: Expression levels of gut-modified *CFTR* in founder animals and recloned piglets. Expression levels of gut-modified *CFTR* in copies per ng RNA inserted in cDNA synthesis are calculated from C_t -values and PCR efficiency. In founder #2477 and recloned piglet #2906, the expression of gut-modified *CFTR* is limited to the small intestine (duodenum, proximal and distal jejunum and ileum). Founder #2129 shows expression in all examined organs, with the highest levels in the proximal jejunum.

For direct comparison of *CFTR* expression in WT and gut-modified CF animals, the expression of a part of the coding region found in both genotypes was analyzed. In CF KO animals, no *CFTR* expression was measurable. The overall expression level of *CFTR* in WT animals was relatively low, lying within a range of several hundred copies per ng inserted RNA for the proximal parts of the small intestine, where the highest expression levels were detected. The whole intestine was the organ with the highest expression levels, showing a strong decline from the duodenum to the colon (see Figure 24 (A)). In the airways, only very small amounts of *CFTR* were expressed. *CFTR* expression in gut-modified *CFTR*$^{-/-}$ piglets corresponded to the expression of gut-modified *CFTR* in terms of organ expression patterns. In five founder animals (#2128, 2130, 2477, 2480 and 2482) and in the recloned piglets (#2870 and 2906), expression of *CFTR* was limited to the small intestine. Three founder animals (#2129, 2479 and 2736) showed expression of *CFTR* in all examined organs. *CFTR* expression levels were negatively correlated with the severity of the intestinal phenotype. Founder #2477 and recloned piglet #2906 showed the strongest *CFTR* expression levels of all examined animals. The correlation of *CFTR* expression pattern and expression levels of these two animals with their intestinal phenotype revealed that the severity of MI was less pronounced when the expression levels of *CFTR* were higher in the distal parts of the small intestine (see Figure 24). However, even in these piglets, the expression levels of *CFTR* were not sufficient to rescue them from the lethal intestinal obstruction and to ensure their survival.

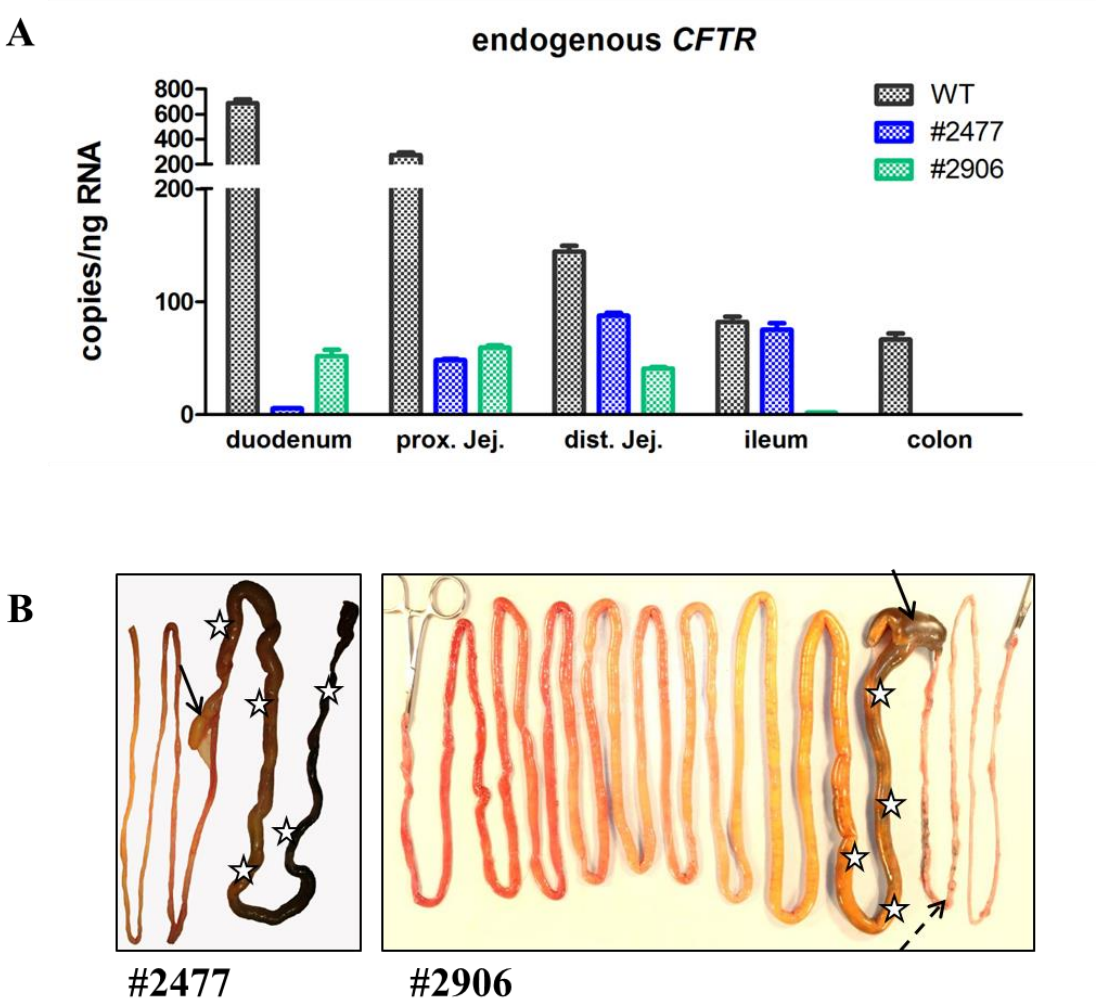

Figure 24: Comparison of *CFTR* expression levels to the intestinal phenotype. (A) Expression levels of *CFTR* in the intestinal tract of WT piglets and the two highest-expressing gut-modified CF piglets. Expression levels of *CFTR* in copies per ng RNA inserted in cDNA synthesis are calculated from C_t -values and PCR efficiency. In the WT piglet, *CFTR* expression levels decrease from duodenum to colon. Piglet #2477 shows the highest levels in the distal parts of the small intestine, in piglet #2906, expression levels of *CFTR* are the highest in the proximal parts of the small intestine. (B) Correlation of *CFTR* expression with intestinal phenotype. The cecum is marked with a black arrow, asterisks indicate the localization of MI. The discontinuous black arrow points to the microcolon. In piglet #2477, meconium has passed through the normal-sized cecum and is stuck in the colon with a normal diameter, in piglet #2906, the meconium is stuck in the distal parts of the jejunum and the enlarged cecum, the colon appears atretic.

To confirm that primers used for qPCR amplified the correct products, a melt curve analysis was performed following each qPCR run (data not shown) and the PCR products were sequenced via the Sanger approach (see Figure 25). The correct amplification of the primers used for the determination of gut-modified *CFTR* had already been proven. All amplified sequences showed 100 % identity with the target sequences. Sequencing confirmed that very low levels of *FABP2* are also expressed in other organs apart from the intestine.

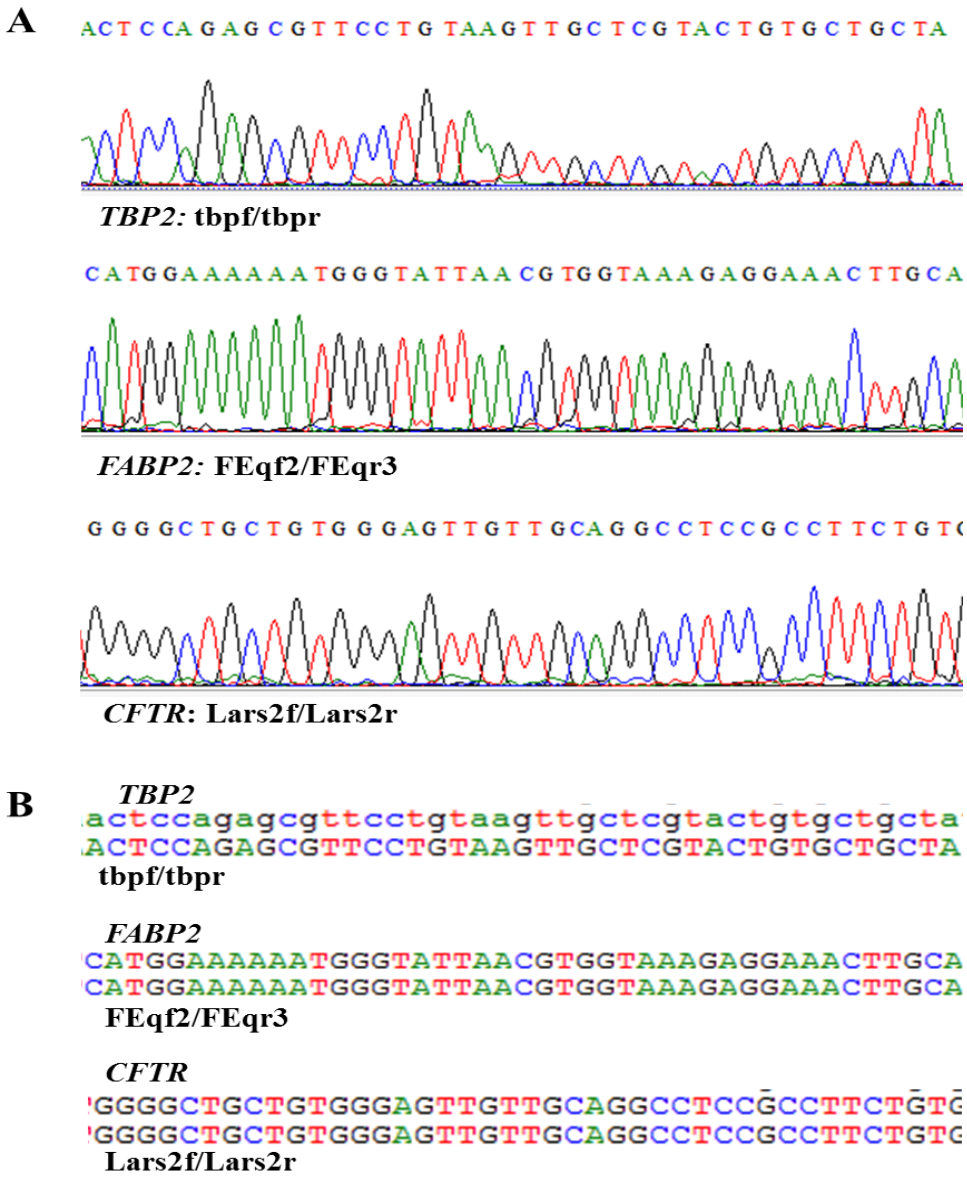

Figure 25: Sequencing of qPCR products. (A) Extract of electropherograms from the sequenced qPCR products. (B) Comparison of amplified sequences and target sequences.

2. Modifier genes contribute to the severity of meconium ileus in *CFTR*$^{-/-}$ piglets

As is known, the severity of the intestinal phenotype in human CF patients is strongly influenced by modifier genes either increasing or decreasing the susceptibility for MI (Blackman, Deering-Brose *et al*. 2006). Therefore, the second approach for the rescue of the lethal intestinal phenotype in CF KO piglets was to study if modifier genes might also play a role in the development of MI in the porcine CF model.

2.1. Establishment of a breeding herd for the production of WT, *CFTR*$^{+/-}$ and *CFTR*$^{-/-}$ piglets

In order to examine whether there was a naturally occurring variability in the severity of MI in CF KO piglets, the intestinal phenotype of a large number of CF KO piglets had to be analyzed. By selective mating of female and male *CFTR*$^{+/-}$ pigs, litters containing piglets of all genotypes were produced for different collaboration projects. To minimize inbreeding, mating between littermates was avoided if possible. In 35 litters with 10.4 animals per litter on average, a total of 364 piglets were born. Approximately following the Mendelian rules, 99 piglets were WT (27.2 %), 91 piglets were CF KO (25 %) and 174 piglets were *CFTR*$^{+/-}$ (47.8 %). It is of note, that in contrast to data reported for male humans carrying one *CFTR* mutation (Mak, Zielenski *et al*. 1999), we could not observe any problems with reduced fertility or infertility in the *CFTR*$^{+/-}$ breeding boars.

Experiments on mucus transport in explanted WT and *CFTR*$^{-/-}$ airways

The main part of CF piglets was produced, genotyped and used for tissue sampling to study mucociliary clearance in explanted tracheas by Anna Ermund and Gunnar C. Hansson from the Mucin Biology Group at the University of Gothenburg. The video microscopy imaging of living tracheal tissue showed that the airways were cleaned by mucus in strands that move towards the larynx and not by a continuous mucus layer. In CF KO airways, mucus strands are

transported with a much slower velocity compared to WT airways - a feature that can be imitated in WT airways when bicarbonate is removed from the Krebs buffer (see Figure 26).

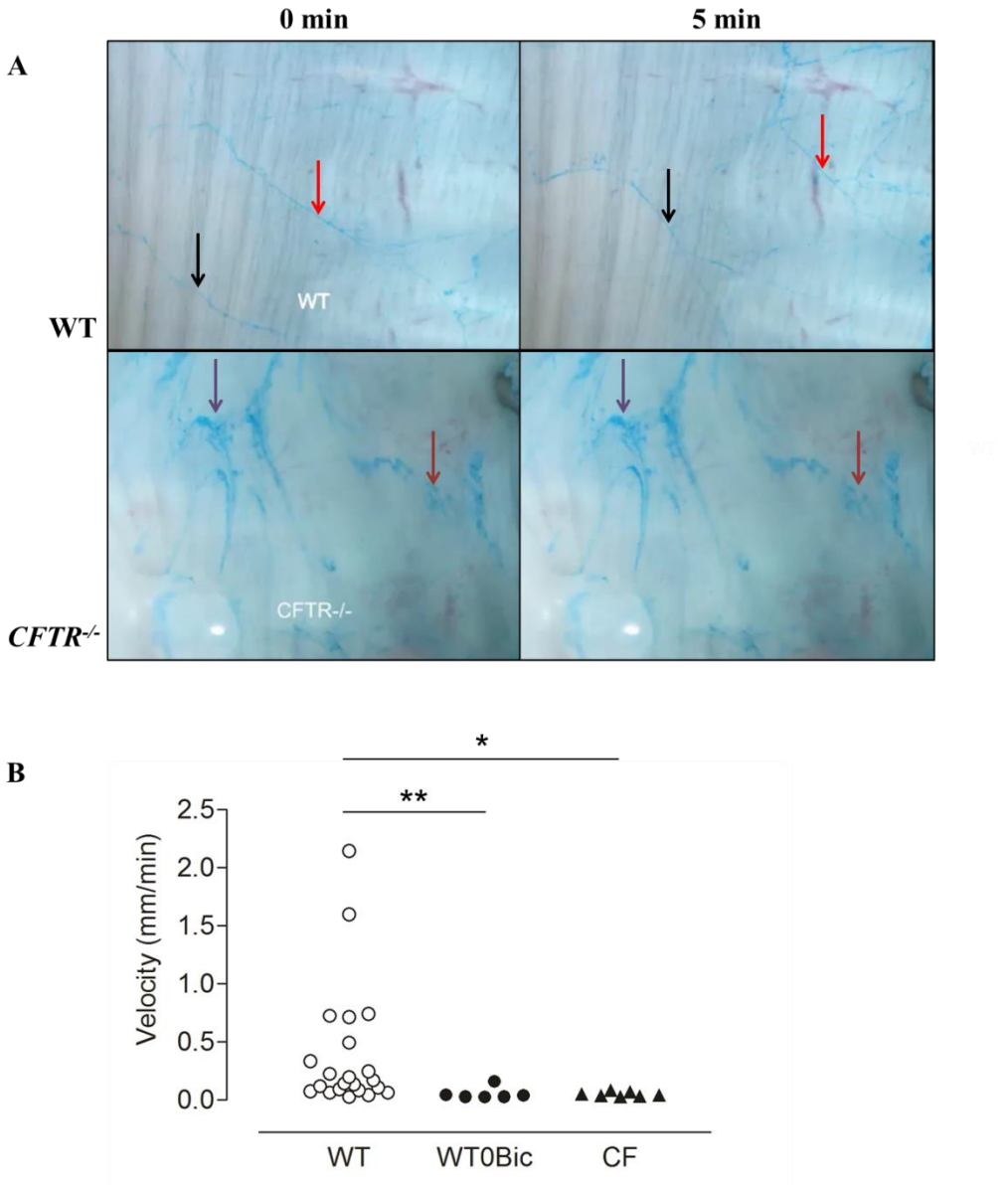

Figure 26: Video microscopy imaging of living WT and *CFTR*$^{-/-}$ tracheal tissue. (A) Mucociliary clearance in living tracheal tissue; first and last frame from video microscopy imaging. Mucus is stained by Alcian blue, arrows of the same color point to identical strands. Mucus does not form a continuous layer but forms strands. Within a period of 5 min, mucus strands have moved in the WT trachea but not in the trachea of CF KO piglets. (B) Calculation of transport

velocity of strands. Statistics calculated with Kruskal-Wallis non-parametric test. Each data point represents the mean of several time lapses of one animal. Data provided by Anna Ermund, Mucin Biology Group, University of Gothenburg.

Mucus strands are secreted by submucosal glands and should therefore mostly consist of Mucin 5b (Muc5b), that is expressed by mucous cells in the submucosal glands and by goblet cells of the surface epithelium (Meyerholz, Lambertz *et al*. 2015). However, immunofluorescent studies with antibodies for Mucin 5ac (Muc5ac) and Muc5b and scanning electron microscopy revealed that mucus strands released by submucosal glands were coated by mucus from goblet cells of the surface epithelium. As goblet cells mainly express Muc5ac, similar amounts of Muc5ac and Muc5b are found in the airway mucus. In terms of mucus secretion and mucin contents, WT and CF KO mucus in the trachea do not differ (see Figure 27).

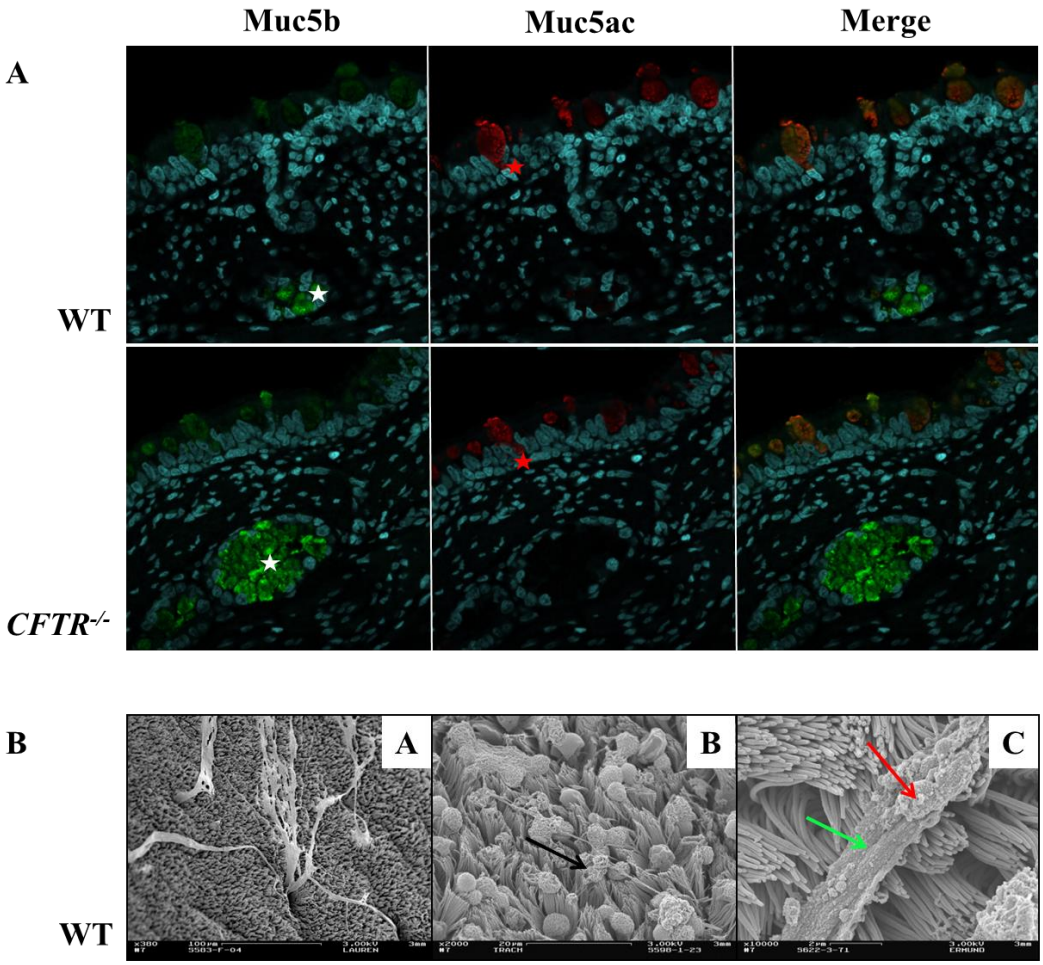

Figure 27: Secretion and composition of airway mucus. (A) Muc5b and Muc5ac staining of WT and CF KO trachea. Nuclear counter stain is performed with Hoechst. Both in WT and CF KO trachea, Muc5b is expressed mainly in mucous cells from submucosal glands (marked with white asterisks), but also in goblet cells of the surface epithelium (marked with red asterisks), Muc5ac is expressed by goblet cells. In both genotypes, mucus strands contain Muc5b and Muc5ac. (B) SEM of WT airways. Mucus strands are released from submucosal glands (A), strands in contact with goblet cells are marked with black arrow (B). Muc5b strands (marked with green arrow) are coated with Muc5ac (marked with red arrow) (C). Data provided by Anna Ermund, Mucin Biology Group, University of Gothenburg.

2.2. Finding *CFTR*$^{-/-}$ piglets with an improved intestinal phenotype

Among a total of 91 CF KO piglets that had been produced by conventional breeding, we found three piglets (#2850, 3137 and 4424) that showed a clearly improved intestinal phenotype when examined after sacrificing. In these piglets, the meconium had passed through the cecum and was stuck in the middle to distal parts of the colon. In addition, the size and diameter of the colon was similar to a WT colon with no signs of a microcolon and no diverticulosis at the mesenterial side of the intestine was detected (see Figure 28). To clarify the relevance of the genetic background for this naturally occurring considerable improvement of the intestinal phenotype, we followed two distinct strategies, one hypothesis-driven "candidate gene" approach and the unbiased "whole-genome" approach. We tested if mutations in the *CLCA4b* gene might have an impact on the severity of MI and searched for single nucleotide polymorphisms (SNPs) in a genome-wide analysis of the three improved piglets and other CF KO animals.

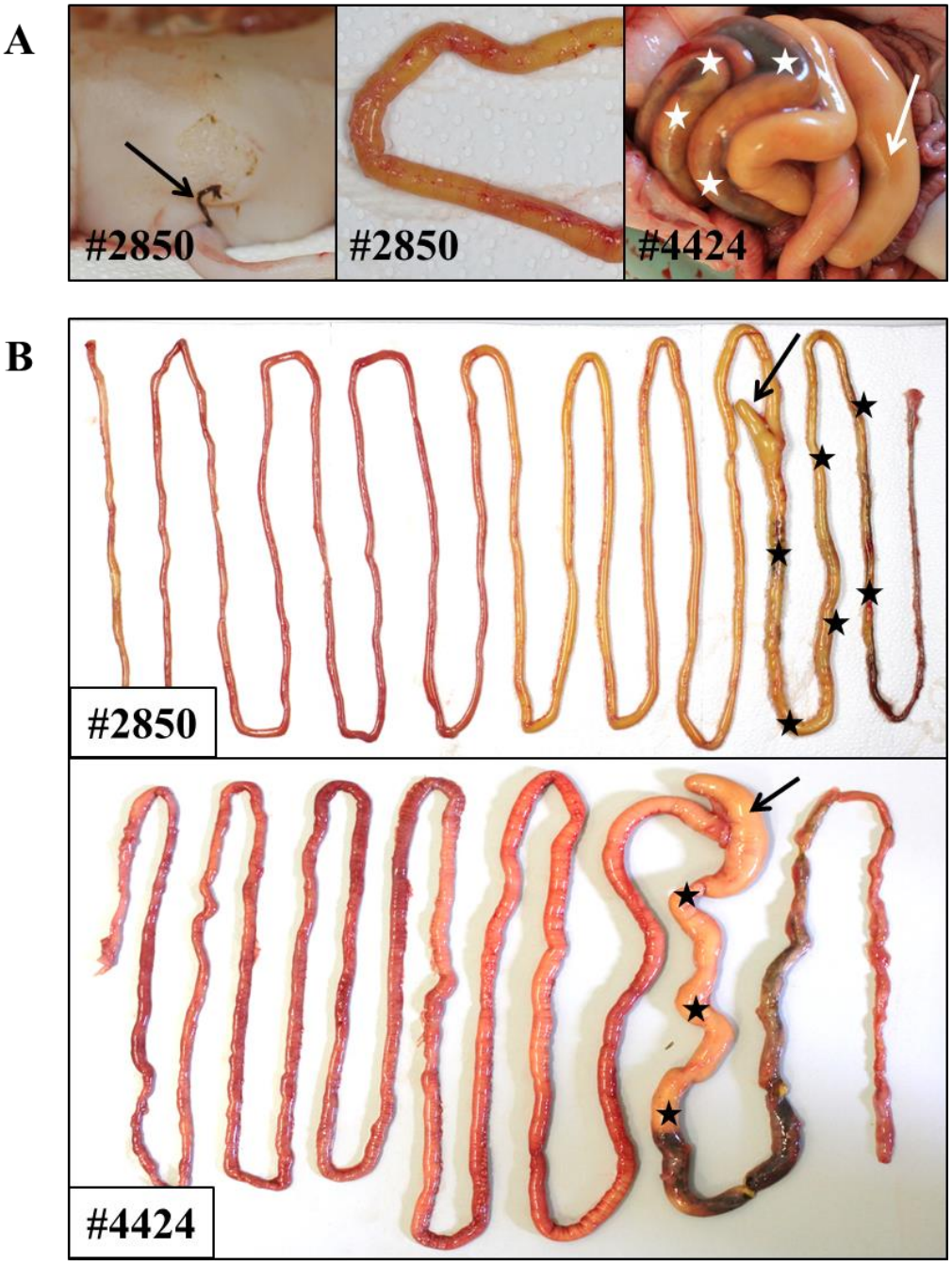

Figure 28: Improved intestinal phenotype in *CFTR*$^{-/-}$ piglets. (A) Features of improvement. Small parts of the meconium are removed naturally (black arrow points to removed meconium) and no herniation of mucosa is detected at the mesenterial side of the intestine. After opening the abdomen, it becomes obvious that the cecum (white arrow) is enlarged but filled with milk, and meconium is visible in the colon gyri (white asterisks). (B) Intestine laid out in full length. Meconium passed through the cecum (black arrow) and milk is found in the

proximal to middle parts of the colon (black asterisks). The diameter of the colon is enlarged in comparison to “normal” CF KO piglets.

Influence of *CLCA4b* integrity on meconium ileus severity in *CFTR*$^{-/-}$ piglets

CLCA4 is known to modulate residual chloride conductance in the intestine of human CF patients (Kolbe, Tamm *et al*. 2013). In the pig genome, a naturally occurring duplication, *CLCA4b,* occurs, that is especially abundant in intestinal cells and co-expressed with CFTR. A large percentage of the pig population has a deleterious mutation within this gene. The 10 bp deletion leads to a loss of the WT splice acceptor site in intron 7, resulting in alternative splicing to a sequence 38 bp upstream of exon 8. This causes a frameshift in protein translation and generates a premature stop codon in exon 8 (see Figure 29 (A)) (Plog, Klymiuk *et al*. 2015). We examined if there was correlation between the *CLCA4b* integrity and the improved intestinal phenotype in the three CF KO piglets. Three primer pairs amplifying the region containing the mutation were compared and primer pair CLCA4b2f/CLCA4b2r was ultimately utilized for PCR (see Figure 29 (B)). Sequencing the candidate region of *CLCA4b* in two of the three improved CF KO piglets (#2850 and #3137) and 15 other CF KO piglets revealed that piglet #2850 was homozygous for the deletion in *CLCA4b*, whereas piglet #3137 was heterozygous. Three other examined CF KO piglets without improved phenotype were homozygous for the deletion, eight heterozygous and in four CF KO piglets only WT alleles were detected. These results indicate that the deletion in *CLCA4b* has no effect on the severity of MI and that *CLCA4b* is therefore no potential modifier gene for the intestinal phenotype in the porcine CF model.

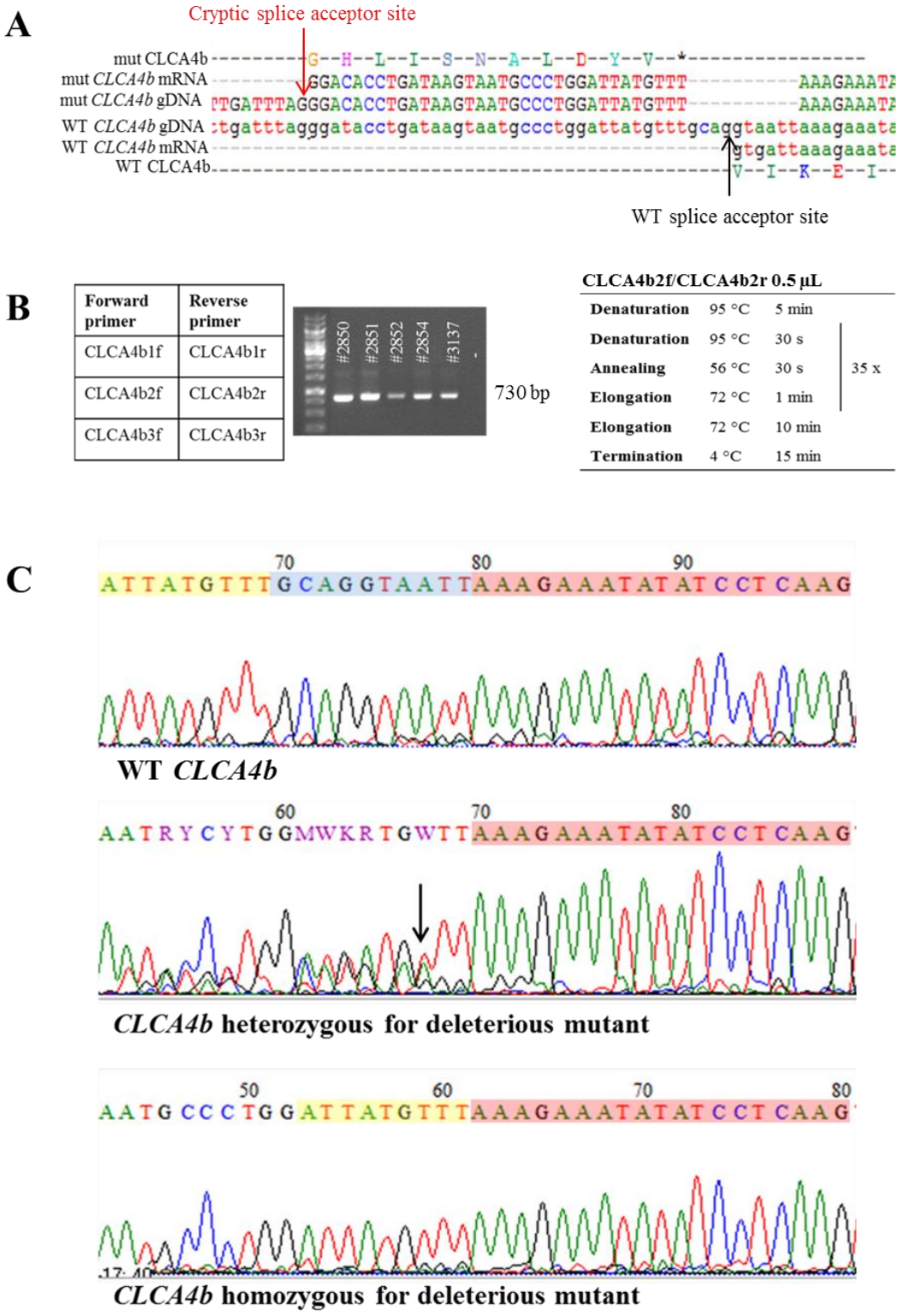

Figure 29: Sequencing of the candidate region in *CLCA4b*. (A) Deletion in *CLCA4b* causes alternative splicing (WT and cryptic splice acceptor sites are marked with a black and red arrow, respectively) and the transcription of a protein with a premature stop codon (marked with asterisk). (B) Testing of primers for the

amplification of the region of *CLCA4b* holding the deleterious mutation. Primers were tested first with a volume of 0.5 µL each and an annealing temperature of 58 °C. Conditions for the PCR utilizing primer pair 2. (C) Excerpt of electropherograms from WT, heterozygous and homozygous piglets. For sequencing purposes, the reverse primer CLCA4b2r was used. Regions at the 5'- and 3'-side of the deletion (10 bases missing in the mutant sequence are highlighted in blue) are highlighted in yellow and red. In the piglets heterozygous for the mutation, characteristic double peaks (see black arrow) are seen at the 5'-side of the red sequence. The first two red peaks at position 68 and 69 are distinct as the first bases at the 3'-side in both the deletion and the yellow sequence are thymidine.

Finding candidate loci that are linked to the improved intestinal phenotype

For a precise description of the degree of relationship between the three CF KO piglets with the improved intestinal phenotype, a pedigree containing all the ancestors and littermates of these three piglets was created. DNA was isolated from the three piglets, all CF KO littermates and the parents and grandparents if stored tissue samples were available and subsequently employed for a genome-wide survey of single nucleotide polymorphism (SNP) variations using the PorcineSNP60 DNA Analysis Kit v2 (Illumina, USA). SNP typing was performed by Doris Seichter, Tierzuchtforschung e.V. München (TZF Grub, Germany) and data was analyzed by Sophie Rothammer and Ivica Medugorac, Chair of Animal Genetics and Husbandry, Faculty of Veterinary Medicine, LMU Munich.

SNP typing revealed that there are two potential modifier loci on chromosome 10 (25.8–25.9 Mb) and on chromosome 16 (4.7–5.2 Mb). The three improved piglets showed homozygosity for a specific haplotype at both loci. CF KO piglets #3343 and #3344 were homozygous for the same haplotype detected in the three improved piglets on chromosome 10 but not on chromosome 16. CF KO piglets #3142, #3146 and #3539 were homozygous for the same haplotype detected in the three improved piglets on chromosome 16, but not on chromosome 10 (see Figure 30). This finding indicates that the severity of the intestinal phenotype might be improved in CF KO piglets that are homozygous for specific haplotypes both on chromosome 10 and chromosome 16.

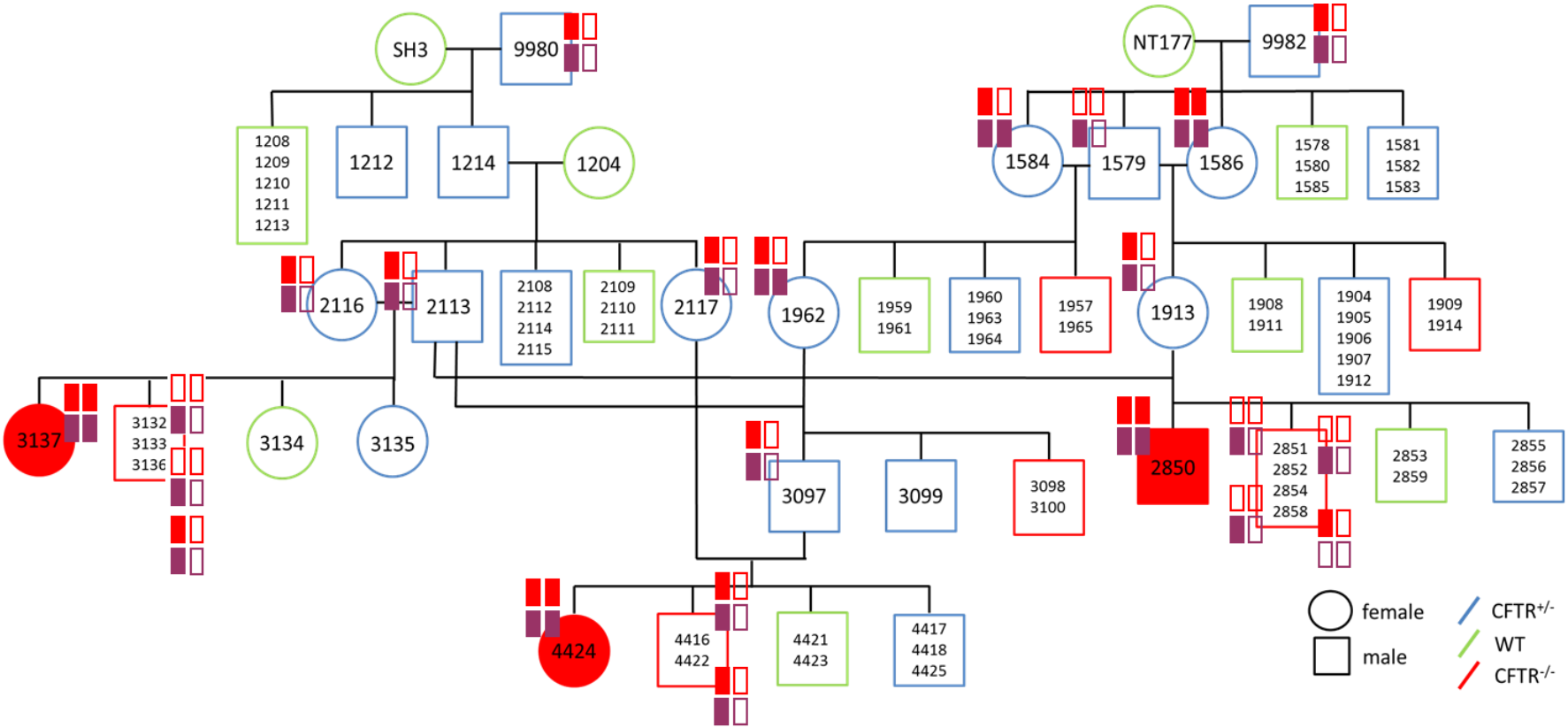

Chr10 25.8-25.9Mb
Chr16 4.7-5.2Mb

Additional CF KO piglets:
(#2113 x #2117 → #3138 – #3147): 4 CF KO: #3138, #3142, #3145, #3146

Corresponding to #2850 (#2113 x #1913 → #3342 – #3354): 4 KO: #3342, #3343, #3344, #3347

Corresponding to #3137 (#2113 x #2116 → #3534 – #3543): 2 KO: #3539, #3543

Figure 30: Pedigree and SNP-typing of three *CFTR*$^{-/-}$ piglets with improved intestinal phenotype. The three improved CF KO piglets #2850, #3137 and #4424 are highlighted in red. Filled and empty boxes indicate the haplotypes of the two alleles (the potential locus on chromosome 10 is highlighted in red, the potential locus on chromosome 16 in purple). The three improved piglets are the only CF KO piglets that are homozygous for a specific haplotype (filled box) for both events.

As we assumed that two separate autosomal recessive events had to combine in order to achieve an improvement of the intestinal phenotype in CF KO piglets, the probability to generate these improved CF KO piglets by mating of *CFTR*$^{+/-}$ pigs was calculated according to Mendelian rules. Only 25 % of a litter are CF KO piglets, therefore, the probability that a piglet is both a CF KO and homozygous for the SNPs found on chromosome 10 and 16, is very low if the parents are not selected for the specific haplotypes (see Table 20). For an efficient production of CF KO piglets that are homozygous for both potential modifiers, it is important for future breeding attempts that all pigs of the breeding herd will be screened for the two candidate loci.

Table 20: Influence of the parents' genotype on the probability to generate *CFTR*$^{-/-}$ piglets with an improved intestinal phenotype.

Genotype of parents		**Probability for piglets homozygous for both events (A/A; B/B)**	**Probability for CF KO piglets homozygous for both events (A/A; B/B)**
P1: A/a; B/b **P2: A/a; B/b**		6.25 %	~1.56 %
P1: A/A; B/b **P2: A/a; B/b**		12.5 %	~3.13 %
P1 A/A; B/b **P2: A/A; B/b**	**P1: A/A; B/B** **P2: A/a; B/b**	25 %	6.25 %
P1: A/A; B/b **P2: A/A; B/B**		50 %	12.5 %
P1: A/A; B/B **P2: A/A; B/B**		100 %	25 %

Parents' (P1 and P2) haplotypes for the two candidate loci A and B are written in capital letters for the desired haplotype and in lowercase for the WT haplotype. Probabilities are calculated according to Mendelian rules.

V. DISCUSSION

Although many important insights into pathological mechanisms have been gained during the last decades and novel forms of therapy have been developed, Cystic Fibrosis still remains a disease that severely reduces the life expectancy of affected patients and thus warrants all the scientific efforts concerning this field (Spielberg and Clancy 2016). Animal models are a unique and essential tool for a better understanding of CF and the testing of new therapeutic approaches. Out of all established animal models for CF, the porcine model shows the closest resemblance to the classic human CF phenotype and thus enables a simplified translation of findings to humans. Studies on neonatal tracheal tissue from CF KO and WT piglets generated by breeding have given important new insights into mucus composition and mucociliary transport in the airways (see Figure 26 and Figure 27) and many collaboration partners are interested in tissue from newborn piglets. However, since not all experiments can be performed on neonatal piglets, the availability of older, living CF pigs is required. For this purpose, the main limitation of the utility of the porcine CF model has to be overcome - the lethal neonatal intestinal obstruction by meconium. In this thesis, two different approaches to rescue the severe intestinal phenotype were evaluated; one approach was the selective transgenic expression of *CFTR* in the intestine, while the second approach investigated the contribution of modifier genes to an improved intestinal phenotype in CF KO piglets. In addition, I characterized the porcine CF model with different molecular biological methods.

The detection of CFTR in the intestine is only successful using one particular antibody under very specific conditions

The investigation of CFTR at protein level proved to be very difficult and it turned out that the detection was only successful in the intestine using one particular antibody, Ab 596, under very specific conditions. Ten commercially available primary antibodies that were described to detect porcine CFTR were

evaluated for their specificity and sensitivity in paraffin-embedded and frozen sections. In general, the advantages of frozen sections are that the antigenicity is often better preserved, whereas the tissue and cellular morphology are better and the handling and storage are easier when paraffin-embedded slides are used (Fischer, Jacobson *et al*. 2008, Wild 2013).

In paraffin-embedded tissue, none of the examined antibodies recognized the correct CFTR protein, even though different antigen retrieval techniques both for heat-induced and proteolytic-induced epitope retrieval were tested. Although the antibodies detected the typical expression pattern of CFTR in WT intestine with the strongest signal intensity in the epithelial crypts and a decrease along the crypt-villus axis, the main problem was that the staining pattern was identical with that of CF KO intestine (see Figure 16). Interestingly, this feature could also be detected in western blots, where several antibodies recognized a band of the correct size both in WT and CF KO tissue (see Figure 17 (A)). A potential explanation for this finding could be the fact that in this thesis the specificity of antibodies was evaluated using porcine KO tissue as a "gold standard" negative control and not only by staining with the secondary antibody; an experiment that has not been done like this before, as no "real" negative control had been available until previously. As CFTR is a member of the ABC transporters that are characterized by highly-conserved motifs in the nucleotide-binding domains (Rees, Johnson *et al*. 2009), antibodies against CFTR might also recognize epitopes on other membrane transport proteins with a distribution pattern similar to CFTR. This idea is fortified by a study in which antibodies against different regions of CFTR recognized not only CFTR, but also immunologically related proteins with a comparable molecular mass and distribution pattern (Walker, Watson *et al*. 1995).

For the detection of human CFTR in frozen sections with the antibodies from the CF folding consortium, a detailed protocol was available (Kreda and Gentzsch 2011). As the amino acid sequences from all purchased antibodies showed a 100 % identity between human and pig, it was expected that this protocol should also work for the specific detection of CFTR in porcine tissue. However, neither in frozen sections nor in methacarn sections with expected antigenicity comparable to frozen sections (Mitchell, Ibrahim *et al*. 1985), a specific staining

of CFTR was detected with this protocol. This indicates that antigen-antibody interactions differ between species in spite of identical epitope sequences.

Only with one very specialized protocol the specific detection of CFTR worked reliably on cryo-sections from the intestine of WT animals, while CF KO tissue was negative. In the WT lung, only a very weak staining of the submucosal glands was detected. This finding can be easily explained by the fact that CFTR antibodies are often not sensitive enough to detect endogenous levels of the protein that is expressed only in very low abundance in many tissues (Doucet, Mendes *et al*. 2003). The expression analysis of *CFTR* at mRNA level showed that *CFTR* expression in the proximal jejunum is about ten times higher than in the lung (see Figure 24). There might be two possible issues contributing to the specific detection of CFTR with this protocol. The freezing method with pre-incubation in 2 % PFA and 30 % sucrose before snap-freezing embedded in OCT compound in an ethanol/dry ice bath should only lead to a better conservation of tissue morphology, but not interfere with the antigenicity of epitopes, which is in general better preserved in frozen than in paraffin-embedded tissue (Wild 2013, Hare, George *et al*. 2014). The second main difference to all other examined protocols was the treatment of sections with Triton X-100. Triton X-100 is known to increase the permeability of tissue for antibodies by destroying the membrane structure (Chen, Cho *et al*. 2010) and might thereby lead to a better detection of CFTR with Ab 596 that recognizes a part of the intracytoplasmatic NBD2 that could otherwise be difficult to access. One problem with studies on the distribution pattern of CFTR is, that even when only experiments on porcine tissue are taken into account, the results are inconsistent. Plog, Mundhenk *et al*. (2010) describe that porcine CFTR is expressed in ciliated epithelial cells and goblet cells in the nasal, tracheal, and bronchial mucosa but not in the alveolar or bronchiolar epithelia or submucosal glands. In contrast, Ballard, Trout *et al*. (1999) localized CFTR mainly to the ducts of submucosal glands and in weaker intensity to cells of the bronchial surface epithelium, an expression pattern corresponding to the weak staining of submucosal glands we detected in WT lung tissue (see Figure 14 (B)). Therefore, it is strongly recommended to repeat the working protocol with other antibodies in order to evaluate if these antibodies can be utilized for the specific detection of CFTR and if they recognize the same

distribution pattern as Ab 596. Only when a panel of antibodies recognizing different regions of CFTR detects the identical distribution pattern, a reliable conclusion on the expression of CFTR in porcine tissue can be reached. As the primary aim was to find an antibody that specifically detected CFTR in paraffin-embedded tissue, a panel of monoclonal antibodies recognizing specific peptide sequences of porcine CFTR were generated by immunization of rats and mice via the hybridoma technique by the AG Kremmer, Institute of Molecular Immunology Helmholtz Center Munich (Rottach, Kremmer *et al*. 2008). These antibodies are currently evaluated using WT and CF KO tissue and will be analyzed in more detail both for their utility for western blot and immunohistochemistry in the future.

Not only the intensity, but also the localization of *CFTR* expression affects the severity of meconium ileus in gut-modified *CFTR*$^{-/-}$ piglets

The correlation of *CFTR* expression levels with the intestinal phenotype in gut-modified *CFTR*$^{-/-}$ piglets revealed that the improvement of the MI was more pronounced when *CFTR* expression levels were higher in the distal parts of the intestine. In contrast, when high *CFTR* expression levels were restricted to the proximal parts of the small intestine, the intestinal phenotype did not differ from normal CF KO piglets. In the ileum of founder #2477 with the clearest improvement of MI, almost the same levels of *CFTR* were detected as in the WT ileum, albeit without an increased survival rate (see Figure 24). This finding remains contrary to a CF mouse model, in which only 5 % of normal *CFTR* expression levels assured the survival from intestinal disease (Dorin, Farley *et al*. 1996). However, a direct translation of findings in CF mice to the porcine CF model is difficult due to differences in the pathological mechanisms involved in the obstructive intestinal disease in these two species. Another study performed by Stoltz, Rokhlina *et al*. (2013) in CF KO piglets states that 20 % of WT *CFTR* mRNA expression in the ileum of gut-corrected *CFTR*$^{-/-}$ piglets is sufficient to rescue the lethal intestinal phenotype. This contradiction might be explained by the fact that in this model *CFTR* expression was only measured in one part of the intestine, the ileum, and not in five different regions of the intestine as in our

study. Therefore, it is unclear, whether higher levels of *CFTR* were detected in these piglets in other parts of the intestine that were the underlying reason for the increased survival and whether the expression levels in the ileum do have a value in predicting the severity of the intestinal phenotype.

We claim that in our examined gut-modified *CFTR*$^{-/-}$ piglets the survival was not rescued, in spite of high *CFTR* expression levels in proximal parts of the intestine, due to the lack of *CFTR* expression in the colon. We hypothesize that the localization of transgenic *CFTR* expression in the colon is as important as the intensity of the expression levels. There are several potential reasons why the prevalence of MI in CF piglets is so much higher than in other animal models for CF (ferret 75 %; mice develop DIOS-like obstruction around weaning) or affected humans (up to 20 %) (Borowitz and Gelfond 2013). Studies performed by Plog, Mundhenk *et al*. (2010) justify the 100 % incidence of MI in pigs with the strong expression of CFTR in the ileum and colon of WT piglets. Apart from the missing CFTR expression in the ileum and colon, other features are known to affect the severity and incidence of MI. The existence of alternative chloride currents in the intestine contributes to a modulation of gastrointestinal disease severity in CF mice and might be a reason for the less pronounced intestinal phenotype in CF mice models in comparison to the porcine model (Rozmahe, Wilschanski *et al*. 1996). CF patients carrying severe mutations in the *CFTR* gene are at a higher risk to develop MI (Dupuis, Keenan *et al*. 2015), so the fact that CF pigs and ferrets carry a null mutation should explain the high incidence of MI in these models. Other findings contributing to the high incidence of MI are the specific anatomy of the porcine large intestine, physiological differences in the secretory mechanisms in the large intestine in relation to other species or the narrow inbred-status of the experimental CF herd (Rogers, Stoltz *et al*. 2008, Sun, Sui *et al*. 2010).

Another indication that missing *CFTR* expression in the colon is primarily responsible for the severe intestinal disease in CF pigs is the atretic microcolon found in CF KO piglets (Meyerholz, Stoltz *et al*. 2010, Klymiuk, Mundhenk *et al*. 2012) that seems to be the main obstacle to the removal of meconium. Whether the atresia of the colon is really caused primarily by a developmental effect due to the lack of *CFTR* or develops subsequently because the functional obstruction

leads to a missing distension by luminal contents (Amodio, Berdon *et al*. 2012), should be analyzed in greater detail. However, the fact that from the first trimester onwards *CFTR* is expressed throughout the intestine in high levels during fetal development, gives a strong hint to the important role of *CFTR* in organ development (Tizzano, Chitayat *et al*. 1993). Only recently, Than, Linnekamp *et al*. (2016) demonstrated the importance of *CFTR* in the regulation of large intestinal stem cells since *CFTR* acts as a tumor suppressor gene for colorectal cancer in mice and humans. This implicates that *CFTR* expression in the distal parts of the intestine is a major contributor to the correct formation and development of the intestine.

An important question in this context is why the expression of *CFTR* is so high in the colon of pigs. This might be due to an adaptive process to the normal physiology of digestion in the porcine large intestine. CFTR-expressing goblet cells in the intestine form the characteristic two-layer mucus that serves as part of the innate immune system in form of a mucosal barrier (Kreda, Davis *et al*. 2012). In the porcine large intestine, dietary fibers are fermented to short chain fatty-acids (Jha and Berrocoso 2016) that stimulate colonic mucin production (Barcelo, Claustre *et al*. 2000) and gut microbiota might even utilize released mucins as energy source (Stanley, Ram *et al*. 1986). The magnified stimulation of mucus production and digestion by gut microbiota might therefore have led to an adaptive increase of goblet cell numbers in the large intestine.

The expression pattern of porcine *FABP2* limits the utility of the promoter to drive a selective expression of *CFTR* in the intestine

In order to achieve a selective expression of *CFTR* in the intestine of gut-modified *CFTR*$^{-/-}$ piglets, the promoter of the porcine *FABP2* gene was employed. The FABP2 protein is involved in the uptake and cellular transport of dietary long fatty-acids and therefore it is expressed predominantly and in high abundance in the intestine (Jiang and Li 2006). As the mRNA of *FABP2* is the most abundant RNA sequence in the intestine (Bass 1988) and the cytosolic FABPs represent up to 2 % of cytosolic proteins in the enterocytes (Ockner and Manning 1974), the expression levels of the transgenic construct were expected to be high. In contrast

to other studies that employed the *FABP2* promoter from the rat for the transgenic expression of *CFTR* in the mouse (Zhou, Dey *et al*. 1994) and pig (Stoltz, Rokhlina *et al*. 2013), we decided to use a homologous promoter because its activity should be stronger and the distribution pattern more precise in the same species (Rathore and Sunilkumar 2005). In 33 % of all examined gut-modified *CFTR*$^{-/-}$ founder animals, however, *CFTR* expression was not limited to the intestine but could be detected, albeit with lower abundance, in other CF-relevant organ systems such as the airways or the pancreas (see Figure 23). Therefore, the utility of these animals would be limited as they would most likely not develop the characteristic CF phenotype. This finding remains contrary to the US transgenic porcine CF model that utilized the rat *FABP2* promoter for the selective expression of *CFTR* in the intestine and did not exhibit any extra-intestinal expression (Stoltz, Rokhlina *et al*. 2013). However, consistent with our results, in a CF mouse model expressing human *CFTR* under the control of the rat *FABP2* promoter, several lines showed an extra-intestinal expression (Zhou, Dey *et al*. 1994), indicating that both rat and porcine *FABP2* expression might not be limited to the intestine. Measuring the expression levels of *FABP2* by quantitative PCR and sequencing of amplification products revealed that very high levels are consistently found in all parts of the small intestine, with highest levels in the jejunum, but also that small levels are detected in all other examined organs (see Figure 22 and Figure 25). Other studies confirm that both rat and porcine *FABP2* transcripts are detected in lower levels in organs other than the intestine (Gordon, Elshourbagy *et al*. 1985, Jiang and Li 2006). Whether the detected *CFTR* expression in extra-intestinal organs in our gut-modified *CFTR*$^{-/-}$piglets was triggered by the low amount of *FABP2* expression in other organs or was caused by the specific integration side of the transgenic vector, could only be clarified by a whole genome sequencing of these piglets. However, expression patterns and the corresponding results in the transgenic mouse model (Zhou, Dey *et al*. 1994) provide a strong indication that the *FABP2* promoter is not suitable to drive an intestine-selective *CFTR* expression.

Another aspect concerning the utility of the *FABP2* as promoter for the expression of *CFTR* is the stage-specific expression during fetal development. As we conclude that *CFTR* expression is essential for the development of the intestine

and *CFTR* expression can be detected as early as in the first trimester of pregnancy in humans (Tizzano, Chitayat *et al*. 1993), a similar developmental expression of *FABP2* might be important to prevent the formation of a microcolon. A closer look at developmental expression patterns of rat and mouse *FABP2* showed that this gene is only expressed during the late trimester of pregnancy in very low levels with a four-fold increase of expression levels within the first 24 h after birth by gene induction (Gordon, Elshourbagy *et al*. 1985, Green, Cohn *et al*. 1992). In contrast, studies on fetal human tissue report a *FABP2* expression very early in the gestational period (Levy, Menard *et al*. 2009). As no studies on the developmental expression pattern of porcine *FABP2* exist, the suitability of the promoter to drive *CFTR* expression during early fetal development remains a feature that should be further investigated.

The last aspect that should be considered in the evaluation of the usefulness of the *FABP2* promoter is that expression analysis of gut-modified *CFTR*$^{-/-}$ piglets indicates the necessity of *CFTR* expression in the large intestine to ensure survival (see Figure 24). Therefore, an ideal promoter should be characterized by high expression in the distal parts of the intestine. *FABP2* expression analysis at mRNA level showed that *FABP2* is predominantly expressed in the small intestine and no measurable amounts are detected in the colon (see Figure 22). Corresponding to this finding, FABP2 protein contents in the human small intestine are significantly higher than in the colon, with highest levels in the jejunum (Pelsers, Namiot *et al*. 2003). The absence of *FABP2* expression in the colon may have been the underlying reason for the severity of MI that could not be improved to a sufficient degree in our gut-modified *CFTR*$^{-/-}$ piglets.

The genetic background of *CFTR*$^{-/-}$ piglets influences the severity of meconium ileus

The finding with the strongest impact on future research concerning the porcine CF model was that the severity of meconium ileus shows variability among CF KO piglets produced by conventional breeding (see Figure 28). Until now all groups working with CF pigs have reported a 100 % penetrance of MI, independent from the mutation in the *CFTR* gene (Rogers, Stoltz *et al*. 2008,

Ostedgaard, Meyerholz *et al*. 2011, Klymiuk, Mundhenk *et al*. 2012). In contrast, in other species a high variability of the severity of the intestinal phenotype is reported in CF, which is mainly influenced by the genetic background. MI in human CF patients is one of several CF manifestations, such as CFRD (Blackman, Commander *et al*. 2013) or susceptibility to chronic infections with *P. aeruginosa* (Emond, Louie *et al*. 2012), which show very high heritability values. This indicates the strong contribution of genetic factors apart from the *CFTR* mutation to the phenotypic variety (Brennan and Schrijver 2016). Already in 1996, in CF mice models the existence of secondary genetic factors influencing the intestinal phenotype was described (Rozmahe, Wilschanski *et al*. 1996). Since, a range of potential candidate genes like members of the solute carrier protein family or multiple apical plasma membrane constituents have been identified by genome-wide association studies (Sun, Rommens *et al*. 2012). However, in this study we could demonstrate for the first time the presence of porcine modifier genes contributing to a variable severity of MI in the CF pig model (see Figure 30).

Only in rare cases modifier genes associated with intestinal obstruction were shown to have the same effect in two different species, like *CLCA1* (Van der Doef, Slieker *et al*. 2010*)* or *MSRA* (Henderson, Doshi *et al*. 2012) in CF mice and humans. Nevertheless, it is important to compare the two candidate loci on chromosome 10 and 16 in the porcine genome to regions in the human genome syntenic to these loci. Thereby we can examine whether genes reported to modify the CF phenotype in humans lay within this region and might therefore also be potential modifier genes for the porcine model. However, first analyses indicate that no described human modifier gene is expressed in the region of interest. Next steps will include a more detailed examination of the two porcine candidate loci in order to determine whether genes with a potential functional correlation with the intestinal obstruction are expressed in this region. The majority of human modifier genes for MI encode proteins that might interact directly with the functional defects leading to the CF phenotype, e.g. by regulation of transepithelial electrolyte and bicarbonate transport (Dorfman, Li *et al*. 2009) or modulation of proteolysis of the abnormal proteinaceous meconium (Henderson, Doshi *et al*. 2012). In future studies it has to be clarified, whether SNPs lie within the coding region of a gene, directly interfering with protein function, or are located at

regulatory regions, affecting the binding of transcription factors and thereby increasing or suppressing gene expression (Bush 2006).

In parallel to a detailed analysis of the two candidate loci it will be essential to produce new CF piglets with an improved intestinal phenotype in order to investigate if these piglets can completely remove meconium and survive the first critical days of life. These piglets can be generated by two different ways – either by reclonation of one of the improved CF piglets via SCNT and ET or by conventional breeding after a screening of the breeding herd for the desired haplotypes. The generation of "gut-improved" CF piglets by SCNT and ET is a fast and efficient method to produce a small number of animals with the desired genotype and is therefore suited for the evaluation of the intestinal phenotype as a kind of "proof of concept" study. However, it has to be taken into account that in the recloned piglets from gut-modified CF founder #2478, the improved intestinal phenotype was not reproducible (see Figure 7) and that recloned "gut-improved" piglets might therefore not exhibit the same level of improvement as the donor animals. In addition, the production of large numbers of viable animals via this method is not feasible due to low cloning efficiency (see Table 14 and Table 15) and a high rate of phenotypical abnormalities (see Figure 7), which might be due to epigenetic reprogramming or genomic damage of the donor cells (Cho, Kim *et al*. 2007). Therefore, all effort will be made to produce these gut-improved CF piglets by conventional breeding in the future. By screening of the breeding herd for the two candidate loci we will be able to selectively mate animals with a specific haplotype to increase the probability of CF KO piglets homozygous for both loci according to Table 20. If "gut-improved" CF KO piglets can survive the first critical days, they will make an ideal animal model for Cystic Fibrosis. In contrast to the porcine CF model with transgenic expression of *CFTR* in the intestine, the severity of meconium ileus is rescued in these piglets by naturally occurring modifier genes, whose existence is also described in human CF patients. Therefore, a living "gut-improved" CF pig will be an ideal large animal model for the investigation of unknown pathological mechanisms and testing of novel forms of therapy. It opens new prospects for CF research and can thereby lead to a better understanding of Cystic Fibrosis or even the development and evaluation of potential curative treatments.

VI. SUMMARY

The pig as an animal model for Cystic Fibrosis – approaches to overcome the lethal intestinal phenotype

Cystic Fibrosis (CF) is one of the most common lethal autosomal recessive hereditary diseases in people from Caucasian origin. Mutations in the gene encoding the anion channel Cystic Fibrosis Transmembrane Conductance Regulator (CFTR) cause defective transepithelial electrolyte transport. The consequence of this pathophysiological mechanism is a multisystemic disease mainly affecting the airways, the gastrointestinal tract and the pancreas. Chronic inflammations and infections of the respiratory tract are the main reasons for the decreased survival rate of CF patients. Although novel drugs, so-called "modulators", targeting specific mutation classes directly at the genetic or protein level have been developed in recent years, treatment options are still primarily limited to symptomatic therapy. So far, five different established animal models are available for CF research. As the porcine CF model bears the strongest resemblance to the classic human CF phenotype, important insights into the underlying pathological mechanisms involved in the development of airway disease have been gained by studying this model organism. The main aspect limiting the suitability of the porcine CF model is the lethal neonatal meconium ileus (MI) that occurs with a penetrance of 100 % and proves to be fatal if not surgically corrected.

In this thesis, I evaluated two different approaches to rescue the lethal intestinal phenotype of CF piglets. The first approach focused on the idea that the transgenic expression of *CFTR* under the control of the intestine-specific fatty-acid binding protein (*FABP2*) promoter should ameliorate the intestinal obstruction in CF piglets without interfering with other typical organ manifestations of CF. Despite an elaborate supporting treatment, none of the transgenic gut-modified piglets was able to remove the meconium completely. The examination of the intestinal phenotype consistently revealed an improvement of MI, indicated by a more distal localization and the absence of diverticulosis. The establishment of a fast genotyping protocol in less than three hours and the sequencing of amplified DNA

confirmed the genetic CF background and the integration of the transgenic vector into the CF genome. By quantitative PCR, I determined the expression level of *CFTR* in different parts of the intestine and other CF-relevant organs and could demonstrate that 33 % of all animals expressed *CFTR* in all organs. In all other tested animals, the expression of *CFTR* was restricted to the small intestine and correlated positively with the expression of *FABP2.* A correlation of the intestinal phenotype with *CFTR* expression levels revealed that the higher the expression levels were in the distal parts of the intestine, the more distinct was the improvement in the phenotype. In addition, I confirmed the absence of CFTR in the intestine and lungs of CF piglets by immunohistochemistry and immunofluorescence.

In the second part of the thesis, I investigated whether modifier genes contributed to the varying severity of meconium ileus that naturally occurred when CF pigs were produced by conventional breeding. In a hypothesis-driven "candidate gene" approach, I demonstrated by sequencing that the integrity of *CLCA4b* does not affect the intestinal phenotype in CF piglets. The genome-wide search for single nucleotide polymorphisms (SNPs) in CF piglets with an improved phenotype in comparison to other CF piglets revealed two potential candidate loci on chromosome 10 and 16, which have to be combined in an autosomal recessive way to improve the intestinal phenotype.

In conclusion, I could demonstrate two different ways to improve the lethal intestinal phenotype in a porcine model for Cystic Fibrosis in this thesis. The intestinal phenotype of transgenic gut-modified CF piglets was clearly alleviated, however, not to a sufficient degree to ensure survival. Presumably, this was caused by the absence of *CFTR* expression in the colon. In addition, the *FABP2* promoter was not suitable to drive an intestine-specific *CFTR* expression with high levels in the distal parts. In contrast, the second approach looks very promising. The discovery of potential modifier genes that contribute to a variable intestinal phenotype in CF piglets harbors great potential for the development of a living porcine CF model.

VII. ZUSAMMENFASSUNG

Das Schwein als Tiermodell für Mukoviszidose - Ansätze zur Behebung des tödlichen intestinalen Phänotyps

Mukoviszidose, auch zystische Fibrose (CF) genannt, gehört zu einer der häufigsten tödlichen autosomal rezessiven Erbkrankheiten bei Menschen mit kaukasischem Hintergrund. Mutationen des *CFTR*-Gens, das für den Anionenkanal Cystic Fibrosis Transmembrane Conductance Regulator (CFTR) codiert, verursachen einen fehlerhaften Elektrolyttransport an der Epitheloberfläche. Die Folge ist eine multisystemische Erkrankung, die vor allem die Luftwege, den Darmtrakt und die Bauchspeicheldrüse betrifft. Chronische Entzündungen und Infektionen des Atemtrakts sind die Hauptursachen für die eingeschränkte Lebenserwartung von CF-Patienten. Obwohl in den letzten Jahren neue Medikamente, sogenannte Modulatoren, entwickelt wurden, die gezielt auf Genom- oder Proteinebene spezielle Mutationsklassen angreifen, beschränkt sich die Behandlung auch heutzutage vorrangig auf eine symptomatische Therapie. Fünf verschiedene etablierte Tiermodelle stehen bislang der CF-Forschung zur Verfügung. Da das Schweinemodell dem klassischen Phänotyp beim Menschen am stärksten ähnelt, konnten anhand dieses Tiermodells wichtige Erkenntnisse über die pathophysiologischen Prozesse, die der Entwicklung der Erkrankung der Atemwege zugrunde liegen, gewonnen werden. Der Nutzen des CF-Schweinemodells ist jedoch enorm eingeschränkt, da es bei neugeborenen CF-Ferkeln mit einer Inzidenz von 100 % zu einem Mekoniumileus (MI) kommt, der ohne Operation tödlich verläuft.

In meiner Dissertation entwickelte ich zwei verschiedene Ansätze, um den tödlichen Phänotyp im Darm von neugeborenen CF-Ferkeln zu beheben. Der erste Ansatz basierte auf der Hypothese, dass eine transgene Expression von *CFTR* unter der Kontrolle des Promoters des nur im Darm exprimierten Gens *FABP2* (fatty-acid binding protein) zu einer Verbesserung des MI führen sollte, ohne dabei andere CF-relevante Organe zu beeinflussen.

Trotz einer ausgeprägten unterstützenden Behandlung konnte keines der transgenen „darmverbesserten“ Ferkel das Mekonium vollständig ausscheiden. Die visuelle Begutachtung des Darmtrakts zeigte bei allen Tieren eine Verbesserung des MI mit einer distaleren Lokalisation und einem Fehlen der Divertikulose. Die Genotypisierung und Sequenzierung der amplifizierten DNA bestätigte die Genetik der CF-Ferkel und die Integration des transgenen Vektors in das Genom. Mit quantitativer PCR wurde die Menge an exprimiertem *CFTR* in verschiedenen Darmabschnitten und anderen CF-relevanten Organen bestimmt. Dabei exprimierten 33 % der untersuchten Tiere *CFTR* in allen Organen. Bei allen anderen getesteten Tieren war die Expression ausschließlich auf den Dünndarm beschränkt und korrelierte positiv mit dem Expressionsmuster von *FABP2*. Die Korrelation zwischen dem Darmphänotyp und der Menge an exprimiertem *CFTR* zeigte, dass die Verbesserung des Darmphänotyps umso ausgeprägter war, je höher die Expression in distaleren Darmabschnitten war. Zusätzlich konnte ich mit immunhistochemischen und Immunfluoreszenz-Methoden bestätigen, dass im Darm und in der Lunge von CF Ferkeln kein CFTR Protein exprimiert wird.

Im zweiten Teil der Dissertation wurde untersucht, ob Modifier-Gene für die unterschiedliche Ausprägung des Darmphänotyps, die natürlicherweise bei gezüchteten CF Ferkeln auftrat, verantwortlich sind. In einem hypothesen-gesteuerten Kandidatengen-Ansatz wurde gezeigt, dass Deletionen im *CLCA4b*-Gen in keinem Zusammenhang mit dem verbesserten Darmphänotyp stehen. Die genomweite Suche nach Einzelnukleotidpolymorphismen, in denen sich CF-Ferkel mit verbessertem Phänotyp von anderen CF-Ferkeln unterscheiden, ergab zwei potentielle Kandidatenregionen auf den Chromosomen 10 und 16, die autosomal rezessiv miteinander kombiniert sein müssen.

Zusammengefasst beschreibt diese Dissertation zwei verschiedene Ansätze, den tödlichen intestinalen Phänotyp in einem Schweinemodell für Mukoviszidose zu beheben. Die Ausprägung des Darmphänotyps in dem transgenen CF-Schweinemodell konnte zwar deutlich verbessert werden, jedoch nicht in einem solchen Maß, dass das Überleben der Tiere gewährleistet wurde. Die Ursache dafür liegt vermutlich in der fehlenden Expression von *CFTR* im Colon. Des Weiteren ist der *FABP2* Promoter ungeeignet, eine darmspezifische *CFTR*-Expression mit hohen Spiegeln im Dickdarm zu bewirken.

Im Gegensatz dazu ist der zweite Ansatz durchaus vielversprechend. Die Entdeckung von möglichen Modifier-Genen, die den Darmphänotyp von CF-Ferkeln beeinflussen, birgt großes Potential für die Entwicklung eines lebenden CF-Schweinemodells.

VIII. INDEX OF FIGURES

IX. INDEX OF TABLES

X. REFERENCE LIST

Adam, R. J., A. S. Michalski, C. Bauer, M. H. Abou Alaiwa, T. J. Gross, M. S. Awadalla, D. C. Bouzek, N. D. Gansemer, P. J. Taft, M. J. Hoegger, A. Diwakar, M. Ochs, J. M. Reinhardt, E. A. Hoffman, R. R. Beichel, D. K. Meyerholz and D. A. Stoltz (2013). "Air trapping and airflow obstruction in newborn cystic fibrosis piglets." Am J Respir Crit Care Med **188**(12): 1434-1441.

Aigner, B., S. Renner, B. Kessler, N. Klymiuk, M. Kurome, A. Wunsch and E. Wolf (2010). "Transgenic pigs as models for translational biomedical research." J Mol Med (Berl) **88**(7): 653-664.

Alton, E. W., D. K. Armstrong, D. Ashby, K. J. Bayfield, D. Bilton, E. V. Bloomfield, A. C. Boyd, J. Brand, R. Buchan and R. Calcedo (2015). "Repeated nebulisation of non-viral CFTR gene therapy in patients with cystic fibrosis: a randomised, double-blind, placebo-controlled, phase 2b trial." The Lancet Respiratory Medicine **3**(9): 684-691.

Amaral, M. and C. Farinha (2013). "Rescuing mutant CFTR: a multi-task approach to a better outcome in treating cystic fibrosis." Current pharmaceutical design **19**(19): 3497-3508.

Amaral, M. D. and K. Kunzelmann (2007). "Molecular targeting of CFTR as a therapeutic approach to cystic fibrosis." Trends in pharmacological sciences **28**(7): 334-341.

Amodio, J., W. Berdon, S. Abramson and C. Stolar (2012). "Microcolon of prematurity: a form of functional obstruction." American Journal of Roentgenology **146**(2): 239-244.

Anderson, D. H. (1938). "Cystic Fibrosis of the pancreas and its relation to celiac disease: a clinical and pathological study." Am J Dis Child **56**: 344-399.

Awadalla, M., S. Miyawaki, M. H. Abou Alaiwa, R. J. Adam, D. C. Bouzek, A. S. Michalski, M. K. Fuld, K. J. Reynolds, E. A. Hoffman, C. L. Lin and D. A. Stoltz (2014). "Early airway structural changes in cystic fibrosis pigs as a determinant of particle distribution and deposition." Ann Biomed Eng **42**(4): 915-927.

Ballard, S. T., L. Trout, Z. Bebök, E. J. Sorscher and A. Crews (1999). "CFTR involvement in chloride, bicarbonate, and liquid secretion by airway submucosal glands." American Journal of Physiology - Lung Cellular and Molecular Physiology **277**(4): L694-L699.

Barcelo, A., J. Claustre, F. Moro, J. Chayvialle, J. Cuber and P. Plaisancie (2000). "Mucin secretion is modulated by luminal factors in the isolated vascularly perfused rat colon." Gut **46**(2): 218-224.

Bass, N. M. (1988). "The cellular fatty-acid binding proteins: aspects of structure, regulation, and function." Int Rev Cytol **111**: 143-184.

Bell, S. C., K. De Boeck and M. D. Amaral (2015). "New pharmacological approaches for cystic fibrosis: Promises, progress, pitfalls." Pharmacology & Therapeutics **145**: 19-34.

Birket, S. E., K. K. Chu, L. Liu, G. H. Houser, B. J. Diephuis, E. J. Wilsterman, G. Dierksen, M. Mazur, S. Shastry and Y. Li (2014). "A functional anatomic defect of the cystic fibrosis airway." American journal of respiratory and critical care medicine **190**(4): 421-432.

Blackman, S. M., C. W. Commander, C. Watson, K. M. Arcara, L. J. Strug, J. R. Stonebraker, F. A. Wright, J. M. Rommens, L. Sun and R. G. Pace (2013). "Genetic modifiers of cystic fibrosis-related diabetes." Diabetes: DB_130510.

Blackman, S. M., R. Deering-Brose, R. McWilliams, K. Naughton, B. Coleman, T. Lai, M. Algire, S. Beck, J. Hoover-Fong, A. Hamosh, M. D. Fallin, K. West, D. E. Arking, A. Chakravarti, D. J. Cutler and G. R. Cutting (2006). "Relative Contribution of Genetic and Non-genetic Modifiers to Intestinal Obstruction in Cystic Fibrosis." Gastroenterology **131**(4): 1030-1039.

Borowitz, D., R. D. Baker and V. Stallings (2002). "Consensus report on nutrition for pediatric patients with cystic fibrosis." Journal of pediatric gastroenterology and nutrition **35**(3): 246-259.

Borowitz, D. and D. Gelfond (2013). "Intestinal complications of cystic fibrosis." Current opinion in pulmonary medicine **19**(6): 676-680.

Boucher, R. (2007). "Evidence for airway surface dehydration as the initiating event in CF airway disease." Journal of internal medicine **261**(1): 5-16.

Bréa, D., F. Meurens, V. Dubois A , J. Gaillard, C. Chevaleyre, M. L. Jourdan, N. Winter, B. Arbeille, M. Si-Tahar, F. Gauthier and S. Attucci (2012). "The pig as a model for investigating the role of neutrophil serine proteases in human inflammatory lung diseases." Biochem J **447**(Pt 3): 363-370.

Brennan, M.-L. and I. Schrijver (2016). "Cystic Fibrosis: A Review of Associated Phenotypes, Use of Molecular Diagnostic Approaches, Genetic Characteristics, Progress, and Dilemmas." The Journal of Molecular Diagnostics **18**(1): 3-14.

Bronsveld, I., F. Mekus, J. Bijman, M. Ballmann, H. R. de Jonge, U. Laabs, D. J. Halley, H. Ellemunter, G. Mastella, S. Thomas, H. J. Veeze and B. Tümmler (2001). "Chloride conductance and genetic background modulate the cystic fibrosis phenotype of ΔF508 homozygous twins and siblings." J Clin Invest **108**(11): 1705-1715.

Bush, A. (2006). Cystic fibrosis in the 21st century, Karger Medical and Scientific Publishers.

Bustin, S. A. (2004). AZ of quantitative PCR, International University Line San Diego, CA.

Chang, E. H., R. S. Lacruz, T. G. Bromage, P. Bringas, M. J. Welsh, J. Zabner and M. L. Paine (2011). "Enamel Pathology Resulting from Loss of Function in the Cystic Fibrosis Transmembrane Conductance Regulator in a Porcine Animal Model." Cells Tissues Organs **194**(2-4): 249-254.

Chang, E. H., A. A. Pezzulo, D. K. Meyerholz, A. E. Potash, T. J. Wallen, L. R. Reznikov, J. C. Sieren, P. H. Karp, S. Ernst, T. O. Moninger, N. D. Gansemer, P. B. McCray, Jr., D. A. Stoltz, M. J. Welsh and J. Zabner (2012). "Sinus hypoplasia precedes sinus infection in a porcine model of cystic fibrosis." Laryngoscope **122**(9): 1898-1905.

Chen, J. H., D. A. Stoltz, P. H. Karp, S. E. Ernst, A. A. Pezzulo, T. O. Moninger, M. V. Rector, L. R. Reznikov, J. L. Launspach, K. Chaloner, J. Zabner and M. J. Welsh (2010). "Loss of anion transport without increased sodium absorption characterizes newborn porcine cystic fibrosis airway epithelia." Cell **143**(6): 911-923.

Chen, X., D.-B. Cho and P.-C. Yang (2010). "Double staining immunohistochemistry." North American Journal of Medical Sciences **2**(5): 241-245.

Cho, S.-K., J.-H. Kim, J.-Y. Park, Y.-J. Choi, J.-I. Bang, K.-C. Hwang, E.-J. Cho, S.-H. Sohn, S. J. Uhm, D.-B. Koo, K.-K. Lee, T. Kim and J.-H. Kim (2007). "Serial cloning of pigs by somatic cell nuclear transfer: Restoration of phenotypic normality during serial cloning." Developmental Dynamics **236**(12): 3369-3382.

Clancy, J. P. and M. Jain (2012). "Personalized Medicine in Cystic Fibrosis." American Journal of Respiratory and Critical Care Medicine **186**(7): 593-597.

Cutting, G. R. (2015). "Cystic fibrosis genetics: from molecular understanding to clinical application." Nat Rev Genet **16**(1): 45-56.

Cystic Fibrosis Foundation. (2016). "CF Clinical Care Guidelines." 2016, from https://www.cff.org/For-Caregivers/CF-Clinical-Care-Guidelines/.

Cystic Fibrosis Foundation. (2016). "Drug development pipeline." Retrieved 05.01.2016, 2016, from https://tools.cff.org/research/drugdevelopmentpipeline/.

Cystic Fibrosis Mutation Database. (2015). "CFMDB Statistics." Retrieved 17 Dec, 2015, from http://www.genet.sickkids.on.ca/StatisticsPage.html.

Davidson, D. J. and M. Rolfe (2001). "Mouse models of cystic fibrosis." Trends in Genetics **17**(10): S29-S37.

Davies, J. C., E. W. F. W. Alton and A. Bush (2007). "Cystic fibrosis." BMJ **335**(7632): 1255-1259.

Debray, D., D. Rainteau, V. Barbu, M. Rouahi, H. E. Mourabit, S. Lerondel, C. Rey, L. Humbert, D. Wendum, C. H. Cottart, P. Dawson, N. Chignard and C. Housset (2012). "Defects in Gallbladder Emptying and Bile Acid Homeostasis in Mice With Cystic Fibrosis Transmembrane Conductance Regulator Deficiencies." Gastroenterology **142**(7): 1581-1591.e1586.

Denning, G. M., L. S. Ostedgaard, S. H. Cheng, A. E. Smith and M. J. Welsh (1992). "Localization of cystic fibrosis transmembrane conductance regulator in chloride secretory epithelia." J Clin Invest **89**(1): 339-349.

di Sant'Agnese, P. A., R. C. Darling, G. A. Perera and E. Shea (1953). "Abnormal electrolyte composition of sweat in cystic fibrosis of the pancreas. Clinical Significance and Relationship to the Disease." Pediatrics **12**(5): 549-563.

Diwakar, A., R. J. Adam, A. S. Michalski, M. M. Tamegnon, A. J. Fischer, J. L. Launspach, R. A. Horan, S. C. Kao, K. Chaloner, D. K. Meyerholz and D. A. Stoltz (2015). "Sonographic evidence of abnormal tracheal cartilage ring structure in cystic fibrosis." The Laryngoscope **125**(10): 2398-2404.

Dodge, J. A., P. A. Lewis, M. Stanton and J. Wilsher (2007). "Cystic fibrosis mortality and survival in the UK: 1947–2003." European Respiratory Journal **29**(3): 522-526.

Dorfman, R., W. Li, L. Sun, F. Lin, Y. Wang, A. Sandford, P. D. Paré, K. McKay, H. Kayserova, T. Piskackova, M. Macek, K. Czerska, D. Sands, H. Tiddens, S. Margarit, G. Repetto, M. K. Sontag, F. J. Accurso, S. Blackman, G. R. Cutting, L. C. Tsui, M. Corey, P. Durie, J. Zielenski and L. J. Strug (2009). "Modifier gene study of meconium ileus in cystic fibrosis: statistical considerations and gene mapping results." Hum Genet **126**(6): 763-778.

Dorin, J., R. Farley, S. Webb, S. Smith, E. Farini, S. Delaney, B. Wainwright, E. Alton and D. Porteous (1996). "A demonstration using mouse models that successful gene therapy for cystic fibrosis requires only partial gene correction." Gene therapy **3**(9): 797-801.

Doucet, L., F. Mendes, T. Montier, P. Delépine, D. Penque, C. Férec and M. D. Amaral (2003). "Applicability of Different Antibodies for the Immunohistochemical Localization of CFTR In Respiratory and Intestinal Tissues of Human and Murine Origin." Journal of Histochemistry & Cytochemistry **51**(9): 1191-1199.

Dupuis, A., K. Keenan, C. Y. Ooi, R. Dorfman, M. K. Sontag, L. Naehrlich, C. Castellani, L. J. Strug, J. M. Rommens and T. Gonska (2015). "Prevalence of meconium ileus marks the severity of mutations of the Cystic Fibrosis Transmembrane Conductance Regulator (CFTR) gene." Genet Med.

Efrati, O., A. Barak, D. Modan-Moses, A. Augarten, D. Vilozni, D. Katznelson, A. Szeinberg, J. Yahav and Y. Bujanover (2003). "Liver cirrhosis and portal hypertension in cystic fibrosis." European journal of gastroenterology & hepatology **15**(10): 1073-1078.

Emond, M. J., T. Louie, J. Emerson, W. Zhao, R. A. Mathias, M. R. Knowles, F. A. Wright, M. J. Rieder, H. K. Tabor and D. A. Nickerson (2012). "Exome sequencing of extreme phenotypes identifies DCTN4 as a modifier of chronic Pseudomonas aeruginosa infection in cystic fibrosis." Nature genetics **44**(8): 886-889.

Farinha, C. M., D. Penque, M. Roxo-Rosa, G. Lukacs, R. Dormer, M. McPherson, M. Pereira, A. G. Bot, H. Jorna and R. Willemsen (2004). "Biochemical methods to assess CFTR expression and membrane localization." Journal of Cystic Fibrosis **3**: 73-77.

Farrell, P. M., B. J. Rosenstein, T. B. White, F. J. Accurso, C. Castellani, G. R. Cutting, P. R. Durie, V. A. LeGrys, J. Massie and R. B. Parad (2008). "Guidelines for diagnosis of cystic fibrosis in newborns through older adults: Cystic Fibrosis Foundation consensus report." The Journal of pediatrics **153**(2): S4-S14.

Fischer, A. H., K. A. Jacobson, J. Rose and R. Zeller (2008). "Cryosectioning Tissues." Cold Spring Harbor Protocols **2008**(8): 4991.

Fisher, J. T., Y. Zhang and J. F. Engelhardt (2011). "Comparative Biology of Cystic Fibrosis Animal Models." Methods Mol Biol **742**: 311-334.

Gibson, L. E. and R. E. Cooke (1959). "A test for concentration of electrolytes in sweat in cystic fibrosis of the pancreas utilizing pilocarpine by iontophoresis." Pediatrics **23**(3): 545-549.

Gill, D. R. and S. C. Hyde (2014). "Delivery of genes into the CF airway." Thorax **69**(10): 962-964.

Goldman, M. J., G. M. Anderson, E. D. Stolzenberg, U. P. Kari, M. Zasloff and J. M. Wilson (1997). "Human β-Defensin-1 Is a Salt-Sensitive Antibiotic in Lung That Is Inactivated in Cystic Fibrosis." Cell **88**(4): 553-560.

Gordon, J., N. Elshourbagy, J. Lowe, W. Liao, D. Alpers and J. Taylor (1985). "Tissue specific expression and developmental regulation of two genes coding for rat fatty-acid binding proteins." Journal of Biological Chemistry **260**(4): 1995-1998.

Gray, M. A., J. P. Winpenny, B. Verdon, H. McAlroy and B. E. Argent (1995). "Chloride channels and cystic fibrosis of the pancreas." Bioscience Reports **15**(6): 531-541.

Green, R. p., S. m. Cohn, J. c. Sacchettini, K. e. Jackson and J. i. Gordon (1992). "The mouse intestinal fatty-acid binding protein gene: nucleotide sequence, pattern of developmental and regional expression, and proposed structure of its protein product." DNA and cell biology **11**(1): 31-41.

Grubb, B. R. and R. C. Boucher (1999). "Pathophysiology of Gene-Targeted Mouse Models for Cystic Fibrosis." Physiological Reviews **79**(1): S193-S214.

Grubb, B. R., A. M. Paradiso and R. C. Boucher (1994). "Anomalies in ion transport in CF mouse tracheal epithelium." American Journal of Physiology-Cell Physiology **267**(1): C293-C300.

Guilbault, C., Z. Saeed, G. P. Downey and D. Radzioch (2007). "Cystic Fibrosis Mouse Models." American Journal of Respiratory Cell and Molecular Biology **36**(1): 1-7.

Guillon, A., C. Chevaleyre, C. Barc, M. Berri, H. Adriaensen, F. Lecompte, T. Villemagne, J. Pezant, R. Delaunay, J. Moënne-Loccoz, P. Berthon, A. Bähr, E. Wolf, N. Klymiuk, S. Attucci, R. Ramphal, P. Sarradin, D. Buzoni-Gatel, M. Si-Tahar and I. Caballero (2015). "Computed Tomography (CT) Scanning Facilitates Early Identification of Neonatal Cystic Fibrosis Piglets." PLoS One **10**(11).

Hameed, S., A. Jaffé and C. F. Verge (2015). "Advances in the detection and management of cystic fibrosis related diabetes." Current opinion in pediatrics **26**(4): 525-533.

Hare, D. J., J. L. George, L. Bray, I. Volitakis, A. Vais, T. M. Ryan, R. A. Cherny, A. I. Bush, C. L. Masters, P. A. Adlard, P. A. Doble and D. I. Finkelstein (2014). "The effect of paraformaldehyde fixation and sucrose cryoprotection on metal concentration in murine neurological tissue." Journal of Analytical Atomic Spectrometry **29**(3): 565-570.

Heijerman, H. (2005). "Infection and inflammation in cystic fibrosis: a short review." Journal of Cystic Fibrosis **4**: 3-5.

Henderson, L. B., V. K. Doshi, S. M. Blackman, K. M. Naughton, R. G. Pace, J. Moskovitz, M. R. Knowles, P. R. Durie, M. L. Drumm and G. R. Cutting (2012). "Variation in MSRA modifies risk of neonatal intestinal obstruction in cystic fibrosis." PLoS Genet **8**(3): e1002580.

Hoegger, M. J., A. J. Fischer, J. D. McMenimen, L. S. Ostedgaard, A. J. Tucker, M. A. Awadalla, T. O. Moninger, A. S. Michalski, E. A. Hoffman, J. Zabner, D. A. Stoltz and M. J. Welsh (2014). "Impaired Mucus Detachment Disrupts Mucociliary Transport in a Piglet Model of Cystic Fibrosis." Science **345**(6198): 818-822.

Itani, O. A., J.-H. Chen, P. H. Karp, S. Ernst, S. Keshavjee, K. Parekh, J. Klesney-Tait, J. Zabner and M. J. Welsh (2011). "Human cystic fibrosis airway epithelia have reduced Cl− conductance but not increased Na+ conductance." Proceedings of the National Academy of Sciences **108**(25): 10260-10265.

Jakab, R. L., A. M. Collaco and N. A. Ameen (2013). "Characterization of CFTR High Expresser cells in the intestine." Am J Physiol Gastrointest Liver Physiol **305**(6): G453-465.

Jha, R. and J. F. D. Berrocoso (2016). "Dietary fiber and protein fermentation in the intestine of swine and their interactive effects on gut health and on the environment: A review." Animal Feed Science and Technology **212**: 18-26.

Jiang, Y.-Z. and X.-W. Li (2006). "Molecular Cloning and Tissue-specific Expression of Intestinal-type Fatty-acid Binding Protein in Porcine." Acta Genetica Sinica **33**(2): 125-132.

Judge, E. P., J. M. L. Hughes, J. J. Egan, M. Maguire, E. L. Molloy and S. O'Dea (2014). "Anatomy and Bronchoscopy of the Porcine Lung. A Model for Translational Respiratory Medicine." American Journal of Respiratory Cell and Molecular Biology **51**(3): 334-343.

Kappler, M., M. Feilcke, C. Schröter, A. Kraxner and M. Griese (2009). "Long-term pulmonary outcome after meconium ileus in cystic fibrosis." Pediatric Pulmonology **44**(12): 1201-1206.

Karimi, A., R. R. Gorter, C. Sleeboom, C. M. F. Kneepkens and H. A. Heij (2011). "Issues in the management of simple and complex meconium ileus." Pediatr Surg Int **27**(9): 963-968.

Katkin, J. and K. Schultz (2010). "Cystic fibrosis: overview of gastrointestinal disease." UpToDate. Waltham, MA: UpToDate.

Kelly, T. and J. Buxbaum (2015). "Gastrointestinal Manifestations of Cystic Fibrosis." Digestive Diseases and Sciences **60**(7): 1903-1913.

Kessler, W. H. a. A. D. H. (1951). "Heat prostration in fibrocystic disease of the pancreas and other conditions." Pediatrics **8**(5): 648-656.

Klymiuk, N., L. Mundhenk, K. Kraehe, A. Wuensch, S. Plog, D. Emrich, M. C. Langenmayer, M. Stehr, A. Holzinger, C. Kroner, A. Richter, B. Kessler, M. Kurome, M. Eddicks, H. Nagashima, K. Heinritzi, A. D. Gruber and E. Wolf (2012). "Sequential targeting of CFTR by BAC vectors generates a novel pig model of cystic fibrosis." J Mol Med (Berl) **90**(5): 597-608.

Knowles, M. R., J. M. Robinson, R. E. Wood, C. A. Pue, W. M. Mentz, G. C. Wager, J. T. Gatzy and R. C. Boucher (1997). "Ion composition of airway surface liquid of patients with cystic fibrosis as compared with normal and disease-control subjects." J Clin Invest **100**(10): 2588-2595.

Kolbe, E. W., S. Tamm, S. Hedtfeld, T. Becker, B. Tummler and F. Stanke (2013). "CLCA4 variants determine the manifestation of the cystic fibrosis basic defect in the intestine." Eur J Hum Genet **21**(6): 691-694.

Konstan, M. W., S. M. Butler, M. E. B. Wohl, M. Stoddard, R. Matousek, J. S. Wagener, C. A. Johnson and W. J. Morgan (2003). "Growth and nutritional indexes in early life predict pulmonary function in cystic fibrosis." The Journal of Pediatrics **142**(6): 624-630.

Kreda, S. M., C. W. Davis and M. C. Rose (2012). "CFTR, Mucins, and Mucus Obstruction in Cystic Fibrosis." Cold Spring Harbor Perspectives in Medicine **2**(9): a009589.

Kreda, S. M. and M. Gentzsch (2011). "Imaging CFTR protein localization in cultured cells and tissues." Cystic Fibrosis: Diagnosis and Protocols, Volume II: Methods and Resources to Understand Cystic Fibrosis: 15-33.

Kurome, M., B. Kessler, A. Wuensch, H. Nagashima and E. Wolf (2015). Nuclear Transfer and Transgenesis in the Pig. Nuclear Reprogramming. N. Beaujean, H. Jammes and A. Jouneau, Springer New York. **1222:** 37-59.

Leung, A., P. Wong, J. Yankaskas and R. Boucher (1996). "cAMP-but not Ca (2+)-regulated Cl-conductance is lacking in cystic fibrosis mice epididymides and seminal vesicles." American Journal of Physiology-Cell Physiology **271**(1): C188-C193.

Levy, E., D. Menard, E. Delvin, A. Montoudis, J. F. Beaulieu, G. Mailhot, N. Dube, D. Sinnett, E. Seidman and M. Bendayan (2009). "Localization, function and regulation of the two intestinal fatty-acid-binding protein types." Histochem Cell Biol **132**(3): 351-367.

Luan, X., A. Campanucci Vó, M. Nair, O. Yilmaz, G. Belev, T. E. Machen, D. Chapman and J. P. Ianowski (2014). "Pseudomonas aeruginosa triggers CFTR-mediated airway surface liquid secretion in swine trachea." Proc Natl Acad Sci U S A **111**(35): 12930-12935.

MacKenzie, T., A. H. Gifford, K. A. Sabadosa, H. B. Quinton, E. A. Knapp, C. H. Goss and B. C. Marshall (2014). "Longevity of Patients With Cystic Fibrosis in 2000 to 2010 and Beyond: Survival Analysis of the Cystic Fibrosis Foundation Patient RegistryLifetime of Patients With Cystic Fibrosis in 2000 to 2010 and Beyond." Annals of Internal Medicine **161**(4): 233-241.

Mak, V., J. Zielenski, L.-C. Tsui, P. Durie, A. Zini, S. Martin, T. B. Longley and K. A. Jarvi (1999). "Proportion of cystic fibrosis gene mutations not detected by routine testing in men with obstructive azoospermia." Jama **281**(23): 2217-2224.

Marino, C. R., L. M. Matovcik, F. S. Gorelick and J. A. Cohn (1991). "Localization of the cystic fibrosis transmembrane conductance regulator in pancreas." Journal of Clinical Investigation **88**(2): 712.

Matsui, H., B. R. Grubb, R. Tarran, S. H. Randell, J. T. Gatzy, C. W. Davis and R. C. Boucher (1998). "Evidence for Periciliary Liquid Layer Depletion, Not Abnormal Ion Composition, in the Pathogenesis of Cystic Fibrosis Airways Disease." Cell **95**(7): 1005-1015.

Meyerholz, D. K., A. M. Lambertz, L. R. Reznikov, G. K. Ofori-Amanfo, P. H. Karp, P. B. McCray, M. J. Welsh and D. A. Stoltz (2015). "Immunohistochemical Detection of Markers for Translational Studies of Lung Disease in Pigs and Humans." Toxicologic Pathology.

Meyerholz, D. K., D. A. Stoltz, E. Namati, S. Ramachandran, A. A. Pezzulo, A. R. Smith, M. V. Rector, M. J. Suter, S. Kao, G. McLennan, G. J. Tearney, J. Zabner, P. B. McCray, Jr. and M. J. Welsh (2010). "Loss of cystic fibrosis transmembrane conductance regulator function produces abnormalities in tracheal development in neonatal pigs and young children." Am J Respir Crit Care Med **182**(10): 1251-1261.

Meyerholz, D. K., D. A. Stoltz, A. A. Pezzulo and M. J. Welsh (2010). "Pathology of gastrointestinal organs in a porcine model of cystic fibrosis." Am J Pathol **176**(3): 1377-1389.

Mitchell, D., S. Ibrahim and B. A. Gusterson (1985). "Improved immunohistochemical localization of tissue antigens using modified methacarn fixation." Journal of Histochemistry & Cytochemistry **33**(5): 491-495.

Navis, A. and M. Bagnat (2015). "Loss of cftr function leads to pancreatic destruction in larval zebrafish." Developmental Biology **399**(2): 237-248.

Navis, A., L. Marjoram and M. Bagnat (2013). "Cftr controls lumen expansion and function of Kupffer's vesicle in zebrafish." Development **140**(8): 1703-1712.

O'Sullivan, B. P. and S. D. Freedman (2009). "Cystic fibrosis." The Lancet **373**(9678): 1891-1904.

Ockner, R. K. and J. A. Manning (1974). "Fatty-acid-binding protein in small intestine identification, isolation, and evidence for its role in cellular fatty-acid transport." Journal of Clinical Investigation **54**(2): 326.

Olivier, A. K., K. N. Gibson-Corley and D. K. Meyerholz (2015). "Animal models of gastrointestinal and liver diseases. Animal models of cystic fibrosis: gastrointestinal, pancreatic, and hepatobiliary disease and pathophysiology." American Journal of Physiology - Gastrointestinal and Liver Physiology **308**(6): G459-G471.

Olivier, A. K., Y. Yi, X. Sun, H. Sui, B. Liang, S. Hu, W. Xie, J. T. Fisher, N. W. Keiser and D. Lei (2012). "Abnormal endocrine pancreas function at birth in cystic fibrosis ferrets." The Journal of clinical investigation **122**(122 (10)): 3755-3768.

Ostedgaard, L. S., D. K. Meyerholz, J. H. Chen, A. A. Pezzulo, P. H. Karp, T. Rokhlina, S. E. Ernst, R. A. Hanfland, L. R. Reznikov, P. S. Ludwig, M. P. Rogan, G. J. Davis, C. L. Dohrn, C. Wohlford-Lenane, P. J. Taft, M. V. Rector, E. Hornick, B. S. Nassar, M. Samuel, Y. Zhang, S. S. Richter, A. Uc, J. Shilyansky, R. S. Prather, P. B. McCray, Jr., J. Zabner, M. J. Welsh and D. A. Stoltz (2011). "The DeltaF508 mutation causes CFTR misprocessing and cystic fibrosis-like disease in pigs." Sci Transl Med **3**(74): 74ra24.

Ostedgaard, L. S., D. K. Meyerholz, D. W. Vermeer, P. H. Karp, L. Schneider, C. D. Sigmund and M. J. Welsh (2011). "Cystic fibrosis transmembrane conductance regulator with a shortened R domain rescues the intestinal phenotype of CFTR-/- mice." Proc Natl Acad Sci U S A **108**(7): 2921-2926.

Pelsers, M. M. A. L., Z. Namiot, W. Kisielewski, A. Namiot, M. Januszkiewicz, W. T. Hermens and J. F. C. Glatz (2003). "Intestinal-type and liver-type fatty-acid-binding protein in the intestine. Tissue distribution and clinical utility." Clinical Biochemistry **36**(7): 529-535.

Pezzulo, A. A., X. X. Tang, M. J. Hoegger, M. H. Alaiwa, S. Ramachandran, T. O. Moninger, P. H. Karp, C. L. Wohlford-Lenane, H. P. Haagsman, M. van Eijk, B. Banfi, A. R. Horswill, D. A. Stoltz, P. B. McCray, Jr., M. J. Welsh and J. Zabner (2012). "Reduced airway surface pH impairs bacterial killing in the porcine cystic fibrosis lung." Nature **487**(7405): 109-113.

Phennicie, R. T., M. J. Sullivan, J. T. Singer, J. A. Yoder and C. H. Kim (2010). "Specific Resistance to Pseudomonas aeruginosa Infection in Zebrafish Is Mediated by the Cystic Fibrosis Transmembrane Conductance Regulator." Infect Immun **78**(11): 4542-4550.

Pierucci-Alves, F., V. Akoyev, J. C. Stewart, L. H. Wang, K. S. Janardhan and B. D. Schultz (2011). "Swine Models of Cystic Fibrosis Reveal Male Reproductive Tract Phenotype at Birth." Biol Reprod **85**(3): 442-451.

Plog, S., N. Klymiuk, S. Binder, M. J. Van Hook, W. B. Thoreson, A. D. Gruber and L. Mundhenk (2015). "Naturally Occurring Deletion Mutants of the Pig-Specific, Intestinal Crypt Epithelial Cell Protein *CLCA4b* without Apparent Phenotype." PLoS ONE **10**(10): e0140050.

Plog, S., L. Mundhenk, M. K. Bothe, N. Klymiuk and A. D. Gruber (2010). "Tissue and cellular expression patterns of porcine CFTR: similarities to and differences from human CFTR." J Histochem Cytochem **58**(9): 785-797.

Potash, A. E., T. J. Wallen, P. H. Karp, S. Ernst, T. O. Moninger, N. D. Gansemer, D. A. Stoltz, J. Zabner and E. H. Chang (2013). "Adenoviral gene transfer corrects the ion transport defect in the sinus epithelia of a porcine CF model." Mol Ther **21**(5): 947-953.

Proesmans, M., F. Vermeulen and K. De Boeck (2008). "What's new in cystic fibrosis? From treating symptoms to correction of the basic defect." Eur J Pediatr **167**(8): 839-849.

Rathore, K. S. and G. Sunilkumar (2005). "Homologous promoter use in genetic modification." ISB News Report, September: 6-7.

Ratjen, F. A. (2009). "Cystic fibrosis: pathogenesis and future treatment strategies." Respiratory care **54**(5): 595-605.

Reddy, M. M., M. J. Light and P. M. Quinton (1999). "Activation of the epithelial Na+ channel (ENaC) requires CFTR Cl- channel function." Nature **402**(6759): 301-304.

Reddy, M. M. and P. M. Quinton (2001). "Selective activation of cystic fibrosis transmembrane conductance regulator Cl- and HCO3- conductances." JOP **2**(4 Suppl): 212-218.

Rees, D. C., E. Johnson and O. Lewinson (2009). "ABC transporters: the power to change." Nat Rev Mol Cell Biol **10**(3): 218-227.

Reznikov, L. R., Q. Dong, J. H. Chen, T. O. Moninger, J. M. Park, Y. Zhang, J. Du, M. S. Hildebrand, R. J. Smith, C. O. Randak, D. A. Stoltz and M. J. Welsh (2013). "CFTR-deficient pigs display peripheral nervous system defects at birth." Proc Natl Acad Sci U S A **110**(8): 3083-3088.

Riordan, J. R. (2005). "Assembly of functional CFTR chloride channels." Annu. Rev. Physiol. **67**: 701-718.

Riordan, J. R., J. M. Rommens, B.-s. Kerem, N. Alon, R. Rozmahel, Z. Grzelczak, J. Zielenski, S. Lok, N. Plavsic and J.-L. Chou (1989). "Identification of the cystic fibrosis gene: cloning and characterization of complementary DNA." Science **245**(4922): 1066-1073.

Rochholz, E. L. (1857). Alemannisches Kinderlied und Kinderspiel aus der Schweiz... von Ernst Ludwig Rochholz, J. J. Weber.

Rogers, C. S., W. M. Abraham, K. A. Brogden, J. F. Engelhardt, J. T. Fisher, P. B. McCray, Jr., G. McLennan, D. K. Meyerholz, E. Namati, L. S. Ostedgaard, R. S. Prather, J. R. Sabater, D. A. Stoltz, J. Zabner and M. J. Welsh (2008). "The porcine lung as a potential model for cystic fibrosis." Am J Physiol Lung Cell Mol Physiol **295**(2): L240-263.

Rogers, C. S., Y. Hao, T. Rokhlina, M. Samuel, D. A. Stoltz, Y. Li, E. Petroff, D. W. Vermeer, A. C. Kabel, Z. Yan, L. Spate, D. Wax, C. N. Murphy, A. Rieke, K. Whitworth, M. L. Linville, S. W. Korte, J. F. Engelhardt, M. J. Welsh and R. S. Prather (2008). "Production of CFTR-null and CFTR-DeltaF508 heterozygous pigs by adeno-associated virus-mediated gene targeting and somatic cell nuclear transfer." J Clin Invest **118**(4): 1571-1577.

Rogers, C. S., D. A. Stoltz, D. K. Meyerholz, L. S. Ostedgaard, T. Rokhlina, P. J. Taft, M. P. Rogan, A. A. Pezzulo, P. H. Karp, O. A. Itani, A. C. Kabel, C. L. Wohlford-Lenane, G. J. Davis, R. A. Hanfland, T. L. Smith, M. Samuel, D. Wax, C. N. Murphy, A. Rieke, K. Whitworth, A. Uc, T. D. Starner, K. A. Brogden, J. Shilyansky, P. B. McCray, Jr., J. Zabner, R. S. Prather and M. J. Welsh (2008). "Disruption of the CFTR gene produces a model of cystic fibrosis in newborn pigs." Science **321**(5897): 1837-1841.

Rosenfeld, M., J. Emerson, J. Williams-Warren, M. Pepe, A. Smith, A. B. Montgomery and B. Ramsey (2001). "Defining a pulmonary exacerbation in cystic fibrosis." The Journal of pediatrics **139**(3): 359-365.

Rottach, A., E. Kremmer, D. Nowak, P. Boisguerin, R. Volkmer, M. C. Cardoso, H. Leonhardt and U. Rothbauer (2008). "Generation and characterization of a rat monoclonal antibody specific for PCNA." Hybridoma **27**(2): 91-98.

Rozmahe, R., M. Wilschanski, A. Matin, S. Plyte, M. Oliver, W. Auerbach, A. Moore, J. Forstner, P. Durie, J. Nadeau, C. Bear and L.-C. Tsui (1996). "Modulation of disease severity in cystic fibrosis transmembrane conductance regulator deficient mice by a secondary genetic factor." Nat Genet **12**(3): 280-287.

Schellekens, D. H., J. Grootjans, S. A. Dello, A. A. van Bijnen, R. M. van Dam, C. H. Dejong, J. P. Derikx and W. A. Buurman (2014). "Plasma intestinal fatty-acid–binding protein levels correlate with morphologic epithelial intestinal damage in a human translational ischemia-reperfusion model." Journal of clinical gastroenterology **48**(3): 253-260.

Scholte, B. J., D. J. Davidson, M. Wilke and H. R. De Jonge (2004). "Animal models of cystic fibrosis." Journal of Cystic Fibrosis **3**: 183-190.

Sheppard, D. N. and M. J. Welsh (1999). "Structure and Function of the CFTR Chloride Channel." Physiological Reviews **79**(1): S23-S45.

Snouwaert, J. N., K. K. Brigman, A. M. Latour, N. N. Malouf, R. C. Boucher, O. Smithies and B. H. Koller (1992). "An Animal Model for Cystic Fibrosis Made by Gene Targeting." Science **257**(5073): 1083-1088.

Spielberg, D. R. and J. P. Clancy (2016). "Cystic Fibrosis and Its Management Through Established and Emerging Therapies." Annual Review of Genomics and Human Genetics **17**(1)

Stanley, R. A., S. Ram, R. Wilkinson and A. Roberton (1986). "Degradation of pig gastric and colonic mucins by bacteria isolated from the pig colon." Applied and environmental microbiology **51**(5): 1104-1109.

Stoltz, D. A., D. K. Meyerholz, A. A. Pezzulo, S. Ramachandran, M. P. Rogan, G. J. Davis, R. A. Hanfland, C. Wohlford-Lenane, C. L. Dohrn, J. A. Bartlett, G. A. t. Nelson, E. H. Chang, P. J. Taft, P. S. Ludwig, M. Estin, E. E. Hornick, J. L. Launspach, M. Samuel, T. Rokhlina, P. H. Karp, L. S. Ostedgaard, A. Uc, T. D. Starner, A. R. Horswill, K. A. Brogden, R. S. Prather, S. S. Richter, J. Shilyansky, P. B. McCray, Jr., J. Zabner and M. J. Welsh (2010). "Cystic fibrosis pigs develop lung disease and exhibit defective bacterial eradication at birth." Sci Transl Med **2**(29): 29ra31.

Stoltz, D. A., T. Rokhlina, S. E. Ernst, A. A. Pezzulo, L. S. Ostedgaard, P. H. Karp, M. S. Samuel, L. R. Reznikov, M. V. Rector, N. D. Gansemer, D. C. Bouzek, M. H. Alaiwa, M. J. Hoegger, P. S. Ludwig, P. J. Taft, T. J. Wallen, C. Wohlford-Lenane, J. D. McMenimen, J. H. Chen, K. L. Bogan, R. J. Adam, E. E. Hornick, G. A. t. Nelson, E. A. Hoffman, E. H. Chang, J. Zabner, P. B. McCray, Jr., R. S. Prather, D. K. Meyerholz and M. J. Welsh (2013). "Intestinal CFTR expression alleviates meconium ileus in cystic fibrosis pigs." J Clin Invest **123**(6): 2685-2693.

Strom, C. M., D. Huang, C. Chen, A. Buller, M. Peng, F. Quan, J. Redman and W. Sun (2003). "Extensive sequencing of the cystic fibrosis transmembrane regulator gene: Assay validation and unexpected benefits of developing a comprehensive test." Genet Med **5**(1): 9-14.

Strom, C. M., R. Janeszco, F. Quan, S. Wang, A. Buller, M. McGinniss and W. Sun (2006). "Technical Validation of a Tm Biosciences Luminex-Based Multiplex Assay for Detecting the American College of Medical Genetics Recommended Cystic Fibrosis Mutation Panel." J Mol Diagn **8**(3): 371-375.

Sun, L., J. M. Rommens, H. Corvol, W. Li, X. Li, T. Chiang, F. Lin, R. Dorfman, P. Busson, R. V. Parekh, D. Zelenika, S. Blackman, M. Corey, V. Doshi, L. Henderson, K. Naughton, W. K. O'Neal, R. G. Pace, J. R. Stonebraker, S. D. Wood, F. A. Wright, J. Zielenski, A. Clement, M. L. Drumm, P. Y. Boëlle, G. R. Cutting, M. R. Knowles, P. R. Durie and L. J. Strug (2012). "Multiple apical plasma membrane constituents are associated with susceptibility to meconium ileus in individuals with cystic fibrosis." Nat Genet **44**(5): 562-569.

Sun, X., A. K. Olivier, B. Liang, Y. Yi, H. Sui, T. I. A. Evans, Y. Zhang, W. Zhou, S. R. Tyler, J. T. Fisher, N. W. Keiser, X. Liu, Z. Yan, Y. Song, J. A. Goeken, J. M. Kinyon, D. Fligg, X. Wang, W. Xie, T. J. Lynch, P. M. Kaminsky, Z. A. Stewart, R. M. Pope, T. Frana, D. K. Meyerholz, K. Parekh and J. F. Engelhardt (2014). "Lung Phenotype of Juvenile and Adult Cystic Fibrosis Transmembrane Conductance Regulator–Knockout Ferrets." Am J Respir Cell Mol Biol **50**(3): 502-512.

Sun, X., A. K. Olivier, Y. Yi, C. E. Pope, H. S. Hayden, B. Liang, H. Sui, W. Zhou, K. R. Hager, Y. Zhang, X. Liu, Z. Yan, J. T. Fisher, N. W. Keiser, Y. Song, S. R. Tyler, J. A. Goeken, J. M. Kinyon, M. C. Radey, D. Fligg, X. Wang, W. Xie, T. J. Lynch, P. M. Kaminsky, M. J. Brittnacher, S. I. Miller, K. Parekh, D. K. Meyerholz, L. R. Hoffman, T. Frana, Z. A. Stewart and J. F. Engelhardt (2014). "Gastrointestinal Pathology in Juvenile and Adult CFTR-Knockout Ferrets." Am J Pathol **184**(5): 1309-1322.

Sun, X., H. Sui, J. T. Fisher, Z. Yan, X. Liu, H.-J. Cho, N. S. Joo, Y. Zhang, W. Zhou and Y. Yi (2010). "Disease phenotype of a ferret CFTR-knockout model of cystic fibrosis." The Journal of clinical investigation **120**(9): 3149.

Sun, X., Z. Yan, Y. Yi, Z. Li, D. Lei, C. S. Rogers, J. Chen, Y. Zhang, M. J. Welsh and G. H. Leno (2008). "Adeno-associated virus–targeted disruption of the CFTR gene in cloned ferrets." The Journal of clinical investigation **118**(4): 1578.

Than, B. L. N., J. F. Linnekamp, T. K. Starr, D. A. Largaespada, A. Rod, Y. Zhang, V. Bruner, J. Abrahante, A. Schumann, T. Luczak, A. Niemczyk, M. G. O'Sullivan, J. P. Medema, R. J. A. Fijneman, G. A. Meijer, E. Van den Broek, C. A. Hodges, P. M. Scott, L. Vermeulen and R. T. Cormier (2016). "CFTR is a tumor suppressor gene in murine and human intestinal cancer." Oncogene.

Tizzano, E. F., D. Chitayat and M. Buchwald (1993). "Cell-specific localization of CFTR mRNA shows developmentally regulated expression in human fetal tissues." Human Molecular Genetics **2**(3): 219-224.

Tuggle, K. L., S. E. Birket, X. Cui, J. Hong, J. Warren, L. Reid, A. Chambers, D. Ji, K. Gamber, K. K. Chu, G. Tearney, L. P. Tang, J. A. Fortenberry, M. Du, J. M. Cadillac, D. M. Bedwell, S. M. Rowe, E. J. Sorscher and M. V. Fanucchi (2014). "Characterization of Defects in Ion Transport and Tissue Development in Cystic Fibrosis Transmembrane Conductance Regulator (CFTR)-Knockout Rats." PLoS One **9**(3).

Uc, A., R. Giriyappa, D. K. Meyerholz, M. Griffin, L. S. Ostedgaard, X. X. Tang, M. Abu-El-Haija, D. A. Stoltz, P. Ludwig, A. Pezzulo, M. Abu-El-Haija, P. Taft and M. J. Welsh (2012). "Pancreatic and biliary secretion are both altered in cystic fibrosis pigs." Am J Physiol Gastrointest Liver Physiol **303**(8): G961-968.

Uc, A., A. K. Olivier, M. A. Griffin, D. K. Meyerholz, J. Yao, M. Abu-El-Haija, K. M. Buchanan, O. G. Vanegas Calderón, M. Abu-El-Haija, A. A. Pezzulo, L. R. Reznikov, M. J. Hoegger, M. V. Rector, L. S. Ostedgaard, P. J. Taft, N. D. Gansemer, P. S. Ludwig, E. E. Hornick, D. A. Stoltz, K. L. Ode, M. J. Welsh, J. F. Engelhardt and A. W. Norris (2015). "Glycemic regulation and insulin secretion are abnormal in cystic fibrosis pigs despite sparing of islet cell mass." Clin Sci (Lond) **128**(2): 131-142.

Van der Doef, H., M. Slieker, D. Staab, B. Alizadeh, M. Seia, C. Colombo, C. van der Ent, R. Nickel, H. Witt and R. Houwen (2010). "Association of the CLCA1 p. S357N variant with meconium ileus in European patients with cystic fibrosis." Journal of pediatric gastroenterology and nutrition **50**(3): 347-349.

van der Doef, H. P. J., F. T. M. Kokke, C. K. van der Ent and R. H. J. Houwen (2011). "Intestinal Obstruction Syndromes in Cystic Fibrosis: Meconium Ileus, Distal Intestinal Obstruction Syndrome, and Constipation." Curr Gastroenterol Rep **13**(3): 265-270.

Van Goor, F., S. Hadida, P. D. Grootenhuis, B. Burton, D. Cao, T. Neuberger, A. Turnbull, A. Singh, J. Joubran and A. Hazlewood (2009). "Rescue of CF airway epithelial cell function in vitro by a CFTR potentiator, VX-770." Proceedings of the National Academy of Sciences **106**(44): 18825-18830.

Walker, J., J. Watson, C. Holmes, A. Edelman and G. Banting (1995). "Production and characterisation of monoclonal and polyclonal antibodies to different regions of the cystic fibrosis transmembrane conductance regulator (CFTR): detection of immunologically related proteins." Journal of Cell Science **108**(6): 2433-2444.

Welsh, M. J., C. S. Rogers, D. A. Stoltz, D. K. Meyerholz and R. S. Prather (2009). "Development of a porcine model of cystic fibrosis." Trans Am Clin Climatol Assoc **120**: 149-162.

Welsh, M. J. and A. E. Smith (1993). "Molecular mechanisms of CFTR chloride channel dysfunction in cystic fibrosis." Cell **73**(7): 1251-1254.

Whitelaw, C. B. A., T. P. Sheets, S. G. Lillico and B. P. Telugu (2016). "Engineering large animal models of human disease." The Journal of pathology **238**(2): 247-256.

Widdicombe, J. H. and J. J. Wine (2015). "Airway Gland Structure and Function." Physiological Reviews **95**(4): 1241-1319.

Wild, D. (2013). The immunoassay handbook: theory and applications of ligand binding, ELISA and related techniques, Newnes.

Wilke, M., R. M. Buijs-Offerman, J. Aarbiou, W. H. Colledge, D. N. Sheppard, L. Touqui, A. Bot, H. Jorna, H. R. de Jonge and B. J. Scholte (2011). "Mouse models of cystic fibrosis: phenotypic analysis and research applications." J Cyst Fibros **10 Suppl 2**: S152-171.

Wilschanski, M., L. L. Miller, D. Shoseyov, H. Blau, J. Rivlin, M. Aviram, M. Cohen, S. Armoni, Y. Yaakov, T. Pugatch, M. Cohen-Cymberknoh, N. L. Miller, A. Reha, V. J. Northcutt, S. Hirawat, K. Donnelly, G. L. Elfring, T. Ajayi and E. Kerem (2011). "Chronic ataluren (PTC124) treatment of nonsense mutation cystic fibrosis." European Respiratory Journal **38**(1): 59-69.

Wright, J. T., C. L. Kiefer, K. I. Hall and B. R. Grubb (1996). "Abnormal Enamel Development in a Cystic Fibrosis Transgenic Mouse Model." Journal of Dental Research **75**(4): 966-973.

Zhou, L., C. R. Dey, S. E. Wert, M. D. DuVall, R. A. Frizzell and J. A. Whitsett (1994). "Correction of lethal intestinal defect in a mouse model of cystic fibrosis by human CFTR." Science **266**(5191): 1705-1708.

XI. ACKNOWLEDGEMENT

First of all, I would like to thank Prof. Dr. Eckhard Wolf for providing me the opportunity to do my doctoral thesis at the Chair for Molecular Animal Breeding and Biotechnology (LMU-Munich) in such an interesting topic and for reviewing this manuscript.

I would like to sincerely thank Dr. Nikolai Klymiuk, Dr. Andrea Bähr and Dr. Elisabeth Kemter for their consistent support, input and help during my thesis.

I am thankful to all my colleagues at the Moorversuchsgut, to senior scientists as well as my fellow graduate students (Anna, Sofia, Kilian, Erika, Arne and Janet) and our technical assistants (Ingrid, Eva and Tatjana, thanks for all your help!). Special thanks go to the whole “stable team”, the veterinarians and especially the animal caretakers Harald Paul and Josef Bichler.

Furthermore, I would like to thank Anna Ermund and Gunnar C. Hansson from the Mucin Biology Group at the University of Gothenburg for great collaboration and for all the data they shared with me.

I would also like to express my gratitude to ethris for giving me the opportunity to work in such an interesting field by providing financial support.

Finally, I would like to thank the people who helped me the most during these years – my parents, my sister Lydia, Christoph and my friends. Thanks a lot for all your support. Without you, this work would not have been possible.